Topology Control and Opportunistic Routing in Underwater Acoustic Sensor Networks

by

Rodolfo Wanderson Lima Coutinho

Thesis submitted to the
Faculty of Graduate and Postdoctoral Studies
In partial fulfillment of the requirements
For the Ph.D. degree in
Computer Science

School of Information Technology and Engineering
Faculty of Engineering
University of Ottawa

Abstract

Underwater wireless sensor networks (UWSNs) are the enabling technology for a new era of underwater monitoring and actuation applications. However, there still is a long road ahead until we reach a technological maturity capable of empowering high-density large deployment of UWSNs. To the date hereof, the scientific community is yet investigating the principles that will guide the design of networking protocols for UWSNs. This is because the principles that guide the design of protocols for terrestrial wireless sensor networks cannot be applied for an UWSN since it uses the acoustic channel instead of radio-frequency-based channel.

This thesis provides a general discussion for high-fidelity and energy-efficient data collection in UWSNs. In the first part of this thesis, we propose and study the symbiotic design of topology control and opportunistic routing protocols for UWSNs. We propose the CTC and DTC topology control algorithms that rely on the depth adjustment of the underwater nodes to cope with the communication void region problem. In addition, we propose an analytical framework to study and evaluate our mobility-assisted approach in comparison to the classical bypassing and power control-based approaches. Moreover, we develop the GEDAR routing protocol for mobile UWSNs. GEDAR is the first OR protocol employing our innovative depth adjustment-based topology control methodology to re-actively cope with communication void regions.

In the second part of this thesis, we study opportunistic routing (OR) underneath duty-cycling in UWSNs. We propose an analytical framework to investigate the joint design of opportunistic routing and duty cycle protocols for UWSNs. While duty-cycling conserves energy, it changes the effective UWSN density. Therefore, OR is proposed to guarantee a suitable one-hop density of awake neighbors to cope with the poor and time-varying link quality of the acoustic channel. In addition, we propose an analytical framework to study the impact of heterogeneous and on-the-fly sleep interval adjustment in OR underneath duty-cycling in UWSNs. The proposed model is aimed to provide insights for the future design of protocols towards a prolonged UWSN lifetime.

The developed solutions have been extensively compared to related work either analytically or through simulations. The obtained results show the potentials of them in several scenarios of UWSNs. In turn, the devised analytical frameworks have been providing significant insights that will guide future developments of routing and duty-cycling protocols for several scenarios and setting of UWSNs.

List of Publications

Referred Journal Papers

1. R. W. L. Coutinho, A. Boukerche, L. F. M. Vieira and A. A. F. Loureiro, "Joint Duty-Cycling and Opportunistic Routing for Mobile Underwater Sensor Networks," *IEEE Transactions on Mobile Computing*, 2016. Under review.

2. R. W. L. Coutinho, A. Boukerche, L. F. M. Vieira and A. A. F. Loureiro, "Modeling and Performance Evaluation of Communication Void Handling in Underwater Sensor Networks," *Computer Networks*, 2016. Second round.

3. R. W. L. Coutinho, A. Boukerche, L. F. M. Vieira and A. A. F. Loureiro, "Topology Control: A New Challenge for Underwater Sensor Networks," *ACM Computing Surveys*, 2017. Second round.

4. R. W. L. Coutinho, A. Boukerche, L. F. M. Vieira and A. A. F. Loureiro, "On the Design of Green Protocols for Underwater Sensor Networks," *IEEE Communications Magazine*, vol. 54, no. 10, pp. 67-73, Oct. 2016. doi: `10.1109/MCOM.2016.7588231`.

5. R. W. L. Coutinho, A. Boukerche, L. F. M. Vieira and A. A. F. Loureiro, "Design guidelines for opportunistic routing in underwater networks," *IEEE Communications Magazine*, vol. 54, no. 2, pp. 40-48, Feb. 2016. doi: `10.1109/MCOM.2016.7402259`.

6. R. W. L. Coutinho, A. Boukerche, L. F.M. Vieira, A. A. F. Loureiro, "A novel void node recovery paradigm for long-term underwater sensor networks," *Ad Hoc Networks*, Volume 34, pp. 144-156, Nov. 2015. doi: `10.1016/j.adhoc.2015.01.012`.

7. R. W. L. Coutinho, A. Boukerche, L. F. M. Vieira and A. A. F. Loureiro, "Geographic and Opportunistic Routing for Underwater Sensor Networks," *IEEE Transactions on Computers*, vol. 65, no. 2, pp. 548-561, Feb. 1 2016. doi: `10.1109/TC.2015.2423677`.

Referred Conference Papers

1. R. W. L. Coutinho, A. Boukerche, L. F.M. Vieira, A. A. F. Loureiro, "EnOR: Energy Balancing Routing Protocol for Underwater Sensor Networks," *Proceedings of the IEEE International Conference on Communications*, 2017. Accepted.

2. R. W. L. Coutinho, A. Boukerche, L. F.M. Vieira, A. A. F. Loureiro, (***In Portuguese***). "Um Protocolo de Roteamento para o Consumo Balanceado de Energia em Redes de Sensores Aquáticas," *Proceedings of the 35th Brazilian Symposium on Computer Networks and Distributed Systems (SBRC)*, 2017. Accepted

3. R. W. L. Coutinho, A. Boukerche, L. F.M. Vieira, A. A. F. Loureiro, "Modeling the sleep interval effects in duty-cycled underwater sensor networks," *Proceedings of the IEEE International Conference on Communications (ICC)*, pp. 1 - 6, 2016. doi: 10.1109/ICC.2016.7510983.

4. R. W. L. Coutinho, A. Boukerche, L. F.M. Vieira, A. A. F. Loureiro, "A novel centrality-based scheme for topology control in underwater sensor networks," *Proceedings of the 19th ACM International Conference on Modeling, Analysis and Simulation of Wireless and Mobile Systems (MSWiM)*, 2016. doi: 10.1145/2988287.2989162.

5. R. W. L. Coutinho, A. Boukerche, L. F.M. Vieira, A. A. F. Loureiro, "Modeling of Opportunistic Routing meeting Duty Cycle in Underwater Sensor Networks," *Proceedings of the 18th ACM International Conference on Modeling, Analysis and Simulation of Wireless and Mobile Systems (MSWiM)*, pp. 125 - 132, 2015. doi: 10.1145/2811587.2811608.

6. R. W. L. Coutinho, A. Boukerche, L. F.M. Vieira, A. A. F. Loureiro, "GEDAR: Geographic and opportunistic routing protocol with Depth Adjustment for Mobile Underwater Sensor Networks," *Proceedings of the IEEE International Conference on Communications (ICC)*, pp. 251 - 256, 2014. doi: 10.1109/ICC.2014.6883327.

7. R. W. L. Coutinho, A. Boukerche, L. F.M. Vieira, A. A. F. Loureiro, "Transmission Power Control-based Opportunistic Routing for Wireless Sensor Networks," *Proceedings of the 17th ACM International Conference on Modeling, Analysis and Simulation of Wireless and Mobile Systems (MSWiM)*, pp. 219 - 226, 2014. doi: 10.1145/2641798.2641813.

8. **(Best paper award)** R. W. L. Coutinho, A. Boukerche, L. F.M. Vieira, A. A. F. Loureiro, "Local Maximum Routing Recovery in Underwater Sensor Networks: Performance and Trade-offs," *Proceedings of the 22th IEEE International Symposium on Modeling, Analysis & Simulation of Computer and Telecommunication Systems (MASCOTS)*, pp. 112 - 119, 2014. doi: 10.1109/MASCOTS.2014.22.

9. R. W. L. Coutinho, L. F.M. Vieira, A. A. F. Loureiro, "DCR: Depth-Controlled Routing protocol for underwater sensor networks," *Proceedings of the IEEE Symposium on Computers and Communications (ISCC)*, pp. 453 - 458, 2013. doi: 10.1109/ISCC.2013.6754988.

10. R. W. L. Coutinho, L. F.M. Vieira, A. A. F. Loureiro, "Movement Assisted-Topology Control and Geographic Routing Protocol for Underwater Sensor Networks," *Proceedings of the 16th ACM International Conference on Modeling, Analysis and Simulation of Wireless and Mobile Systems (MSWiM)*, pp. 189 - 196, 2013. doi: 10.1145/2507924.2507956.

Acknowledgements

I am greatly indebted to my advisors Prof. Azzedine Boukerche (uOttawa), Canada, and Prof. Antonio A. F. Loureiro (UFMG), Brazil, for their encouragement, guidance, and support throughout my graduate studies. Both of you gave me valuable pieces of advice not only about research and the process of accomplishing it but also about life. Uncountable times I appealed for both of you when I faced a research or bureaucratic problem that seemed to be insuperable. You all have always been willing to guide me to find a solution and both of you always intervened when the problem was bigger than I could handle it. And there were many ☺. Thank you all so much, Professors!

I am also very thankful to Prof. Luiz F. Veira (UFMG) for introducing me to and helping me with this fascinating and challenging research topic on underwater sensor networks. This research field is really amazing! Thank you.

The staff and faculty members of the *Universidade Federal de Minas Gerais* (UFMG) and the University of Ottawa, undoubtedly, were cooperative and aided me to go throughout this process. I would like to thank everyone there for their support. Special thanks and acknowledgment must go to Renata, Sônia, Linda, Sheila, Stella, Maristela, Laura Roach, Annik Dion and Maria Bento.

I thank my friends and colleagues in the UWL/WISEMAP Lab (Brazil) and PARADISE Research Lab (Canada) for their help whenever I needed and willingness to make the Lab an enjoyable and fun work environment.

Definitely, I would like to express my deepest gratitude to my dear wife Aline da Silva Brito. This accomplishment would not be possible without your unconditional assistance, patience, and love in good and bad moments. I love you so much! I could not succeed and realize my dream without your support. I will be eternally indebted for your presence in my life.

I always gonna be truly grateful to my parents, *Tia*, brothers, and sister. They were very supportive and did whatever they could to assist me in my own education, during my entire academic life. They always encouraged and helped me even with this long geographical distance between us.

This research was partially supported by the NSERC TRANSIT Project and NSERC DIVA Strategic Network Research Program during my stay in Canada, and the Coordination for the Improvement of Higher Education Personnel (CAPES), during my stay in Brazil.

Contents

List of Tables

List of Figures

Glossary of Terms

ACK Acknowledge

ARQ Automatic Repeat-Request

AWGN Additive White Gaussian Noise

BP British Petroleum

BPSK Binary Phase Shift Keying

CC Cooperative Communication

CCDF Complementary Cumulative Distribution Function

CDF Cumulative Density Function

CTC Centralized Topology Control

DBR Depth-Based Routing

DCR Depth-Controlled Routing

DFS Depth First Search

DTC Distributed Topology Control

EPA Expected Packet Advancement

FBR Focused Beam Routing

GOR Geographic and Opportunistic Routing

GPS Global Positioning System

GR Geographic Routing

GUF Greedy Upward Forwarding

GUF+DA Greedy Upward Forwarding with Depth Adjustment Void-Handling

GUF+PA Greedy Upward Forwarding with Power Control Void-Handling

GUF+VA Greedy Upward Forwarding with Bypassing Void Region

HH-VBF Hop-by-Hop Vector-based Forwarding

IoUT Internet of Underwater Things

LPL Low Power Listening

LPP Low Power Probing

MAC Medium Access Control

MCM Meandering Current Mobility

NACK Negative Acknowledge

NADV Normalized Advancement

OR Opportunistic Routing

PRNet Packet Radio Network

QoS Quality of Service

RF Radio Frequency

RMS Root Mean Square

RTS Request to Send

SEA Sensor Equipped Aquatic

SNR Signal-to-Noise Ratio

UAV Underwater Autonomous Vehicle

UWSN Underwater Wireless Sensor Network

VANET Vehicular Ad Hoc Network

VAPR Void-Aware Pressure Routing

VBF Vector-Based Forwarding

WSN Wireless Sensor Network

Chapter 1

Introduction

The ocean covers more than 70% of the Earth's surface and it is vital for human life. It helps in driving weather and regulating Earth's temperature, provides primary resources for humans and serves as a medium for commerce and transport [1]. However, more than 95% of the volume of the ocean remains unexplored and, even more alarming, unseen by human eyes [2]. The solid knowledge and understanding of the ocean are daunting. Nevertheless, they are necessary to the consciously, sustainably and properly exploration and protection of this environment. Unfavorably, the reality regarding technologies for large-scale data collection from the ocean is not exciting. Either sensor nodes without underwater communication capabilities or wired-interconnected underwater sensor nodes have been used for underwater monitoring applications. These approaches are expensive, not scalable and intolerant to faults.

In this content, underwater sensor networks (UWSNs) have been attracting increasing attention from scientific and industrial communities. The use of underwater sensor nodes, enabled with wireless communication capabilities, have the potentials to realize real-time underwater monitoring and actuation applications, with an on-line system reconfiguration and failure detections capabilities [3]. Therefore, this technology is expected to make possible a new era in scientific and industrial underwater monitoring and exploration applications, such as the monitoring of marine life, pollutant content, geological processes on the ocean floor, oilfields, climate, and tsunamis and sea-quakes; to collect oceanographic data, ocean and offshore sampling, navigation assistance, and mine recognition, in addition being used for tactic surveillance applications. These applications will help in filling the gap of our knowledge regarding the ocean and aquatic environments in general.

Nevertheless, deployments of underwater sensor networks are still limited to experimental settings. Nowadays, a large-scale deployment of an underwater sensor network is expensive. This is due to the high cost of ship missions for the deployment, operation, and maintenance of the network. Ship missions can last several days since sensors might be attached to docks, anchored buoys, sea floors, underwater autonomous vehicles (UAVs), low-power gliders, or underpowered drifters, depending on the desired network architecture [4]. Additionally, underwater sensor nodes and AUVs are naturally expensive, due to their acoustic modem transceiver and the appropriate hardware for protecting the circuitry.

Yet, efficient data collection is challenging in UWSNs. Often, underwater sensor nodes are equipped with acoustic modems to wirelessly communicate with each other. This is because high-frequency radio waves are strongly absorbed in water and optical waves suffer from heavy scattering and are restricted to short-range-line-of-sight applications. Underwater communication links are affected by high path loss, noise, multipath signal propagation, limited bandwidth capacity, Doppler spreading and high power consumption [5]. Moreover, temporary connectivity loss can occur due to shadow zones. Therefore, the wireless link between neighbors can perform poorly or even be down at any given moment, which will increase packet retransmissions will increase, as an attempt to deliver data packets, and will result in more packet collisions, delay and energy consumption.

1.1 Thesis Statement

Research problem: In wireless communication systems, the underwater acoustic channel is recognized as one of the harshest communication media in use today [5]. The underwater acoustic channel is highly unreliable and costly. One big challenge in UWSNs is, then, how can we achieve high rates of data delivery with a low energy consumption.

Key idea: In this thesis, we propose the symbiotic design of topology control and opportunistic routing towards efficient data collection in the envisioned large-scale underwater acoustic sensor networks.

The suitable, autonomous and on-the-fly organization of UWSN topology, through topology control algorithms, might mitigate undesired effects of the underwater wireless

communication and, consequently, improve networking services and protocols. The topology of a network dictates how the nodes interconnect with each other. The proper organization of the UWSN topology might mitigate undesired effects of the underwater wireless communication and, consequently, improve networking services and protocols. Topology control, for instance, will be fundamental to deal with the involuntary network topology changes in UWSNs occasioned by the mobility of the nodes and time-varying link quality effects, which diminish the performance of networking services and protocols.

In turn, opportunistic routing (OR) helps to mitigate the effects of the underwater channel and enhance the poor quality of underwater acoustic physical links, by taking advantage of the broadcast nature of the wireless transmission medium. However, some of their drawbacks (*e.g.*, communication void region problem, high delay, and redundant data packet transmission) are accented in underwater acoustic communication, which can severely diminish UWSN's performance if not carefully considered.

However, each approach has disadvantages that, when combined, could diminish significantly the performance of an UWSNs. Therefore, we propose analytical frameworks, topology control algorithms, and routing protocols to study the symbiotic design of topology control and opportunistic routing in UWSNs, as well as its characteristics, drawbacks and how it can mitigate the effects of the underwater acoustic channel and improve data collection in UWSNs.

1.2 Objectives

The main objectives of this thesis are to propose analytical frameworks and develop protocols for high-fidelity and energy-efficient data collection in UWSNs. Specifically, we aim the design of joint mobility-assisted and duty-cycled-based topology control with opportunistic routing to mitigate the drawbacks of the acoustic channel in UWSNs.

The design of networking protocols for underwater sensor networks is demanding. Due to the characteristics of the underwater environment and acoustic channel, the wide knowledge acquired in the context of wireless ad hoc networks and RF-based wireless sensor networks cannot be directly applied in designing networking protocols for UWSNs. Moreover, energy constraints, computational limitations, dynamic and unpredictable mobility, and other challenges well-known and well-investigated in wireless ad hoc and sensor networks are even more critical and arduous in UWSNs.

Overall speaking, this thesis aims to provide a general discussion about the symbiotic design of topology control and opportunistic routing towards efficient data collection in

UWSNs. We intend to identify and understand difficulties and requirements for enabling efficient data collection. We intend to investigate the potentials of topology control and opportunistic routing in dealing with the drawbacks of the underwater acoustic channel. We intend to understand the weakness of topology control and opportunistic routing, that will be accented in the harsh environment of underwater acoustic communication.

1.3 Contribution

In the following we list the contributions made in this thesis, in the order they appear in this document.

- **An analytical framework to study void-handling paradigms.** One classical problem of geographic and opportunistic routing (GOR) is the communication void region. This problem happens whenever there is no neighboring node closer to the destination than the current forwarder node. This contribution consists in modeling and evaluation of the three methodologies (*i.e.*, power control, mobility assisted and bypassing void area) for the design of void handling protocols for GOR protocols in UWSNs.

- **Two mobility assisted topology control algorithms.** This contribution concerns on the development of two topology control protocols (the CTC and DTC) for reducing disconnected nodes in sparse underwater sensor networks for short-term monitoring applications. In these protocols, disconnected and void nodes determined from an AUV-based localization system are moved to new depth locations to resume greedy forwarding geographic routing in static UWSNs. This approach increases data delivery by improving network connectivity and routing efficiency.

- **GEDAR opportunistic routing protocol.** This contribution concerns on the proposal of an opportunistic routing protocol for mobile underwater sensor networks. The novelties of the proposed protocol are twofold. Firstly, GEDAR was the first position-based opportunistic routing protocol for mobile UWSNs. Secondly and most importantly, GEDAR innovates in leveraging the depth adjustment capability of mobile underwater sensor nodes for handling with the communication void region problem.

- **An analytical framework to study the joint design of opportunistic routing and duty-cycling protocols.** This contribution consists in proposing an

analytical framework to study the "collision" of opportunistic routing and duty-cycling for energy efficient and reliable data collection in mobile UWSNs. We first propose a novel version, for the scenario of opportunistic routing, of the following three approaches used to design duty-cycling protocols: naive asynchronous duty cycle, low power listening (LPL) and low power probing (LPP). After that, we proposed an analytical framework to study the trade-offs, in terms of energy cost and data delivery reliability, and to obtain insights into the future design of protocols for UWSNs.

- **An analytical framework to study the on-the-fly adjustment of the sleep interval of joint duty-cycling and opportunistic routing.** This contribution consisting in devising an analytical framework to study the effects, in terms of energy consumption and data delivery, of the on-the-fly sleep interval adjustment. We formulate the sleep interval adjustment as an optimization problem towards the maximization of the minimum residual energy of the nodes using opportunistic routing in mobile UWSNs. Results showed that the sleep interval adjustment outperforms the use of a homogeneous and fixed sleep interval on the nodes.

- **Design guidelines for the design opportunistic routing in UWSNs.** This contribution discusses the benefits and challenges of opportunistic routing in underwater sensor networks and provides some guidelines for the further design of routing protocols.

1.4 Thesis Outline

The remainder of this thesis is organized as follows. Chapter 2 provides an introductory overview about underwater acoustic sensor networks. Chapter 3 presents an overview of opportunistic routing in UWSNs. Chapter 4 surveys the state-of-the-art about topology control in UWSNs. Chapter 5 introduces and defines several concepts used throughout of this work. Chapter 6 models the communication void region problem and void-handling techniques in underwater sensor networks. Chapter 7 proposes a novel geographic routing protocol and two topology control algorithms for non-mobile underwater sensor networks. Chapter 8 designs an anycast, geographic and opportunistic routing protocol, named of GEDAR, for mobile UWSNs. GEDAR implements a void-handling procedure, which is based on topology control through the depth adjustment of the void nodes. Chapter 9 devises an analytical framework to study the joint design of opportunistic routing and

duty cycling protocols in mobile underwater sensor networks. Chapter 10 proposes an analytical framework to investigate the effects of the sleep interval on the energy consumption of duty-cycled UWSNs, which employ opportunistic routing protocol at the network layer. Finally, Chapter 11 summarizes the contributions of this thesis and we present some research directions for future works.

Chapter 2

Underwater Acoustic Sensor Networks: Basic Concepts

In this Chapter, we discuss some aspects of underwater sensor networks (UWSNs) that were considered in this thesis. In Section 2.1, we present the motivation for the development and deployment of UWSNs. In Section 2.2, we present some considered UWSN architectures. In Section 2.3, we discuss the main challenges when designing routing protocols for UWSNs. In Section 2.4, we review the widely considered underwater acoustic channel model. Finally, we present our final remarks in Section 2.5.

2.1 Introduction

On April 20, 2010, the biggest oil spill in the history of the United States began after an explosion on the British Petroleum (BP)-owned Deepwater Horizon drilling platform in the Gulf of Mexico. It is estimated that, during the 87 days of the leak, more than 100 million gallons of crude oil were pumped into the ocean, affecting approximately 16,000 miles of coastline. The explosion killed 11 people and injured 17 others. There were over 8,000 animals dead only six months after the spill. The BP company estimated that total spill-related expenses would be approximately of $37.2 billion. However, these expenses over the years may be even higher.

Underwater wireless sensor networks (UWSNs) — sensor network formed by underwater sensor nodes with sensing, processing, storage and underwater wireless communication capabilities — will pave the way for a new era of underwater monitoring and actuation applications. These special kind of ad hoc [6, 7, 8] and sensing network [9]

have a great potential for preventing, monitoring and even helping to solve incidents resembling the aforementioned one, which may cause tragic environmental problems and heavy economic loss. UWSNs also have the potential to be part of the technological apparatus of oil and gas companies, for accurate and intelligent inspection of offshore platforms and deposits and incident and damage monitoring activities, especially nowadays as fossil fuel exploration is moving towards both deep-water and ultra-deep water offshore fields and arctic zones [10]. Finally, it is worth mentioning that UWSN has become a fast growing field. The envisioned landscape of applications that will be enabled by UWSNs has tremendous potential to change the current reality where no more than 5% of the volume of the oceans were explored.

In spite of its benefits, an underwater sensor network, if it is not well designed for the particular application, can incur impractical economic and environmental expenses. These can result from the high cost of ship missions for deployment, operation and maintenance. Ship missions can last several days, since sensors must be attached to docks, anchored buoys, seafloors, underwater autonomous vehicles (UAVs), low-power gliders, or underpowered drifters, depending on the desired network architecture [4]. Besides, underwater sensor nodes and autonomous vehicles (UAVs) are naturally expensive, due to their acoustic modem transceiver and the appropriate hardware for protecting the circuitry. They have high energy consumption due to the characteristics of underwater acoustic communication, which can stop the underwater monitoring and exploration missions prematurely.

Additionally, to enable large deployments of UWSNs, networking solutions toward efficient underwater data collection need to be investigated and proposed. In this context, the suitable, autonomous and on-the-fly organization of UWSN topology, through topology control algorithms, might mitigate undesired effects of the underwater wireless communication and, consequently, improve networking services and protocols. In the remaining sections of this Chapter we discuss some aspects of UWSNs that are related to the contributions made in this thesis.

2.2 Architectures of Underwater Sensor Networks

In the following, we describe some UWSN architectures that can be considered for underwater monitoring applications.

2.2.1 Communication-less architecture

In a not-so-distant past, underwater sensor nodes without communication capabilities were employed to gather data from oceans. In this kind of monitoring solution, static or mobile underwater sensor nodes are deployed and, after that, they start recording data from time to time, about the variables or events of interest. At the end of the mission, the nodes are then captured and the collected data are offloaded.

The main disadvantage of the aforementioned approach comes from the lack of underwater communication between the nodes. Therefore, during the monitoring mission, which can last for several months or even years, it is impossible to know the location of the nodes, what data they are collecting and even if they are working properly. Moreover, there is a high delay in obtaining the collected data, and, until the end of the monitoring mission, it is not possible to perform any on-line system reconfiguration and failure detection procedure [3].

2.2.2 Wired underwater sensor network architecture

This architecture is based on fixed sensor nodes moored at the sea floor. Data is delivered to the monitoring center through wires or optical fiber, as in the NEPTUNE project[1] (please refer to Figure 2.1a). Usually, this architecture is expensive and used for deployments of monitoring applications in a relatively small region of a marine habitat. Its main advantage is the possibility of collecting multimedia content, obtained from high-quality video cameras and microphones[2].

2.2.3 Satellite-based underwater sensor network architecture

In this approach, underwater nodes move vertically and offload the collected data through satellite links (see Figure 2.1b). This is the case of the RAFOS instruments[3] [11] used in the Argo project, which measures the temperature, salinity and velocity of the upper ocean [12].

The RAFOS instruments have an operational cycle where, most part of the time, the devices drift at different depths and collect data during their movements. Each instrument, at the end of its cycle, surfaces and transmits all stored data to ground stations, using radio-frequency links to orbiting satellites.

[1] http://www.neptunecanada.ca

[2] http://www.oceannetworks.ca/sights-sounds/live-video

[3] http://www.whoi.edu/instruments/viewInstrument.do?id=1061

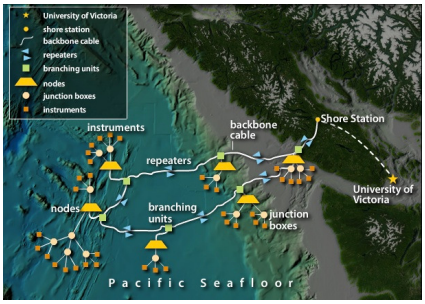

(a) The NEPTUNE Observatory

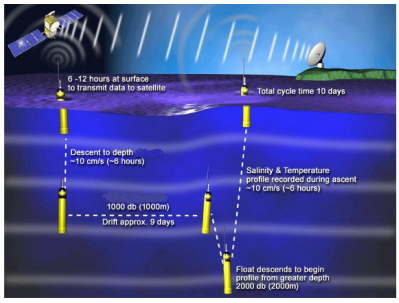

(b) Rafos float

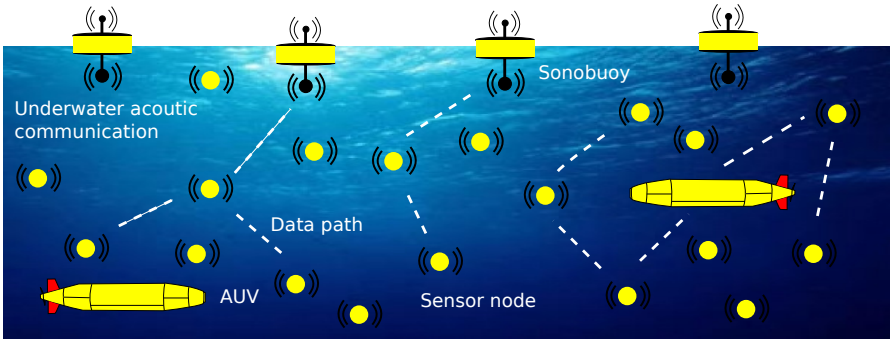

(c) SEA Swarm UWSN architecture

Figure 2.1: Example of underwater monitoring architectures

In comparison to the communication-less approach, there is no need to wait until the end of the monitoring mission to obtain the gathered data. However, there still exists a considerable delay corresponding to the duration of the nodes' operational cycle, i.e., the time between two consecutive ascent operations where the instrument surfaces (about a 10-day interval).

2.2.4 SEA Swarm underwater sensor network architecture

Lee et al. [13] described the Sensor Equipped Aquatic (SEA) swarm architecture as a sensor cloud that drifts with water currents. In fact, the advances in underwater sensor, vehicular and wireless communication technologies have enabled the scenario of an underwater sensor cloud, as shown in Figure 2.1c.

In this architecture, a UWSN is comprised of sensor nodes and surface sonobuoys (sinks). Underwater sensor nodes are equipped with acoustic transceivers that allow them to wirelessly communicate with each other. Sonobuoys are equipped with both radio-frequency (RF) and acoustic transceivers, in which they use acoustic communication to

send commands and collect data from underwater sensor nodes and RF communication to deliver the collected data to a monitoring center through satellite communication, for instance. Due to the underwater wireless communication capability, in this architecture is possible to achieve real-time data collection, on-line system reconfiguration, failure detection and fault-tolerant applications.

In the SEA Swarm network architecture, due to the big challenges concerning the efficient deployment of underwater nodes [14], topology control will be essential for improving connectivity and coverage, as well as to deal with the drawbacks of the underwater acoustic channel and improve the network performance. For instance, topology control through the controlled depth adjustment of underwater nodes or mobility of autonomous underwater vehicles (UAV) can be performed to move nodes for specific locations to interconnect network partitions.

2.3 Routing

In general, data routing in wireless ad hoc networks is severely impaired by the network topology [15, 16, 17]. In UWSNs, the design of routing protocols is still more challenging, due to the spatiotemporal varying nature of the acoustic link quality that unpredictably changes the network topology. In this scenario, geographic (position or depth-based) routing has been preferable for UWSNs [18, 19, 13, 20, 21, 22, 23, 24].

Geographic routing does not require the establishment and maintenance of end-to-end routing paths from each sender node to the destinations, as happens in proactive and reactive routing paradigms. In this approach, a forwarder node, aware of its geographical location and the location of its neighboring nodes, transmits a message to a locally optimal next-hop node closest to the destination (greedy forwarding strategy). Therefore, there is no need of excessive and systematic flooding for route discovery and maintenance, which would diminish the network performance, due to the overhead and message collisions, and result in a high waste of energy.

Geographic routing entails one-hop neighboring information to forward data messages. However, this routing approach is still impaired by the unpredictable and dynamic changes in the UWSN topology. For instance, based on the location and interconnection of the nodes, communication void regions may appear in the network. Communication voids happen whenever a sender node (void node) is located at a maximum local, i.e., it does not have a neighboring node in closer proximity to the destination. When a data message reaches such void nodes, it should be routed through an alternative path or is

discarded.

Often, void-handling procedures have been employed by geographic routing protocols in UWSNs. A void-handling procedure is used for routing data messages from void nodes to a node that can resume the greedy forwarding strategy. Since data messages are routed from void nodes, instead of being discarded, void-handling procedures avoid the degradation of the network performance and application.

In this context, topology control might have a fundamental role either to organize the network topology to eliminate void regions [22, 25] or to adjust it to recover from void regions [26]. Power control-based void-handling procedures, for instance, can be used to increase the communication range at void nodes aiming to find a new neighboring node that can resume the greedy forwarding strategy. Moreover, topology control-based void-handling procedures can move void or neighboring sensor nodes to new depths to eliminate void regions or UAV to collect data from void nodes.

2.4 Underwater Acoustic Channel

In the following, we review the underwater acoustic channel model, frequently employed in mathematical frameworks and simulation-based solutions for UWSNs. The idea is to highlight the communication challenges that diminish the performance of UWSNs, which might be addressed using a topology control.

The passive sonar equation characterizes the signal-to-noise (SNR) of an emitted underwater signal at the receiver as [27]:

$$SNR = SL - A(d, f) - N(f) + DI \geq SINR_{\text{th}}, \tag{2.1}$$

where SL is the source level, $A(d, f)$ is the transmission loss, $N(f)$ is the noise level, DI is the directivity index, and $SINR_{\text{th}}$ is a decoding threshold. In Eq. 2.1, all quantities are in dB re μ Pa.

The Urick's model [28] has been widely used to capture the underwater acoustic signal attenuation. More realistic models to predict acoustic attenuation can be found in literature, such as Rogers model and Bellhop software, but the Urick model is simple to evaluate and can provide a useful approximation whenever their parameters are properly chosen. This model is based on empirical equations for acoustic power spreading and absorption loss.

The path loss describes the attenuation of a single, unobstructed propagation path, over a distance d for a signal of frequency f, due to a large scale fading. The path loss

is mainly caused by the *geometrical spreading* and *signal attenuation* associated with frequency dependent absorption. It is calculated as:

$$10 \log A(d, f)/A_0 = k \times 10 \log d + d \times 10 \log a(f)^d, \tag{2.2}$$

where k is the spreading factor and $a(f)$ is the absorption coefficient. The absorption coefficient $a(f)$, in dB/km for f in kHz, is described by the Thorp's formula [29], given by:

$$10 \log a(f) = \frac{0.11 \times f^2}{1 + f^2} + \frac{44 \times f^2}{4100 + f^2} + 2.75 \times 10^{-4} f^2 + 0.003. \tag{2.3}$$

The geometry of propagation is described using the spreading factor k. Its commonly used values are $k = 2$ for spherical spreading, $k = 1$ for cylindrical spreading, and, for a practical scenario, k is given as 1.5.

The noise that affects the underwater acoustic channel is originated from *ambient* and *site-specific* sources. It can be modeled using four sources [30]: turbulence (N_t), shipping (N_s), waves (N_w), and thermal noise (N_{th}). The overall ambient noise is $N(f) = N_t(f) + N_s(f) + N_w(f) + N_{\text{th}}(f)$. For frequency f in kHz, shipping s ranging between 0 and 1 (light to dense) and wind in m/s, the four noise components in dB re μ Pa per Hz are given by:

$$\begin{aligned} 10 \log N_t(f) &= 17 - 30 \log f \\ 10 \log N_s(f) &= 40 + 20(s - 0.5) + 26 \log f - 60 \log(f + 0.03) \\ 10 \log N_w(f) &= 50 + 7.5 w^{1/2} + 20 \log f - 40 \log(f + 0.4) \\ 10 \log N_{th}(f) &= -15 + 20 \log f. \end{aligned} \tag{2.4}$$

It is worth mentioning that noise decreases with frequency and turbulence, shipping activities, breaking waves and thermals are the primary sources of ambient noise.

In Eq. 2.1, the source level (SL) is also related to the transmitted signal intensity I_t (μPa) at 1 m from the source, expressed as

$$SL = 10 \log \frac{I_t}{1 \mu Pa}. \tag{2.5}$$

Solving Eq. 2.5, the transmitted signal intensity is given by Eq. 2.6, where the constant converts μ Pa to W/m^2.

$$I_t = 10^{SL/10} \times 0.67 \times 10^{-18}. \tag{2.6}$$

Finally, the transmission power P_t in Watts needed to achieve intensity I_t at a distance of 1 m from the source in direction to the receiver is

$$P_t = 2\pi \times H \times I_t, \tag{2.7}$$

where H is the water depth in meters.

Finally, it is important to mention that the bandwidth of the underwater acoustic channel depends on the transmission power, radio frequency and transmission distance. The $1/A(l, f)N(f)$ factor is a function of the distance and frequency.

In summary, the aforementioned characteristics severely degrade the link reliability. Due to underwater acoustic channel characteristics, the link between neighbors can perform poorly or can even be down during some time. Temporary lost connectivity can be experienced because of shadow zones. As main consequence, a possible increasing number of message retransmissions should occur to try to deliver it. This will increase message collisions, delay and energy consumption.

2.5 Concluding Remarks

This Chapter presented an introductory discussion about the potentials and challenges of underwater sensor networks. We discussed the motivation for the research and development of UWSNs. Moreover, we highlighted the main challenges faced when designing routing protocols for UWSNs. We reviewed the underwater acoustic channel model and we pointed out how topology control can be used to mitigate the drawbacks of the acoustic channel and improve the performance of UWSN applications.

Chapter 3

Opportunistic Routing in UWSNs: Overview and Design Guidelines

The unique characteristics of the underwater acoustic channel have imposing many challenges that limit the utilization of underwater sensor networks. In this context, opportunistic routing has greater potential for mitigating drawbacks from underwater acoustic communication and improving network performance.

In this Chapter, we discuss the two main building blocks for the design of opportunistic routing protocols for underwater sensor networks: candidate set selection and candidate coordination procedures (Section 3.2). In Section 3.3, we propose classifying candidate set selection procedures into sender-side, receiver-side and hybrid approaches; and, in Section 3.4, candidate coordination procedures into timer-based and control packet-based approaches. Finally, we present the final remarks in Section 3.5.

3.1 Introduction

Opportunistic routing (OR) [31] has been shown a promising paradigm to design routing protocols for UWSNs [32]. In traditional multihop routing, a packet is transmitted to a specific next-hop node using a unicast communication. If the next-hop node does not receive it, the packet should be retransmitted. After a finite number of unsuccessful retransmissions, the packet is discarded. In OR, a set of candidate nodes is involved for advancing the packet toward the destination. Accordingly, a packet is sent leveraging the broadcast nature of the wireless transmission. The candidates that receive the packet will continue, coordinately, forwarding it in a prioritized way, such that a low priority

node transmits the packet if none of the high priority nodes have done so. Therefore, a packet is retransmitted only if none of the candidates have received it.

Opportunistic routing paradigm has benefits and drawbacks that must be considered when it is used to design routing protocols for underwater networks. OR increases packet delivery and decreases the number of packet collisions, since the probability that at least one candidate would correctly receive the packet is high compared to the traditional unicast routing. However, the packet delivery end-to-end delay is high due to the nodes' transmission coordination. Yet, the harsh underwater communication environment can result in poor transmission nodes' coordination, culminating in redundant packet transmissions, increasing packet collisions, and delay and energy consumption. Moreover, the assignment of the same high priority for some candidates may deplete their energy sooner, leading to partitions in the network.

3.2 The Components of Opportunistic Routing

Opportunistic routing protocols are composed of two main building blocks:

- *Candidate set selection*: This procedure is responsible for selecting a subset of neighboring nodes to continue forwarding the packet towards the destination. In this work, we categorize candidate set selection procedures in sender-side based, receiver-side based and hybrid approaches.

- *Candidate set coordination*: This procedure is responsible for coordinating the packet forwarding operation between the next-hop candidate nodes. Moreover, this procedure is also responsible for determining suppression of the redundant packet transmissions of low priority nodes. In this work, we categorize the candidate set coordination in timer-based and control packet-based approaches.

Figure 3.1 depicts the OR building blocks and the categorization we have proposed to better describe some design principles of each approach. If we use an OR protocol in underwater sensor networks, we must execute the following steps when a node has a data packet to deliver to a surface sonobuoy. First, the candidate set selection procedure determines a subset of the neighboring nodes (candidate set) to forward the packet. Second, either the candidate nodes' ID or other indicative information is included in the packet header to be used by the candidate nodes. After that, the current forwarder node broadcasts the packet. Candidate nodes that have successfully received the packet

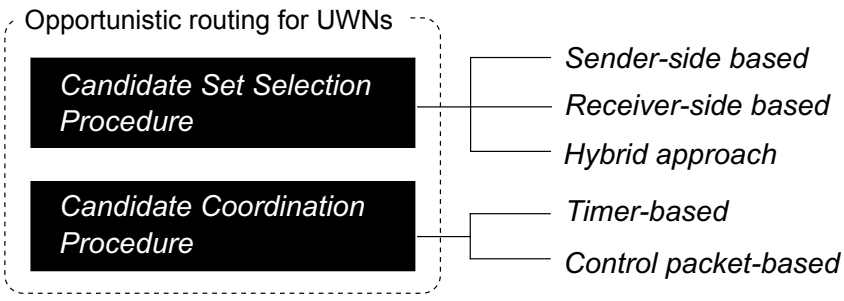

Figure 3.1: Opportunistic routing building blocks for underwater sensor networks

initiate the forwarding procedure according to their priority levels. Finally, low priority candidate nodes suppress the packet transmission when it is sent by a high priority node.

3.3 Candidate Set Selection Procedures

The candidate set selection procedure is responsible for choosing a subset of the neighboring nodes to continue forwarding the packet. A fitness function or a single metric, such as the expected distance progress or expected transmission count, is used to determine the suitability of each neighbor. The neighbors are sorted according to their suitability, and are then included in the next-hop candidate set, which eventually becomes subject to restriction, such as a limited number of candidates or a one-hop candidate set delay.

In terrestrial wireless networks, it is common to have candidate set selection procedures that consider the whole network topology, or a recurrence function to determine the fitness of each neighbor. For instance, Li et al. [33] analyze the candidate set selection problem, developing a dynamic programming algorithm to determine an optimal solution that will minimize the expected number of transmissions. A similar strategy seems inappropriate for an underwater sensor network, due to the high cost of disseminating the topology information to all the nodes, given the unique characteristics of the underwater acoustic channel and node mobility.

We concentrate only on local procedures for the candidate set selection. In those approaches, the next-hop candidate set is determined by each neighboring node or by the current forwarder node with k-hop neighborhood information, for a small value of k (*e.g.*, $k = 1$ or $k = 2$). In a broader manner, candidate set selection procedures can be classified in *sender-side*, *receiver-side* and *hybrid* procedures. In the following, we describe each category, and present some proposed OR protocols in underwater sensor networks.

3.3.1 Sender-side procedures

In sender-side candidate set selection procedures, the current forwarding node is responsible for selecting the next-hop forwarder candidate set. It selects the forwarder nodes based on neighborhood information. Usually, nodes use periodic beaconing to acquire neighborhood information. Based on the neighborhood information and on the next-hop selection metric or function, the current forwarder node determines which neighbors are enabled to continue forwarding the packet towards the destination. After that, the enabled neighbors are sorted and included into the next-hop candidate set, according to their priorities. Finally, the unique ID of the chosen nodes is included in the packet header. Frequently, a bloom filter or membership checking data structures are used to avoid long packet headers, which would increase the packet error rate.

With approaches that fall into this category, as the neighborhood is known in advance, more complex and multi-objective fitness functions, which consider application and underwater acoustic channel characteristics, can be used to select the next-hop candidate set. For instance, buffer and distance information of the neighbors can be used by the next-hop candidate set selection procedure in a real-time application (*e.g.*, oil spill monitoring) to ensure an acceptable packet reception ratio with a limited delay. Moreover, only nodes close enough to hear the transmission of each other can be selected to belong to the next-hop candidate set, in order to mitigate the problem of hidden terminals. The main drawback of this approach stems from the need to keep updated neighborhood information at the nodes, considering the node mobility caused by ocean currents. The use of beacon messages can overload the channel and increase packet collisions, because of the slow propagation through acoustic channels.

Hydrocast [13] routing protocol is an example of underwater OR protocol that implements a sender-side based candidate set selection procedure. Its candidate set selection procedure employs neighbors with a positive packet advancement, *i.e.*,closer to the sea surface. The protocol first calculates the fitness of each node using normalized advancement (NADV). Second, the neighbor with the highest NADV and all nodes distant at most βR of it, are chosen to form a cluster. Those steps are repeated until no neighbor remains. For instance, in Figure 3.2a, *clusters 1, 2* and *3* are determined after the aforementioned step. Each cluster is then expanded by including all nodes with a shorter distance to nodes already in the cluster than the communication range. In the example of Figure 3.2b, Node n_2 is included into *cluster 1*, and Nodes n_1 and n_3 into *cluster 2*. Finally, the cluster with the greatest expected progress (a normalized sum

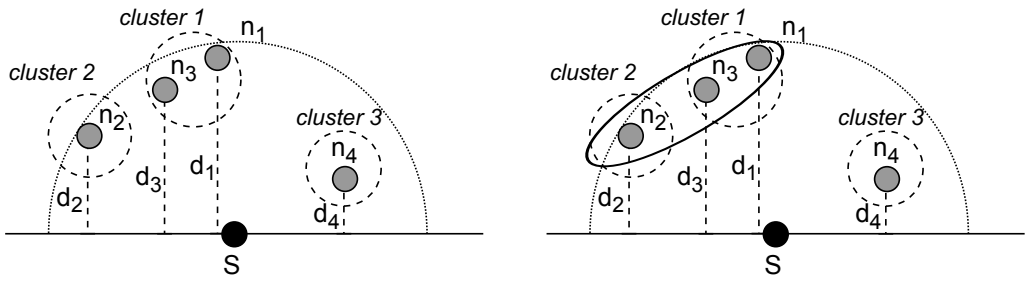

(a) Part 1 (b) Part 2

Figure 3.2: Hydrocast candidate set selection procedure

of advancements made by the nodes) is selected and the IDs of its nodes is included in the packet header. With minor variations, the aforementioned next-hop candidate set selection procedure is used by many other OR protocols in underwater sensor networks, such as in GEDAR [34]. A main disadvantage of Hydrocast is that it employs a simplified underwater channel model to calculate the NADV, which may not reflect the reality in some scenarios.

3.3.2 Receiver-side procedures

In receiver-side candidate set selection procedures, the neighboring nodes are responsible for determining whether they are included in the next-hop forwarder candidate set of a received packet. The current forwarder includes some control information (*e.g.*,its depth or distance to the destination) in the packet header, and then, broadcasts it. Each receiver node, from the information contained into the packet, determines locally whether it is a next-hop candidate node, according to the rule adopted by the protocol. If the neighboring node is a candidate, it determines its forwarding priority and forwards the packet if and when it should do so.

The receiver-side based next-hop candidate set selection procedures are simple and scalable, requiring no neighborhood information. Because of this, energy conservation and an increased underwater acoustic channel utilization can be achieved. Moreover, these procedures are indicated for high traffic load applications, such as pollution monitoring, since there are no control packets competing for access to the acoustic channel and colliding with the data packets. However, the candidate coordination and redundant packet suppression can be inefficient, leading to a high number of duplicated packet transmissions, which unnecessarily consume energy and do not provide any innovative information to the destination, being discarded when it is reached.

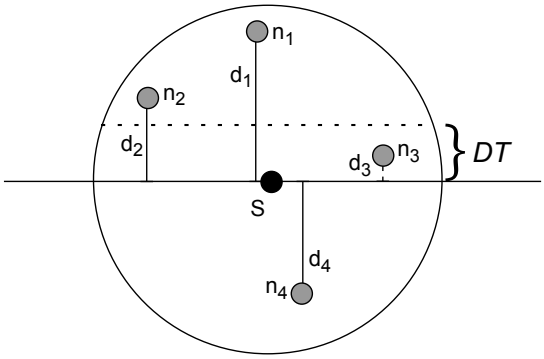

Figure 3.3: DBR candidate set selection procedure

VBF [18] and DBR [35] routing protocols are examples of underwater OR protocols that implement a receiver-side based candidate set selection procedure. In the DBR routing protocol, the current forwarder node includes its depth information in the packet and broadcasts it. Upon receiving a packet, each neighboring node compares its depth with the sender's depth. The neighbor is a next-hop candidate if it is closer to the sea surface than the current forwarder node, and this depth difference is higher than a DT depth threshold. For instance, considering the current forwarder node S in Figure 3.3, Nodes n_3 and n_4 will discard the received packet because n_3 and n_4 do not have a depth difference higher than DT, and do not advance the packet towards the surface, respectively. Nodes n_1 and n_2 are candidates for forwarding the packet. In this example, Node n_1 is the high priority node. Node n_2 only forwards the packet if n_1 fails to do so. In the VBF routing protocol, packets are routed along a virtual pipe (please refer to Figure 3.4a). The location information of the sender and the destination are included into the packet header to be used for the purpose of next-hop candidate selection. When a node receives a packet, it determines whether it is inside the routing pipe by calculating its distance to the vector formed by the sender and destination location information. If its distance to the vector is smaller than W, the node is a next-hop candidate. Otherwise, the node discards the packet. VBF and DBR protocols suffer from similar drawbacks. Networks with higher densities are susceptible to a large number of duplicated transmissions. This is because both protocols do not employ any type of mechanism for restricting the number of candidates in the set, and do not address the hidden terminal problem. In low-density scenarios, data delivery will be compromised, as VBF and DBR do not employ a communication void region mechanism.

In the VBF routing protocol [18], packets are routed along a virtual pipe (please refer to Figure 3.4a). The location information of the sender and the destination are included

into the packet header to be used to the next-hop candidate selection purpose. When a node receives a packet, it determines whether it is inside the routing pipe by calculating its distance to the vector formed by the sender and destination location information. If its distance to the vector is smaller than W, the node is a next-hop candidate. Otherwise, the node discards the packet.

3.3.3 Hybrid procedures

In hybrid candidate set selection procedures, the next-hop forwarder candidate set is determined by the current forwarder node and its neighbors, in two distributed steps. When a node has a packet to transmit, it informs its situation and requests information (*e.g.*, battery level or link reliability) from its neighborhood through a broadcast of a control packet. Neighbor nodes meeting the criteria (*e.g.*, positive progress to the destination) will respond to the current forwarder node with the requested information. In the end, the current forwarder node selects the next-hop candidate set based on received packets.

In the solutions belonging to this category, the neighborhood condition is known on demand, in contrast to the procedures based on the sender-side based candidate set selection, where beaconing happens periodically. Moreover, short packets to the next-hop candidate selection and coordination are less likely to be lost, resulting in an improvement in candidate coordination performance. This approach is highly suitable for low traffic load monitoring applications, such as periodic ocean temperature or salinity monitoring applications. However, this two-way procedure can increase end-to-end delay, due to the slow propagation through underwater acoustic channels.

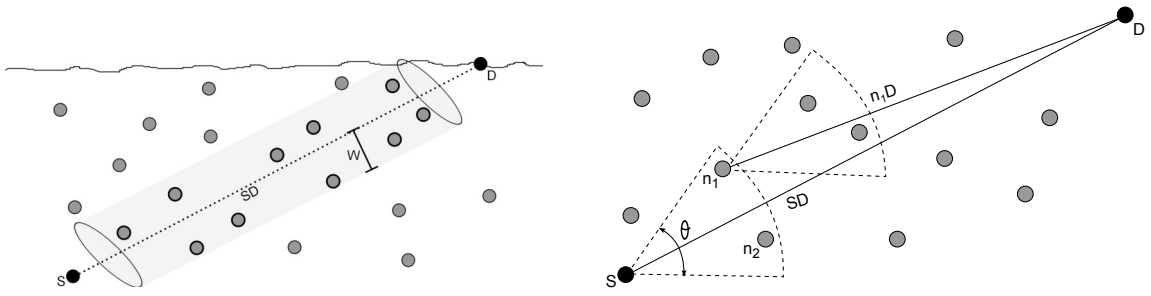

(a) VBF candidate set selection procedure (b) FBR candidate set selection procedure

Figure 3.4: Candidate set selection procedures

FBR [36] and CARP [37] are examples of underwater routing protocols that imple-

ment a hybrid candidate set selection procedure. It is worth noting that these protocols are not opportunistic in the sense that only one neighbor node is selected as next-hop forwarder, *i.e.*, only one candidate as the next hop. However, we present them as an example of a hybrid solution, since they can be easily extended to incorporate the opportunistic routing nature by determining a sorted list of next-hop candidate nodes. In both routing protocols, when a node has a packet to send, it broadcasts a control packet to inform its neighbors and to obtain additional information. Each neighbor meeting the desired requirement to be a forwarder candidate replies to the current forwarder node. The desired requirement is to lie within a cone of angle $\pm\theta/2$ emanating from the transmitter towards the destination in FBR (*e.g.*, Nodes n_1 and n_2 in Figure 3.4b) and having a hop count to the destination less than the source node in CARP. The next-hop candidate is selected among the neighbors that replied to the sender request, based on their load or proximity to the destination, and a link quality goodness function in FBR and CARP, respectively.

3.4 Candidate Coordination Procedures

The transmission coordination of the next-hop forwarder candidate nodes is a crucial component of OR design protocol. With the inclusion of many nodes in the candidate set, link reliability improves and the average number of transmissions required to deliver a packet is reduced. However, the candidates must forward the packet in a coordinated manner, such that a lower priority node will transmit the packet only if the higher priority nodes fail to do so. This will avoid transmission of unnecessary and redundant packets, which will consume energy and fail to provide any additional information, being discarded at the destination.

The coordination of candidate transmission is a more difficult problem in underwater networks than in terrestrial networks. While a candidate set with only two or three nodes may be sufficient for obtaining a high packet delivery probability in terrestrial radio frequency-based wireless networks, in underwater networks this number should be greater due to high signal attenuation and shadow zones.

In this Chapter, we categorize candidate coordination procedures based on *timer-based coordination* and *control packet-based coordination*. We anticipate that current state-of-the-art OR protocols have mostly used timer-based procedures for candidate coordination. This is due to its simplicity and the absence of extra packet transmissions, which might overload the underwater acoustic channel and increase energy consumption.

Table 3.1: Holding time function of some timer-based candidate coordination procedures

OR protocol	**Holding time function**
VBF [18]	$T_{h_{VBF}} = \sqrt{\alpha} \times T_{delay} + \frac{R-d}{v}$
DBR [35]	$T_{h_{DBR}} = \frac{2\tau}{\delta}.(R-d)$
Hydrocast [13]	$T_{h_{Hydrocast}} = \alpha(R-d)$

In the following we discuss the advantages and disadvantages of each category.

3.4.1 Timer-based candidate coordination

Upon receiving a packet in the timer-based coordination procedure, each candidate node holds it for a period of time or a number of transmission slots, according to its priority. The candidate will suppress its transmission if it receives an indication during its waiting period that the packet was forwarded by a high priority node. Usually, this indication is the reception of the same packet, now coming from a high priority node or an acknowledgment (ACK) packet. Otherwise, the node forwards the packet when its holding time expires.

The main advantage of this approach is the absence of extra control packets, which can further degrade network performance. However, as no control packet is used to coordinate and inform low priority nodes, duplicated date packet transmissions can occur when the nodes are far from one another and cannot hear transmissions. In this case, duplicated data packet transmissions have a more negative impact on network performance and energy consumption than the use of control packets, due to their differences in size.

Hydrocast [13], VBF [18] and DBR [35] routing protocols are examples of OR protocols for underwater sensor networks which employ timer-based candidate coordination procedures. Their packet holding time function is presented in Table 3.1, where R is the node's communication range and d is the packet advancement made by the node. The VBF holding time function has two terms. The first term determines holding time based on the node's desirability factor (in other words, its priority), and a pre-defined maximum delay, such that it waits less time when the nodes' priority is higher. The second term computes the remaining time needed for all the nodes in the current forwarder's communication range to receive the packet. DBR and Hydrocast implement a linear function of a receiver node, such that the closer the node approaches the sea surface, the less time it waits. The difference between their holding time function is the manner in

which the constant factor is determined. Since the node in DBR does not know about the other candidates, the constant factor considers the packet propagation time in the worst scenario possible, in which the highest and lowest priority nodes are distant δ m from each other. In Hydrocast, this packet propagation time can be computed at each packet transmission, since the next-hop candidate nodes and their priorities are known by the current forwarder node.

3.4.2 Control packet-based candidate coordination

Using control packet-based candidate coordination procedure, a candidate node upon receiving a packet will respond with a short control packet, if high priority candidates have failed to do so. The control packet transmission notifies the current forwarder node of the successful receipt of the packet, and informs the other low candidate nodes that they should suppress their transmissions. Usually, control packet-based candidate coordination approaches designed for terrestrial wireless networks fall into one of the categories below [31]:

- *ACK-based*: The current forwarder node sends the data packet, and the candidates respond with an acknowledgment packet according to their priorities;
- *RTS/CTS-based*: The current forwarder node sends an RTS packet, the candidates respond with a CTS packet according to priority, and finally, the data packet is sent to the candidate that replied to the RTS transmission.

The abovementioned design principles have severe drawbacks when applied to underwater sensor network scenarios. ACK-based approaches require all candidates close enough to the transmission to be heard by others [31]. Otherwise, duplicated packet transmissions will take place and degrade network performance. RTS/CTS-based candidate coordination might perform poorly in underwater sensor network scenarios, since a high priority node may successfully receive a short RTS packet, become the next-hop forwarder responding with the CTS packet, and eventually become unable to receive the data packet, as it is longer than RTS and its delivery probability is significantly lower.

Currently, to the best of our knowledge, there is no opportunistic routing protocol designed for underwater sensor networks, which exclusively use control packet-based candidate coordination. Hydrocast routing protocol [13], which employs a timer-based candidate coordination, uses an ACK packet transmission before the candidate forwards the data packet; this functions as an alert reinforcement to inform low priority nodes,

since it is more probable that the neighbor will receive the short ACK packet than the high priority node data packet transmission.

3.5 Concluding Remarks

This Chapter presented detailed design guidelines for opportunistic routing protocols in underwater networks. We described a general framework of OR for UWSNs in particular, and we have investigated the design of their candidate set selection and coordination procedures. We divided candidate set selection procedures into sender-side based, receiver-side based and hybrid-based. We have categorized the candidate coordination procedures into timer-based and control packet-based approaches. For each category of candidate set selection and coordination procedures, we discussed its principles, advantages and disadvantages, relating them to the underwater acoustic communication characteristics, since these characteristics (together with network scenario and application) guide the design of opportunistic routing protocols. Finally, we put into perspective the advantages and disadvantages of the candidate set selection and coordination categories combined during the design of OR protocols for underwater sensor networks.

Chapter 4

Topology Control: A New Challenge for Underwater Networks

Topology control has been studied in wireless ad hoc and sensor networks, since the early years of packet radio networks. Due to its benefits, topology control recently started to be investigated in the context of underwater sensor networks. However, the vast knowledge acquired so far in this topic cannot be directly applied in UWSNs. In this context, research efforts have been devoted to investigating the potentials and shortcoming of topology control in UWSNs, and to establish the principles for further protocol designs in this network.

In this Chapter, we survey the state-of-the-art of topology control in UWSNs. Based on our literature review, in Section 4.2, we classify the current topology control algorithms for UWSNs in power control (Section 4.3), wireless interface management (Section 4.4), and mobility assisted-based (Section 4.5) protocols. Finally, in Section 4.6, we present the final remarks of this Chapter.

4.1 Introduction

The network topology dictates how the nodes interconnect each other. It directly impacts on the performance of networking protocols. In UWSNs, the topology changes frequently because of involuntary mobility of underwater nodes and time-varying link quality effects. Depending on the UWSN architecture and the environment where it is deployed in, underwater sensor nodes (*e.g.*, free-floating nodes) will move influenced the effect of meandering sub-surface currents and vortices [38]. Consequently, the interconnection

between the nodes will change along the time. In fact, depending on the network density, even slow-moving coastal current will be enough to significantly change the network topology, diminish the connectivity and make the sensor network unattainable after a few hours.

Time-varying link quality is the second critical factor impacting the topology of UWSNs. The temperature of the water can change the way of sound is refracted; the morphology of the sea bottom and other environmental factors also impact on acoustic signal propagation [39]. In fact, experimental measurements showed that strength of received signal transmitted using underwater acoustic channel varies along the time due to the channel fading [40]. Moreover, temporary losses of connectivity can be experienced due to shadow zones.

Topology control will be fundamental in the hash scenario of UWSNs. The conscious and purposeful topology control through the adjustment of several network parameters can stabilize and smooth the undesirable changes in the network topology. In this Chapter, we highlight the potential of topology control for improving the performance of UWSNs, survey the current state-of-the-art of topology control and present an in-depth discussion of the advantages and disadvantages of solutions already proposed for UWSNs.

4.2 The Proposed Classification Methodology

Topology control algorithms might be classified based on different perspectives. For example, topology control algorithms could be classified in:

1. **global** and **local**, according to the considered information about the topology. In the former, the overall network topology information is considered for the topology control. In the latter, the local information of the topology, *i.e.*, a k-hop ($k = 1$ or $k = 2$) neighborhood information, is considered for the topology control.

2. **centralized** or **distributed**, according to the nature of the solution. In the former, a unique node or entity is responsible for computing the new network topology. In the latter, a set or each node is responsible for making decisions to organize the network topology.

3. **proactive** or **reactive**, whether it runs periodically or as a consequence of some topological event in the network (*e.g.*, nodes' failures).

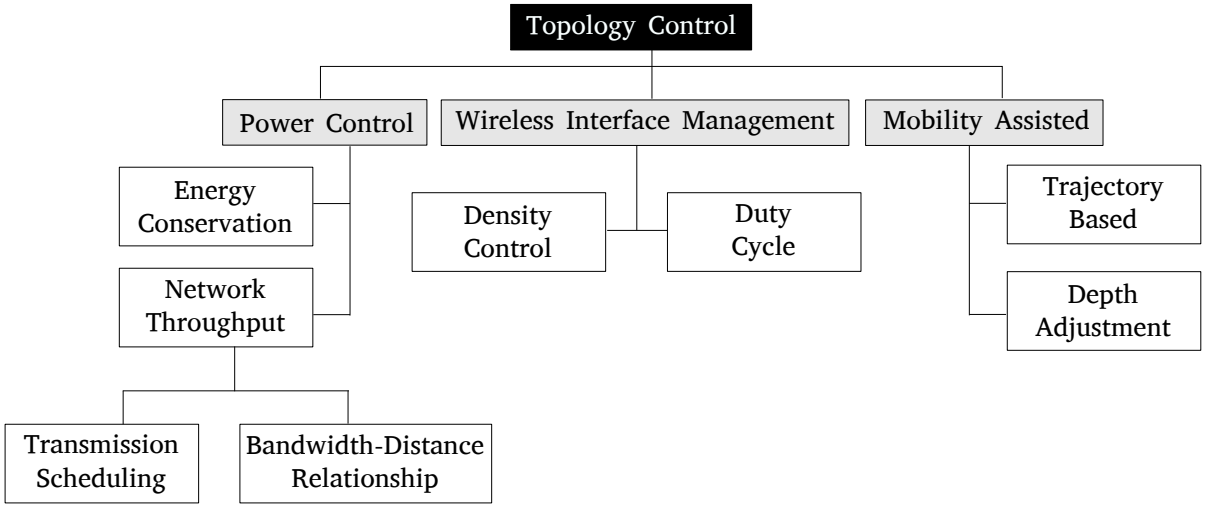

Figure 4.1: Taxonomy of topology control in UWSNs

4. **homogeneous** or **non-homogenegous** [41]. It is based on the resulting communication range at the nodes. In the former, a unique communication range value is determined for all the nodes. In the latter, the topology control algorithm will assign the appropriate communication range r_c to each node. This value is determined from range between $r_{\min} \leq r_c \leq r_{\max}$; or

5. **coverage–, connectivity–,** or **energy–oriented**, according to the main goal of the topology control algorithm. In the literature, it has been observed that several of the topology control algorithms are strictly related with a desired goal.

In this thesis, however, we adopt the following criteria to classify topology control protocols in UWSNs: *the main methodology they have used to conscious and purposeful change the topology of the network*. Following this criteria, we believe the proposed classification might exhaustively cover topology control algorithms designed for UWSNs. Therein, we classify topology control algorithms as power control-, wireless interface mode management-, and mobility assisted-based solutions. This classification is broader enough to encompass the future design of topology control protocols for envisioned software defined networking-based UWSN and heterogeneous UWSNs. This is because these three approaches are the way to create and/or remove acoustic links in the network topology, independently of the characteristics of the considered scenario. Finally, it is important to mention that the desired goal when controlling the topology might be achieved from the use of each topology control category. For instance, energy efficiency can be

Table 4.1: Power control-based topology control approaches

Sub-category	**Basic solution**	**Challenges**
Energy conservation	Assigns a minimum transmission power to each node to ensure network connectivity.	Complex and impractical channel models; Spatial and time-varying link quality; Shadow zones; Multipath propagation; Uncertainty communication range value.
Network throughput	Assigns the optimal transmission power according to the distance, aiming to increase bandwidth or the proper communication range to increase spatial reuse.	

achieved through the proper power control of the nodes [42], by means of the wireless interface management through duty-cycling in UWSNs [43], as well as using mobility assisted topology control through the movement of some nodes to new depths [25].

4.3 Power Control–based Topology Control

Transmission power control-based topology control algorithms assign the proper transmission power level to each node, with the objective of improving some network performance metric (*e.g.*, energy consumption, throughput, and delay). The changes in the network topology happen as nodes create and drop communication links by increasing and reducing their transmission power. In general, these algorithms are proposed for reducing energy consumption. However, in underwater acoustic sensor networks, this approach has been mainly proposed to mitigate the drawbacks of underwater acoustic communication and improve network performance. In the following, we survey power control-based topology control proposals, whose main goals are as energy conservation and network throughput, as summarized in Table 4.1.

4.3.1 Energy conservation

Mostly, power control-based topology control algorithms are designed for energy conservation. This is due to the fact that UWSNs are battery operated and ship missions to replace of batteries are expensive and can last for several days.

In this regard, it was shown that short-range multi-hop communication is preferable for UWSNs, in spite of the possibility of using long-range communication links of the order of several kilometers [44]. Casari and Harris [45] and Casari et al. [46] investigated

the benefits, in terms of energy conservation, of using short-range multi-hop UWSN communication instead of direct communication to sink nodes. Porto and Stojanovic [42] concluded that the optimal transmission power that should be assigned to each node is the minimum value still guaranteeing connectivity between each node and the sink.

In fact, the use is short-range multi-hop communication is desired in energy-constrained wireless ad hoc networks. This is because radio transceivers are the main source of energy consumption [47] and the energy required for message transmission is proportional to the distance between the communicating pair nodes [48]. However, the suitable transmission power assignment is challenging and faces the following general trade-off. The use of long-range communication links improve network connectivity and reduce end-to-end delay as messages take fewer hops to be delivered. Disadvantageously, high message collision rate might happen since interference zones are larger. Conversely, short-range communication links increase throughput due to the increment of the spatial reuse, but they can lead to high end-to-end delay.

In a scenario of concentric layered UWSN architecture, Al-Bzoor et al. [49] proposed the APCR routing protocol, which selects the appropriate transmission power at the nodes, considering the trade-off between energy consumption and network connectivity. For the routing purpose, each node is assigned to one of the concentric layers, determined from multiple transmission power levels of the sink node. To do so, the sink node transmits Interest messages using different transmission power level. Accordingly, sensor nodes able to receive messages from the sink node transmitted at the lowest power level are assigned to the layer 1. Nodes not assigned to the layer 1 that received the Interest message transmitted with power level 2 are assigned to the layer 2, and so on. Data routing is then performed from nodes at high layers to low layers, toward to the sink. The transmission power adjustment at the nodes is done as follows. Initially, each node sets the highest transmission power level. Then, they reduce the transmission power to the level enough ensuring communication range with the closest neighboring node located in the next layer toward to the sink.

Zhou and Cui [50] and Xu et al. [51] proposed the multi-path power-control transmission (MTP) and layered multi-path power control (LMPC) protocols, respectively. In the multi-path routing setting considered in both proposals, redundant data messages are transmitted along different paths. At the surface sink nodes, the original data message can be recovered from the combination of several (corrupted) received copies. During the data routing, both approaches select the optimal energy cost (*i.e.*, transmission power) at the intermediate nodes in the routing paths. In their studies, the authors formulated the

transmission power selection as an optimization problem with the goal of minimizing the energy consumption. The minimum transmission power level at each intermediate node is then determined, subject to a message error rate below an established threshold. The MTP and LMPC protocols differ in the procedures used to determine the multi-paths and the layered network architecture considered in the LMPC protocol.

Kim et al. [52] proposed a transmission power control allocation solution taking into consideration sea surface information. The height of waves is considered in the proposed transmission power adjustment algorithm, due to the fact that it affects the surface signal reflection, in which, in turn, affects the strength of the received signal at a node. In the proposed algorithm, the higher the RMS wave height is, the stronger transmission power will be used. Surface buoys, equipped with accelerometer and gyro sensors, record their elevation trajectory, and from that, compute the mean water line. This computed value is used to estimate the Root Mean Square (RMS) wave height. The transmission power of nodes and, consequently, the appropriate frequency are then adjusted proportionally to the RMS wave height. The proposed solution reduced energy consumption by decreasing the transmission power of the nodes as the wave height gradually decreases toward zero meters, which is the case where traditional approaches do not perceive variation of channel quality and keep using excessive transmission power.

4.3.2 Network throughput

Power control-based topology control algorithm can also be proposed to improve the UWSN throughput. In this approach, increased network throughput is achieved either by improving transmission scheduling or achievable bandwidth. In the former case, power control assigns an adequate communication range to the nodes in order to increase spatial reuse and, consequently, network throughput. In the latter case, power control determines the appropriate communication range and corresponding optimal frequency to increase the achievable bandwidth. Both approaches are described in the following.

It is also important to mention that a maximized network throughput can also be achieved using an adequate deployment of nodes. For instance, Lmai et al. [53] and Anjangi and Chitre [54] showed that an underwater sensor network with a grid topology can be useful to provide high throughput when optimal transmission schedule is considered. The topology control in these scenarios could be used to fix slight position deviations in the formation of the grid network topology, occasioned by underwater mobility or deployment errors. In this work, however, we do not cover these scenarios since they are

a very special case of deployments and applications of UWSNs.

4.3.2.1 Transmission scheduling

It is well-known that the throughput/goodput of network systems is closely related to the spatial reuse, which in turn represents the number of links that can simultaneously transmit data [55]. In wireless networks, a critical factor limiting the network capacity is the interference among spatially closer nodes. In these networks, due to the broadcast nature of the communication medium, nodes located inside an interference zone of both the transmitter and receiver should be kept silent (*i.e.*, without transmitting) when a transmission is happening. This silence is necessary to avoid message collisions and, consequently, waste of networking resources. In UWSNs, the collision-free transmission coordination among nodes is challenging. As a matter of fact, the design of efficient medium access control (MAC) protocols for UWSNs is daunting, mainly because of the high message propagation delay occasioned by the low acoustic signal propagation speed (≈ 1500 meters/second). Therefore, the effectiveness of using feedback solutions for MAC protocols (*e.g.*, carrier sensing and RTS/CTS exchange) is not common in UWSNs [56]. In fact, contention-free-based approaches (*e.g.*, FDMA, CDMA or TDMA) could lead to a better performance of UWSNs [57].

In this context, power control-based topology control can confine interference and improve spatial reuse, by properly assigning a short-range communication for the nodes. Therefore, some proposals, as will be described in the following, have been proposed to extend traditional transmission scheduling protocols considering a fixed interference range, such as in [58] and [53]. The use of fixed long-range communication links is disadvantageous, as it does not optimize the total number of concurrent transmissions of the network. In this scenario, topology control through transmission power control can maximize the spatial reuse as it is helpful in confining interference while ensuring network connectivity and link reliability.

Bai et al. [59] proposed an optimization formulation of the conflict-free link scheduling problem using correlation and conflict matrices. After that, they proposed a heuristic to find a solution for this NP-Complete problem. Power control is introduced in order to confine interference, ensuring high throughput and low end-to-end delay requirements of real-time applications.

Shashaj et al. [60] proposed scheduling and routing policies, considering the use of power control, aiming to optimize network resources (*e.g.*, bandwidth and energy) in periodic traffic applications of UWSNs. In their solution, transmissions happen according

to a scheduling policy. Afterward, the scheduled message transmissions are performed following the routing policies. Transmission power control is performed based on a set of different discrete transmission power levels. The transmission power assigned to each node is the lowest power level ensuring communication with the selected next-hop node.

Su et al. [55] proposed a spatial reuse index metric to measure the spatial efficiency in wireless networks. They showed that, due to the low spreading loss of acoustic signals, spatial reuse in underwater sensor networks is lower than in RF networks. Thus, the authors proposed the UPC-MAC protocol where power control is independently performed on the senders, applying Nash Equilibrium of a utility function defined to maximize the network throughput and reduce energy consumption.

Differently from the previously mentioned solutions, Anjangi and Chitre [61] propose a transmission scheduling algorithm for randomly deployed underwater networks aiming to increase throughput and reduce energy consumption. A scheduling algorithm determines the time slots in which each node will transmit and receive messages. In their work, power control was used to limit the interference range and, consequently, increase the achievable throughput. They showed by means of simulations that reduced interference range allows transmission schedules with significant gains in throughput since more transmission opportunities will be achieved and throughput gets closer to the upper bound.

It can be observed from the aforementioned proposals that power control has been considered to confine interference. When a suitable transmission power is considered at each node, it can reduce the conflict between the communication links. This increases spatial reuse and, consequently, the network throughput. However, these proposals do not consider using power control to conserve energy as well (as described in Section 4.3.1).

4.3.2.2 Bandwidth-distance relationship

The design of topology control algorithms based on power control can be used to explore the bandwidth-distance relationship of the underwater acoustic channel to improve the performance of UWSNs. It is well-known that, in radio-frequency-based wireless communication, the energy cost for a transmission is proportional to the distance between the communicating nodes. As far the nodes are, a higher transmission power is necessary to ensure a successful message reception (*i.e.*, enough strong received signal). However, in the underwater acoustic channel, the distance between the communication nodes also will affect the useful bandwidth.

Stojanovic [30] showed that for a given communication distance, there is a constraint

on the maximum usable frequency. This constraint is due to the signal absorption, which increases rapidly as the frequency increases. Moreover, the intensity of the ambient noise (*e.g.*, turbulence, shipping, waves and thermal noise) impacting the underwater acoustic signal varies according to the used frequency. Therefore, as showed in [30], there is also a limitation of the useful acoustic bandwidth from below as the noise is high for low frequencies and decays as soon as the frequency increases. This leads to the conclusion that, based on the attenuation-frequency product, there is an optimal frequency f_c for each communication distance in which impairments on the transmitted signal are minimized.

We can mention the following proposals in power control that explore the bandwidth-distance relationship. Porto and Stojanovic [42] extended the DACAP MAC protocol [62] to allow multi-hop communication, *i.e.*, network topology without maximal connectivity. The simple shortest path routing was considered for multi-hop data routing from sensor nodes to the sink. The usage of short-range communication allowed to the use the frequency of 35 kHz. One of the most important result was that the energy consumption decreases as the transmission range decreases. The authors concluded that the optimal transmission range corresponds to the minimal connectivity. Moreover, it was shown that the throughput increases as the transmission range decreases.

Casari and Harris [45] proposed the SBRB, FSBRB and DBRB protocols, which leverage the bandwidth-distance relationship to reduce the number of transmissions for completing a network broadcast (*e.g.*, applications of route dissemination, neighborhood discovery and in-network reprogramming of nodes) and minimize energy consumption and delay. Using the SBR baseline protocol, each node broadcasts the message upon receiving it. However, in the proposed SBRB, FSBRB and DBRB protocols, each node broadcasts the message using an appropriate short-range and frequency based on the necessary transmission power. Long-range links using high transmission power are used to notify all nodes about the progress of a message broadcast. FSBRB is an FEC-enhanced version of SBRB where the message is encoded prior to initiating the broadcast. DBRB differs from SBRB by sending some FEC data, through long-range higher power communication, that can be used by the nodes to correct errors. In the experiments, the authors varied different network densities which require a different minimum transmission power to have a connected network. To conclude, results showed considerable energy savings when nodes could to adjust their transmission power.

Casari et al. [46] explored the bandwidth-distance relationship and investigated the performance of multi-hop transmission policies to transport data from sensor nodes to a

sink node. They considered a network scenario formed by r nodes in a chain topology. In the considered scenario, each node generates N messages and transmits through multihop communication via short-range communication links, having greater bandwidth available, until they reach the sink. The authors investigated two multihop relaying policies as follows. The *relaying-only* policy employs short-range communication and forward messages for all the nodes upstream until they reach the sink. Using the *parallel transmission* policy, each node has the option to use long-range communication to forward some of its message directly to the sink while the rest of the messages are forwarded through multihop short-range communication. In conclusion, obtained results showed that the average delay was small when some messages were transmitted directly to the sink through long-range communication. However, multihop transmissions through short-range communication led to reduced energy consumption.

Jornet and Stojanovic [63] investigated the effects of the number of available power levels allowed to be assigned to the nodes. They highlighted that more transmission power levels would be interesting to allow a finer tuning of the transmission power of the nodes. However, from a practical implementation, a small number of levels is probably more desirable as it reduces the design and implementation complexity of the hardware and protocols. Numerical results showed that there was a reduction in the total power consumption as the number of power levels increased. This was due to the fact that nodes could adjust more accurately their transmission power. Results showed that four power levels were sufficient to achieve a good compromise between energy consumption and implementation complexity for the considered network.

4.4 Wireless Interface Mode Management–based Topology Control

A well-investigated methodology for topology control in wireless sensor networks is the communication radio management of nodes. In wireless networks, the communication interface has different modes of operation: *transmitting*, *receiving*, *idle*, *sleep* and, of course, totally *powered-off*. Yet, each operation mode has different unitary costs of energy. Hence, the overall energy consumption of a node depends on the amount of time it spends with its wireless interface in each mode, as given by the below simplified energy consumption equation:

$$E = T_{\text{tx}} e_{\text{tx}} + T_{\text{rx}} e_{\text{rx}} + T_i e_i. \tag{4.1}$$

Table 4.2: Power consumption of the WHOI micromodem-2

State	**Energy consumption**	**State**	**Energy consumption**
Transmitting	8 W - 48 W	Idle (active)	300 mW
Receiving	300 mW	Hibernating (sleep)	165 μW@5 V

In Eq. 4.1, the variables T_{tx}, T_{rx} and T_i correspond to the amount of time that the wireless interface spent transmitting, receiving and in the idle state, respectively. The terms e_{tx}, e_{rx} and e_i are the energy consumption of transmitting, receiving and idle states per time, respectively.

The WHOI micromodem-2 [64], for instance, designed for underwater acoustic communication, has the costs showed in Table 4.2. Such as the WHOI micromodem-2, there is a significant difference between transmission and receiving/idle costs in acoustic modems. The receiving and idle energy costs, in fact, are low and very similar to typical radio-frequency-based wireless interfaces. In this regard, one might suggest that there is no reason to concern about receiving and idle energy costs in UWSNs, as they could be dominated by the transmission cost.

However, despite the significant difference between transmitting and receiving/idle costs, underwater sensor nodes spend most time of their operational cycle in the idle listening mode as data message transmissions in underwater monitoring applications are very infrequent (*e.g.*, once a week [65]). Therefore, wireless interface mode management in UWSNs also may result in energy conservation [43, 66, 67, 68].

In the aforementioned context, topology control through the wireless interface mode management can conserve energy during times of no communication. It changes the network topology by either keeping a backbone of active nodes for communication purpose, where the remaining of redundant nodes can go to sleep (density control), or by controlling the active period of the nodes to make them available at the same time enabling communication (duty-cycling operation). Both approaches lead to energy conservation since they reduce the amount of time that a node unnecessarily spends listening to the channel. Moreover, this topology control approach might reduce interference by means of the network density control, which decreases message collisions and the need of message retransmissions. Consequently, it will also improve the performance of slotted-based medium access control protocols in UWSNs, and decrease the overhead of neighboring discovery of routing protocols, since only a subset of the nodes will be awake.

Table 4.3: Summary of the wireless interface mode management methodology.

Sub-category	**Basic solution**	**Challenges**
Density control	Keeps a set of nodes awake, at any time, to serve as a communication backbone for data delivery.	Low density deployments; Mobility; Unreliable channels for determining and maintaining a communication backbone;
Duty cycle	Switch synchronously or asynchronously the wireless interface of a node between active and sleep mode periodically.	Time synchronization; Overhead; High delay; Long message preambles; Low reliability of acoustic channel;

Herein, we survey and discuss the topology control protocols in UWSNs based on the management of the wireless interface modes. As already briefly mentioned, we address two approaches, density control and duty cycle, as summarized in Table 4.3. The former approach consists in turning off completely the wireless interface of redundant nodes (from a point of view of sensing and communication) that are not necessary, at the moment, in the process of data collection and delivery. This approach has been widely employed in wireless sensor networks, which have a high-density deployment of nodes. However, it might be inefficient and impracticable for UWSNs, since the network topology is usually sparse. The latter approach has an appealing potential for scenarios of UWSNs. It consists in having the nodes operating in a duty cycle manner. In this approach, each node alternates its wireless interface mode between active and sleep modes. When a node is in the active mode, it is able to send or receive messages. At sleep mode, part of the wireless communication interface circuitry is shut down, which reduces the energy consumption of idle listening.

4.4.1 Density control-based topology control

In general, topology control algorithms of this category select a subset of the deployed nodes to be in the active mode, which are used as a communication backbone for multi-hop data delivery. In order to conserve energy, the unchosen nodes can change their wireless interface state for the sleep mode. The density control-based topology control approach has been particularly employed in terrestrial wireless sensor networks (WSNs) [69] since they usually comprise high-density deployments.

Nowadays, the density control-based topology control approach has been less explored in underwater sensor networks. The main reason for this is the fact that underwater

sensor networks typically involve sparse deployments. Thus, in these networks, each node has a vital role for the network connectivity.

However, as will be pointed out in the following, there are some proposals investigating the benefits and drawbacks of this topology control methodology in UWSNs. Further investigations might be motivated by the facts that (i) the deployment of underwater sensor nodes usually occurs according to the following manner: a group of underwater drift nodes are initially deployed in a small area and they spread out with ocean currents as the time goes by, which makes a high density deployment in the beginning of the monitoring mission; and (ii) underwater nodes might use high communication range, which will result in redundancy.

Harris-III et al. [43, 66] investigated the potentials of idle-time power management and wake-up modes in UWSNs. The evaluation was performed by the analysis of the energy consumption. Simulations led to the conclusion that ultra-low power wake-up mode outperforms sleep cycling for UWSN applications of periodic data transmission at a frequency on the order of minutes to a few hours. The reason for this is the excessive control message transmissions to ensure that the receiver node will be awoken and the high-energy cost for transmissions. In this regard, low-power wake-up systems have been proposed for underwater sensor networks, as described in the following.

Wills et al. [70] designed a low-cost and low-power acoustic modem for enabling high-density deployments of short-range communication-based UWSNs. In the designed acoustic modem, the wake-up receiver module is responsible for (i) monitoring the energy level present in a narrow band of frequencies, and (ii) waking up the receiver through an interrupt, when the energy exceeds a threshold level.

Sanchez et al. [71] designed an RFID-based wake-up system for a low-power acoustic modem. In the proposed solution, a wake-up signal is transmitted to inform the intended receiver about a further message transmission. At the receiver side, an interrupt signal is generated to wake up the micro-controller, whenever the intended receiver detects a wake-up signal matching with its assigned recognition pattern.

Li et al. [72] designed an on-duty circuit for power monitoring and acoustic modem wake-up. In order to control the on-duty circuit, the authors proposed operating modes for the modem as sleep, monitor and working. The wake-up circuit in the monitor mode, triggered by an alarm time, wakes up and switches the modem to the working mode when it detects a wake-up signal received by the transducer.

4.4.2 Duty-cycling-based topology control

In this work, we argue that duty cycle can also be explored for topology control. One might argument that duty-cycling operation does not change the network topology since a pair of communicating nodes will be awake at the same time for data delivery. However, from a point of view of topology control, the proper selection and/or adjust of the sleep interval of the nodes might force the absence/existence of some links during a communication.

Duty-cycling has been extensively investigated to achieve energy-efficiency in energy-constrained wireless ad hoc networks. In a duty-cycled network, each node periodically alternates the state of its wireless interface between active and sleep mode. In this approach, energy conservation is achieved by avoiding to keep nodes idle listening to the channel, especially in low traffic load scenarios of sensor networks.

In general, duty-cycling protocols have been classified in *synchronous* and *asynchronous*, according to the mechanism used to ensure the pairwise communicating nodes awake at the same time, *i.e.*, during the message transmission. In synchronous duty-cycling, the sleep/wakeup schedule of the nodes is aligned, by means of an explicit negotiation. Therefore, a sender node is always aware when its neighbors will be awake and apt to receive data messages. In asynchronous duty cycling, conversely, the duty cycle schedule of the nodes is completely decoupled. Therefore, at an arbitrary time instance, only a subset of nodes might be in the active mode, *i.e.*, awake and apt to receive data messages.

Synchronous and asynchronous duty cycling protocols have peculiar characteristics that will impact on the UWSN performance. Synchronous duty-cycling protocols entail periodic signaling to ensure an alignment between the duty-cycling schedule of the nodes. Moreover, there is the need for synchronized clocks, which require extra computing and communication efforts. This approach seems to be unfeasible in UWSNs because of the overhead for clock synchronization and schedule exchanging. Asynchronous duty-cycling protocols, on the other hand, are simple and do not involve periodic beaconing for schedule alignments. However, these protocols lead to an increasing end-to-end delay, since there is no guarantee that a receiver node will be awake when a sender node has a data message to transmit. Even though, protocols falling into this category seem to be more suitable for the harsh environment of UWSN applications. In the following, we briefly discuss the three main methodologies used for the design of asynchronous duty-cycling protocols:

- **Naive asynchronous duty-cycling:** In duty-cycling protocols based on this methodology, a sender node transmits a data message whenever it is ready. The message is successfully received if there is a neighboring node awake during the transmission. This approach is efficient in terms of energy saving and overhead. However, there is not guarantee that a data message will be successfully delivered to the destination, especially in low-density scenarios of UWSNs.

- **Low power listening (LPL) duty-cycling:** In duty-cycling protocols based on this methodology, a sender node transmits preambles before a data message transmission. The preamble phase is used to ensure that the intended receiver will be awake during the data message transmission. This phase lasts for a period slightly higher than the sleep interval of the receiver node. At the receiver side, whenever it wakes up and detects a preamble transmission, it remains awake to receive the data message transmitted after the preamble phase. It is important to mention that the classical LPL approach is infeasible for UWSNs, due to the long preamble transmissions and the high energy cost of acoustic modems for transmitting. For these networks, the strobed-preamble variant is desired. In the strobed preamble LPL variant [73, 74], short-preambles transmissions are interleaved by silence times. Finally, it is worth mentioning that energy expenditure mostly happens in the sender nodes.

- **Low power probing (LPP) or receiver-initiated duty-cycling:** In duty-cycling protocols based on this methodology, a receiver node transmits a beacon whenever it wakes-up. This transmission is used to inform its awake situation for possible sender nodes in the neighborhood. Thus, a sender node whenever it has a data message to transmit, it waits until the intended receiver wakes up and transmits the beacon.

In the following, we discuss some of the representative duty-cycling proposals for UWSNs, encountered in the literature. Zorzi et al. [75] studied the effects of node density on the energy consumption, considering a duty-cycled UWSN where each node can control its transmission power. As expected, it was observed that one of the main drawbacks of the use of asynchronous duty-cycling is the decrement of the instantaneous network density. This behavior, as already discussed above, might be critical to maintain the network connectivity in the sparse deployments of UWSNs. Yet, the authors showed that this decrease in the number of active nodes, occasioned by duty-cycling, incur in

more energy expenditure per delivered data message. This happens because sender nodes needed to use high transmission power to find an active neighbor node.

Coutinho et al. [68] proposed an analytical framework for performance evaluation of duty-cycling protocols based on the aforementioned three methodologies (naive, low power listening and low power probing) in scenarios of UWSNs using opportunistic routing protocols. The authors evaluated the potentials for energy conservation of these approaches in comparison to the always-on wireless interface configuration scenario. The obtained results showed that naive-based asynchronous duty cycling protocols achieved more efficiency in terms of energy conservation. This is due to the absence of control messages transmissions to ensure both receiver and sender nodes awake at the same time. However, due to the lack of this mechanism, this approach performed poorly in terms of message delivery.

Hong et al. [76], differently from the aforementioned proposals, addressed the problem of sleeping-waking frequency in duty-cycled UWSNs. The motivation of this work comes from the fact that the frequent switching on/off of the wireless interface will waste energy and, consequently, decrease the lifetime. The authors proposed the receiver-oriented sleep scheduling (ROSS) scheme to conserve energy by reducing the sleeping-waking frequency on the nodes. The proposed scheme works in a tree topology of nodes using TDMA scheduling for transmissions. The ROSS scheme allocates the working time of each node from the root to the leave nodes, where each node will be able to sleep immediately after forwarding all received data from its children. Due to the mechanism used to determine the working time of each node, the ROSS scheme achieves higher throughput and lower end-to-end delay in comparison to related MAC protocols proposed for UWSNs.

Coutinho et al. [77] investigated the impact on network lifetime, of the proper selection of the sleep interval of nodes in a duty-cycled UWSNs. The authors proposed an analytical framework to evaluate the impact of sleep interval control at the nodes on the network lifetime. They argued that the amount of time a node spends sleeping must be periodically adjusted to achieve a balanced energy consumption between the nodes. This is due to the fact that long sleep interval conserves energy at the receiver nodes, but it leads to a high-energy consumption on sender nodes due to the strobed preamble transmissions. Obtained results from a sleep interval control optimization formulation, considering traffic load and network density, showed that on-the-fly sleep interval adjustment is preferable as it can prolong network lifetime by reducing the quick battery depletion of central nodes from a routing point of view.

4.5 Mobility Assisted–based Topology Control

In underwater sensor networks, topology control can be done by leveraging the controlled mobility of some underwater nodes. In this approach, the basic idea is to move one or a few underwater nodes for new locations. This displacement can be done with the objective of improving the network functioning or performance.

In the terrestrial wireless sensor network, mobility assisted-based topology control has been extensively designed to restore the network connectivity [78]. This is motivated by the fact that, in these networks, the network connectivity is frequently disrupted by node failures occasioned by either battery depletion or problem in the hardware. In these scenarios, new locations are computed for some mobile nodes. These nodes, then, move to the determined locations and act as bridges between the two previous disconnected network segments.

In the context of UWSNs, mobility assisted-based topology control algorithms have been used to improve data collection [79, 80], data routing [25], coverage [81] or even underwater node localization [82]. Underwater autonomous vehicles (UAVs) or nodes with depth adjustment capabilities can be used for these purposes. The use of UAVs allows more flexible and efficient topology control as they can move in any direction. Ordinary underwater nodes, conversely, have a constrained mobility. They usually can move vertically, *i.e.*, they can adjust their depths. However, this approach is more affordable than UAVs and, therefore, can be deployed in different ways.

The mobility assisted-based topology control is probably the most powerful methodology to change the network topology. We can state that the methodologies previously discussed make "soft" changes in the network topology by enabling or not some communication links. In fact, there are no physical changes regarding the location of the nodes, limiting the possible neighboring nodes that a given node can have. Using mobility assisted-based topology control, conversely, nodes can be relocated and, as consequence, a more effective density control can be accomplished and new sets of neighboring nodes can be enabled. Therefore, this approach can achieve better performance when topology control is used to improve coverage, for instance.

Topology control using a mobility assisted-based approach must carefully select the nodes to be moved and the location where they will be moved to. In most of the network deployments, there is an associated cost to move mobile nodes, such as the energy cost. These costs should be considered when the topology control algorithm selects the nodes and new locations for them. This is to avoid mobile nodes to quickly deplete

Table 4.4: Summary of the mobility assisted-based topology control methodology

Sub-category	**Basic solution**	**Challenges**
Depth adjustment	Underwater sensor nodes are moved vertically for new locations.	Mobility; Movement delay; Energy cost for vertical movement; Low density deployments; Changes in the sensing coverage area;
Trajectory	Autonomous underwater vehicles (UAVs) follow well-defined trajectories to collect data from underwater sensor nodes.	High cost; Energy limitation; Localization and tracking;

their batteries, which might incur disruption in the network connectivity. Therefore, in UWSNs, independent of the use of UAVs or underwater nodes with depth adjustment capabilities, the main research challenge of designing mobility assisted-based topology control is to design efficient protocols for selecting the nodes to be moved and determining their new locations.

In the following, we discuss two mobility assisted-based topology control approaches, summarized in Table 4.4, according to the considered type of mobile nodes.

4.5.1 Trajectory-based topology control

Topology control algorithms for UWSNs in this category have used underwater autonomous vehicles (UAVs) to enable much richer underwater applications relying on multimedia content. To do so, UAVs equipped with optical and acoustic communication visit underwater sensor nodes and collect data from them.

This heterogeneous architecture is aimed to overcome the bandwidth-limited nature of the underwater acoustic channel, which can support data delivery of single readings of environmental variables (*e.g.*, temperature, salinity and pressure level). However, it is insufficient to handle multimedia content, obtained from high resolution cameras, in underwater wireless sensor network applications.

In these applications, optical communication is preferable for data offloading. This is because the optical channel can achieve high data rates, on the order of several Mbps, over short distances. Acoustic communication, conversely, will still play a significant role in these UAV-aided heterogeneous UWSN architecture. It will be used for the transmission of control data among long-range nodes, for instance, to inform about sensed data and

coordinate the UAV trajectory. Thus, the trajectory of the UAV can be determined from the existence of hot-spots.

Some of the main research challenges when designing topology control approaches using UAVs, arise from the design of UAV path-planning algorithms. Since there is an associated cost for the UAV movement and a delay for the displacement of the UAV from its current position to the node to be visited, efficient UAV path-planning solutions must be proposed to minimize the cost and achieve the desired user's expectation in terms of collected data. Moreover, these solutions must consider the technological and environmental constraints and challenges, such as energy, data-storage and speed of wind gushes and roughness of water surface. In the following, we discuss some research efforts in this direction.

Khan et al. [83] proposed the use of a value of information (VoI) metric for path-planing of an UAV to collect data from underwater nodes. Accordingly, the VoI metric is given by an always monotonically decreasing function used to estimate the quality of sensed information. The meaning behind the VoI metric is that a sensed value is more valuable for the application immediately when it is detected and then, it starts loosing value with time. Based on the VoI metric, the authors investigated three path-planning algorithms for the UAV: (i) Lawn mower path planner (LPP), where the next nodes to be visited are the neighboring nodes of the list of visited nodes; (ii) Greedy path planner (GPP), where the next node to be visited is the one maximizing the information, *i.e.*, the next node of utmost importance; and (iii) Random path planner (RPP), where the next node to be visited is randomly selected by the UAV. Simulation results showed that the greedy path planner algorithm outperformed the LPP and RPP algorithms in terms of visits to all considered hot-spots and maximized VoI.

Similarly, Basagni et al. [79] proposed to use the VoI metric for UAV path planning in a submarine surveillance and monitoring application. The authors then proposed an Integer Linear Programming (ILP) formulation for determining UAV paths that maximize the VoI of collected data. The proposed ILP formulation takes into consideration realistic factors of UWSN and applications, such as communication rates, distances and surfacing constraints of UAVs. In addition, the authors proposed the Greedy and Adaptive UAV Path-finding (GAAP) heuristic where the selection of the next node to be visited by the UAV is based on the expected VoI of the node when the UAV arrives on it. Thus, according to the proposed GAAP path-planing algorithm, the UAV decides to visit a node only if the collected data will increase the VoI of the data that will be delivered to the sink.

Forero et al. [80] proposed a dynamic path-planning algorithm for trajectory coordination of multiple UAVs. The proposed algorithm takes into consideration the energy capacity of UAVs, their battery recharge time and data-storage capacity. Moreover, it dynamically routes UAVS, instead of a predetermined trajectory, which allows them to adapt to changes on the network conditions (*e.g.*, volume of data to be collected, remaining energy in the UAVs and battery recharge times).

4.5.2 Depth adjustment-based topology control

In UWSNs, some topology control algorithms use the vertical movement (depth adjustment capabilities) of underwater sensor nodes to perform the topology control. The basic idea behind this approach is to change the network topology by coordinately controlling the depth of some underwater sensor nodes.

Some of the recent underwater sensor nodes have been equipped with depth adjustment capabilities. For instance, the AquaNode [84] uses a which-based apparatus allowing it to move vertically. In this mechanism, each underwater node is attached to a surface buoy or an anchor. Hence, the vertical movement of the node is done through the adjust of the cable. The Drogue node [85], on the other hand, entails a buoyancy-based apparatus for vertical movement. In this approach, an internal buoy is inflated by a pump, bladder or another device. This changes the buoyancy of the node relative to the water. Thus, the node emerges. Each approach has advantages and disadvantages considering the movement speed and energy cost for movement.

An important aspect of topology control algorithms in this category is that they can organize the network topology either in a *proactive* or *reactive* manner, as discussed in the following.

In proactive algorithms, the depth adjustment of the selected nodes is performed immediately after the network deployment. Based on the position of the randomly deployed nodes, a subset of them is determined to be moved to new depths to accomplish the desired goal (*e.g.*, improvement in coverage or network connectivity). Moreover, to achieve better results, proactive depth adjustment-based topology control can be done using the information of the entire network topology.

This procedure can be described as follows. First, an UAV (or a set of them) will travel along the deployment area and collect the location information of the deployed nodes. This can be done together with the UAV-aided underwater node localization systems [86]. Second, the topology control algorithm will determine the set of nodes that

need to be moved and their new depths. This selection is based on the initial topology and the desired goals. Thirdly, UAVs can be employed to inform the selected nodes to move to new depths.

In reactive algorithms, depth adjustment decisions are made locally at some nodes. A given node, based on an event firing the topology control algorithm, determines whether it should move or not. This decision will be motivated by the network status or local topology. For this, the node will use the information of its neighborhood. After that, based on given criteria, the node will select a new depth. Reactive depth adjustment-based topology control algorithms are preferable in mobile UWSNs. They can be used, for instance, for the restoration of the network connectivity, as nodes involuntarily move according to the ocean currents.

Herein, we discuss some preliminary solutions that used this approach for topology control. Accordingly, O'Rourke [84] proposed the use of depth-adjustment of the nodes to improve data delivery. The authors suggested a multi-modal underwater sensor node equipped with both underwater acoustic and radio-frequency modems. Thus, each node can either delivery data through multi-hop acoustic communication or it can surface and use radio-frequency communication. Moreover, the authors proposed a set of algorithms to compute the energy and delay trade-offs of nodes, with the goal of selecting a subset of them to surface and transmit data through radio channels. Preliminary results showed that the greedy algorithm, which raises the nodes closer to the surface, can reduce communication costs and increase the network lifetime.

Similarly, Basha et al. [87] proposed a set of eight algorithms to select the nodes to surface. In this set of algorithms, there are centralized algorithms as well as completely distributed ones. The idea is to select an efficient communication strategy and determine efficient data routing. To select the communication strategy, *i.e.*, underwater communication or surface radio communication, the proposed algorithms consider the energy consumption of vertical movement and the energy costs relative to acoustic and radio-frequency communication.

Coutinho et al. [22, 25, 34] proposed to use depth adjustment of some nodes to improve underwater data routing. In [25], the authors proposed the CTC and DTC algorithms, for topology control through depth adjustment of some nodes, to reduce the fraction of isolated nodes, *i.e.*, without a multi-path to a sink, in sparse UWSN deployments.

Coutinho et al. [22] proposed the DCR geographic routing protocol that uses depth adjustment-based topology control to handle with void nodes. In addition, the authors in [34] proposed the GEDAR opportunistic routing protocol, which uses depth-

adjustment-based topology control, for efficient data delivery in challenging mobile UWSNs. Despite significant differences in the proposed topology control algorithms and UWSN scenarios, the vertical movement principle designed showed to be effective to cope with some shortcomings of the acoustic channel and geographic routing.

In the previous approaches, two critical issues may happen. Firstly, high energy consumption and, second, changes in the sensing coverage area. Energy cost is a shortcoming in some of the underwater node vertical movement technologies. In fact, in the previous solutions, the network energy cost was excessive in highly sparse network deployments. A similar trend was found in the analyses performed in [88]. This is because some nodes must be moved for long distances. Thus, this approach might shorten the UWSN lifetime. Moreover, since some nodes are moved from their deployed depths, this approach may significantly change the initial coverage area. If there is no appropriate control of the nodes that will surface, the application might experience a lack of information of events happening in deep waters.

4.6 Concluding Remarks

Topology control is fundamental to improve the performance in wireless ad hoc and sensor networks. In underwater sensor networks, more specifically, it also is necessary to achieve efficient underwater monitoring and exploration applications. In this networks, topology control has been used for improving networking services and protocols used to support distributed applications.

This Chapter surveyed the initial research efforts on topology control in underwater sensor networks. We classified the current approaches encountered in the literature, according to the main methodology used to consciously make changes in the network topology. In doing so, we discussed the advantages, disadvantages, and challenges of each one, relating them to the challenges of the underwater environment and acoustic channel.

Chapter 5

Preliminaries, Fundamentals and Definitions

This Chapter preliminarily presents some definitions and models that are used throughout this thesis. It is organized as follows. Section 5.1 describes the deployment of underwater acoustic sensor networks for long- and short-term underwater monitoring applications. Section 5.2 provides a general graph-based network modeling. Section 5.3 models the greedy forwarding-based geographic routing approach. Section 5.4 defines and models the communication void region problem of geographic routing in UWSNs. Section 5.5 reviews the mathematical model used to estimate the packet delivery probability in the underwater acoustic channel. Finally, we conclude this Chapter in the Section 5.6.

5.1 Underwater Sensor Network Deployments

Throughout this thesis we consider an underwater acoustic sensor network SEA (Sensor Equipped Aquatic) swarm architecture, as discussed in details in Section 2.2 either composed by static or mobile underwater sensor nodes at the ocean bottom, scattered by sonobuoys, also named of sink nodes, deployed at the surface of the ocean.

Acknowledgment: It is important to mention that a dozen of underwater nodes or UAVs carefully deployed at specific locations (*e.g.*, [89]) is the current practical scenario of an UWSN in the ocean. This limited number of nodes is mainly due to their high cost. However, in this thesis, we follow the randomly high-deployment approach adopted by related work [18, 35, 36, 13, 19]. This approach is not only to test our proposed models

and protocols in adverse settings but also to obtain insights for the future development of networking solutions for high-density UWSNs enabled by low-cost underwater sensor nodes [90].

Broadly, we can distinguish underwater monitoring applications in two classes [91]:

- **Long-term aquatic monitoring applications.** In this class of applications, UWSNs are used to collect non-time-critical information about the monitored event. Usually, a well-defined event at a particular spatial area is the target of the monitoring system. Static UWSNs can be used in these applications. The underwater nodes are attached into buoys or anchors to remain almost static in the desired location. Some aquatic monitoring applications of this category include, water quality, hydroelectric reservoir, marine biology, deep-sea archeology, seismic predictions, pollution detection and oil/gas field monitoring.

- **Short-term aquatic monitoring applications.** In this class of applications, UWSNs are frequently used to collect time-critical information in a 4 D nature, that is, spatial and temporal correlated data. By doing so, underwater sensor nodes are deployed without tethers. They freely drift according to the ocean currents [92]. Some applications of this category include underwater natural resource discovery, anti-submarine mission, loss treasure discovery, tsunamis and sea-quakes monitoring, oceanographic data collection, navigation assistance and pollutant content monitoring.

5.2 Network Model

In this thesis, our network model consists of a set $N = N_n \cup N_s$ of nodes with a communication range of r_c, so that N_n represents the set of sensor nodes, and N_s is the set of sonobuoys. As in the literature, the sensor nodes $N_n = \{n_1, n_2, \ldots, n_{|N_n|}\}$ are randomly deployed in an area of interest $D \in \mathcal{R}^3$. Each node might be equipped with various sensors and with a low-bandwidth acoustic modem. The acoustic modem is used to periodically report, wirelessly, the sensed data to the destinations (sonobuoys) via multi-hop communication. Underwater sensor nodes can adjust its depth by means of inflatable buoys or winch based apparatus.

In a buoyancy-based depth adjustment system, a buoy can be inflated by a pump, bladders or other device to change the buoyancy of the float relative to the water. This

system does not use propulsion mechanisms, reducing the energy cost to the depth adjustment. In winch-based apparatus, sensor nodes are attached to surface buoys or anchors by means of cables. A cable is then adjusted to move and maintain a node in a determined depth. Some works that consider depth adjustment capability of the nodes for coverage improvements [81] and localization systems [82], for instance, did not consider the cost relative to this task.

In mobile UWSNs, Drogue node [85] is a preferable candidate to be used as a sensor node. However, we have considered the vertical movement speed and energy cost values of the depth adjustment mechanism proposed in [93] as that work provides the vertical movement speed and energy cost information. It is worth highlighting that winch-based approaches are energy hungry as compared with buoyancy-based approaches. Thus, each sensor node can move vertically with velocity $v = 2.4\,\mathrm{m/min}$ at an energy cost of $E_m = 1500\,\mathrm{mJ/m}$.

The sonobuoys $N_s = \{s_1, s_2, \ldots, s_{|N_s|}\}$ are special nodes randomly deployed at the sea surface. Each sonobuoy is equipped with Global Positioning System (GPS) to determine its location. Moreover, they are equipped with both acoustic and radio transceiver modems; each sonobuoy uses acoustic links to send commands and to receive data from underwater sensor nodes, and the radio links are used to forward the data packets to a monitoring center for future processing.

Like [35] and [94], we consider that if a packet arrives at any sonobuoy, it can be delivered to the monitoring center. This assumption is reasonable because acoustic communication is more hard than radio frequency communication since sound propagates (speed of $1.5 \times 10^3\,\mathrm{m/s}$ in water) five orders of magnitudes slower than radio (with a propagation speed of $3 \times 10^8\,\mathrm{m/s}$ in air).

We represent the network topology as an undirected graph $G(t) = (V, E(t))$ at time t, where $V = N$ is the set of vertices corresponding to the sensor nodes and sonobuoys; and, $E(t) = \{e_{ij}(t)\}$ is the finite set of links between them. For long-term monitoring scenarios, we have static sensor network. In this case, the topology is time-invariant unless the nodes purposely move for new depths.

Two nodes u and $v \in V$ are *neighbors* at time t and are *directly connected* via a *link*, if they can directly, mutually, and consistently communicate over an acoustic channel at time t. We define $N_u(t)$ as the set of underwater sensor nodes that are node u's neighbors with $u \notin N_u(t)$.

5.3 Geographic Routing Paradigm

In this thesis, we concern about geo-opportunistic routing protocols for UWSNs. Geographic routing has been proven to be a promising paradigm for the design of energy-efficient routing protocols for underwater sensor networks. Geographic routing protocols are simple and scalable. They do not require the establishment or maintenance of complete routes to destinations. Moreover, there is no need to transmit routing messages to update states.

During multihop data forwarding, the current forwarder node selects its local optimal neighbor node as a next-hop forwarder to continue forwarding the packet. The choice of this next-hop node is made from the position or depth information of the current forwarder node, its neighbors and of the destination. The idea is to advance the packet as close as possible to the destination at each hop.

We use the greedy forwarding strategy to perform the next-hop forwarding selection. In this strategy, a packet is routed at each hop to a locally optimal next-hop node towards the destination. We use the *packet advancement (ADV)* [95] to select the best next-hop candidate as:

$$ADV(n_j) = D(n_j, s^*_{n_j}) - D(n_i, s^*_{n_i}), \tag{5.1}$$

where n_i and n_j are the source and neighbor nodes, respectively. $D(n, s)$ denotes the Euclidean distance from a node n and the sonobuoy s. Sonobuoy $s^*_{n_i}$ is the closest sonobuoy to n_i, according to

$$s^*_{n_i} = \underset{s \in \mathcal{N}_s}{\operatorname{argmin}}\{D(n_i, s)\}. \tag{5.2}$$

Let $\mathcal{F}_{n_i} = \{n_j \in N(n_i) : ADV(n_j) > 0\}$ be the set of neighbor candidates of n_i that can be selected as a next-hop. From Eqs. 5.1 and 5.2, if n_i lacks a direct connectivity with a sonobuoy, it will select the next-hop as:

$$n^*_j = \underset{n_k \in \mathcal{F}_{n_i}}{\operatorname{argmax}}\{ADV(n_k)\}. \tag{5.3}$$

5.4 Communication Void Region Problem

The main disadvantage of geographic routing protocols is the *communication void region problem*. Communication void region problem limits the applicability of geographic routing and significantly degrades its performance [96]. This serious shortcoming has

been widely investigated in radio frequency-based wireless ad hoc networks. However, less attention has been devoted in the scenarios of UWSNs.

Herein, we present some definitions related to the communication void region problem used throughout this thesis.

Definition 1 (Communication void region) *This occurs when the current forwarder node cannot deliver data packets directly to the destination, and does not have a neighbor node closer to the destination than itself to continue forwarding.*

Definition 2 (Void node) *These are the nodes located within communication void regions. When a packet becomes stuck in the void nodes, it should be either routed using a void handling algorithm, or discarded.*

Definition 3 (Void handling algorithm) *This is the mechanism employed by the geographic routing protocol to route data packets to their destinations when they cannot be delivered using the greedy forwarding strategy.*

Chen and Varshney [97] discuss different approaches for the void node problem in 2 D networks. In contrast, Durocher et al. [98] show that no k-local routing algorithm guarantees the delivery of messages in 3 D networks modeled as a ball graph.

5.5 A Review of the Packet Delivery Probability

In this section, we review the underwater packet delivery probability $p(d, m)$ for a packet of m bits transmitted, by means of an acoustic link, between any pair of underwater nodes with a distance of d meters from each other.

First, we use Eq. 5.4 to calculate the path loss on a transmitted acoustic signal over a distance d for a signal of frequency f.

$$A(d, f) = d^k a(f)^d. \tag{5.4}$$

In Eq. 5.4, the absorption coefficient $a(f)$, in dB/km for f in kHz, is described by the Thorp's formula [29] given by:

$$10 \log a(f) = \frac{0.11 \times f^2}{1 + f^2} + \frac{44 \times f^2}{4100 + f} + 2.75 \times 10^{-4} f^2 + 0.003. \tag{5.5}$$

The average Signal-to-Noise Ratio (SNR) over distance d is thus given as:

$$\Gamma(d) = \frac{E_b/A(d,f)}{N_0} = \frac{E_b}{N_0 d^k a(f)^d}, \tag{5.6}$$

where E_b and N_0 are constants that represent the average transmission energy per bit and noise power density in a non-fading additive white Gaussian noise (AWGN) channel. As in [99] and [100], we use Rayleigh fading to model small scale fading where SNR has the following probability distribution:

$$p_d(X) = \int_0^\infty \frac{1}{\Gamma(d)} e^{-\frac{X}{\Gamma(d)}}. \tag{5.7}$$

The probability of error can be evaluated as:

$$p_e(d) = \int_0^\infty p_e(X) p_d(X) dX. \tag{5.8}$$

Here, $p_e(X)$ is the probability of error for an arbitrary modulation at a specific value of SNR X. In this thesis, we use the Binary Phase Shift Keying (BPSK) modulation that is widely used in the state-of-the-art acoustic modems [13, 94, 5, 101, 102].

In BPSK, each symbol carries a bit. In [103], the probability of bit error over distance d is given as:

$$p_e(d) = \frac{1}{2}\left(1 - \sqrt{\frac{\Gamma(d)}{1+\Gamma(d)}}\right). \tag{5.9}$$

Thus, for any pair of nodes with distance d, the delivery probability of a packet with size m bits is simply given by:

$$p(d,m) = (1 - p_e(d))^m. \tag{5.10}$$

5.6 Concluding Remarks

This Chapter discussed some preliminary concepts that will be used in the remainder of this thesis. In this Chapter, we reviewed the typical non-mobile and mobility UWSN architectures. We also provided our general graph-based network modeling, as well as a mathematical model of the greedy forwarding routing strategy and communication void region. Finally, we reviewed the packet delivery probability between two communicating underwater sensor nodes.

Chapter 6

An Analytical Framework of the Communication Void Region Problem

In this Chapter, we model our proposed mobility assisted and the two main methodologies in the literature that have been used for the design of void-handling algorithms in UWSNs. The devised analytical framework is aimed to fill the gap in the literature of analytical tools that allows the performance evaluation of the trade-offs of each paradigm along different scenarios of UWSNs.

The proposed model provides insights for the further design of void-handling algorithms in different underwater application and sensor network configurations. Numerical results show that the widely used bypassing void region approach is not effectively for moderate- and high-density UWSN scenarios. Conversely, topology control-based approaches (power control and mobility-assisted) are preferable as they create additional links. However, the use of void-handling procedures increased the network energy consumption, which made each paradigm unsuitable for specific scenarios revealed by the proposed modeling.

This Chapter is organized as follows. Section 6.1 presents our proposed classification of void-handling algorithms for UWSNs, and reviews the works encountered in the literature. Section 6.2 describes some preliminary concepts used by our proposed model. Section 6.3 presents the analytical framework proposed for evaluating the performance of the void-handling algorithms. Section 6.4 presents the performance evaluation of the analytical model. Finally, Section 6.5 presents our chapter remarks.

6.1 Literature Review and Proposed Classification

In this section, we review the void-handling algorithms proposed for geographic and opportunistic routing protocols in underwater wireless sensor networks. The communication void region problem and its related concepts, used recurrently throughout the text where defined in Section 5.4.

In traditional geographic routing using the greedy upward (pressure-based) forwarding strategy, the next-hop forwarder selection is made according to Algorithm 1. Accordingly, each node selects its neighboring node closer to the surface of the sea (Lines 3-8). When a node has a data packet to send, it inserts the unique address of its next-hop forwarder into the packet header and broadcasts it. Nodes that have correctly received the packet compare whether they are the next-hop forwarder of the sender. The forwarder node will relay the packet towards the surface, to be received by a sonobuoy. The packet will be discarded by the other nodes. When a node is in a communication void region (Figure 6.1a), it should employ a void-handling algorithm or discard the packet.

Algorithm 1 Greedy upward routing algorithm

1: $\text{next\_hop}_v \leftarrow$ undefined
2: $\text{depth}_{nh} \leftarrow \infty$
3: **for** $u \in N_e(v)$ **do**
4: **if** $depth(u) < depth_{nh}$ **then**
5: $\text{next\_hop}_v \leftarrow$ u
6: $\text{depth}_{nh} \leftarrow$ depth(u)
7: **end if**
8: **end for**

When a node is in a communication void region and cannot determine a next-hop forwarder according to Algorithm 1, a void-handling algorithm should be used. In the following, we classify the proposed recovery algorithms in three categories as: *bypassing void region-*, *power control-*, and *mobility assisted-based* solutions. We discuss the general design principles, advantages and drawbacks of each these categories, highlighting the main protocols encountered in the literature. These aspects are summarized in Table 6.1.

6.1.1 Bypassing void region-based approaches

The majority of void-handling algorithms for UWSNs are designed from the bypassing void region-based strategy, as shown in the example of Figure 6.1b. Void-handling al-

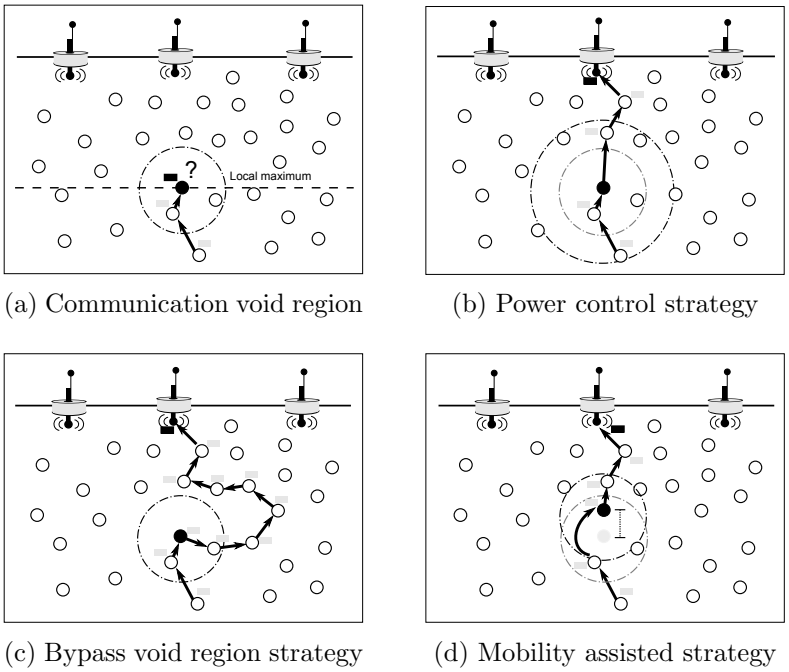

(a) Communication void region (b) Power control strategy

(c) Bypass void region strategy (d) Mobility assisted strategy

Figure 6.1: Communication void region problem and void-handling strategies

Table 6.1: Proposed classification of void-handling methodologies in UWSNs

Methodology	**Basic Principle**	**Advantages**	**Disadvantages**
Power control	Void nodes increase their communication range to find a next-hop node.	Simple, scalable, no changes in the sensing coverage area.	Increase energy consumption, packet error and collisions.
Bypassing void region	An alternative path circumventing the void region is determined.	No changes in the sensing coverage area.	Overhead to find alternative paths, long routing paths, which increase packet collisions and end-to-end delay.
Mobility assisted	Void nodes are vertically moved to new locations.	No increment of the number hops and interference zone.	Change the initial sensing coverage.

Algorithm 2 Bypassing void region–based void node recovery algorithm

```
1: ▷ m: an incoming beacon message
2: if m.seq_num > seq_num or (m.seq_num = seq_num & m.hop_count + 1 <
   hop_count) then
3:    NDF_dir(sender) ← m.DF_dir
4:    hop_count ← m.hop_count + 1
5:    next_hop_v ← m(sender)
6:    if depth(v) > depth(sender) then
7:       DF_dir ← UP
8:    else
9:       DF_dir ← DOWN
10:   end if
11: end if
12:
13: if DF_dir = UP then
14:   next_hop_v ← undefined
15:   depth_nh ← depth(v)
16:   for u ∈ N_e(e) do
17:      if depth(u) < depth_nh and NDF_dir(u) = UP then
18:         next_hop_v ← u
19:         depth_nh ← depth(u)
20:      end if
21:   end for
22: end if
```

gorithms using this strategy should discover and maintain an alternative routing path from the void node to a non-void node that can resume the greedy upward forwarding routing.

The main disadvantages of this strategy are twofold. First, the network can experience excessive energy consumption of control packets. Second, data packets are routed along more hops, increasing the delay for delivering the packet, as well as network interference. Algorithm 2 shows a simple heuristic to route data packets along void regions based on the VAPR [94] routing protocol. In this algorithm, packets are routed circumventing the communication void region known by means of periodic beacons.

Herein, we discuss UWSNs' routing protocols employing bypass void region-based

recovery algorithm. In Vector-based Routing (VBF) protocol [18], data packets are routed along a virtual "routing pipe". The routing pipe is formed by the vector, known as forwarding vector, calculated from the sender and destination location information. A node that has successfully received a packet continues to forward it, if its distance to the forwarding vector is less than a predefined threshold. Otherwise, the packet is discarded. The disadvantages of VBF arise from the node density inside the routing pipe. High densities cause redundant packet transmissions. Low densities lead to packet losses, due to the problem of void region.

To mitigate the effects of node density in VBF, Nicolaou et al. [104] proposed the Hop-by-Hop Vector-based Forwarding (HH-VBF) routing protocol. HH-VBF uses a different virtual pipe per-hop from each forwarder to the sink, to cope with the absence of nodes lying within the virtual forwarding pipe of VBF in sparse network scenarios. VBVA [105] routing protocol, also designed to improve VBF, attempts to bypass the boundary of the void region by shifting the forwarding vector of the data packet, and by a back-pressure method when the vector-shifting method fails (convex voids).

Hydrocast routing protocol [13] uses the pressure (depth) information of the nodes to greedily route data packets towards the surface of the sea. In each hop, the forwarder node selects a subset of its neighbors, named as candidates, with shallower depths than its own. The candidates continue the multihop routing in a prioritized way, such that a node will forward the packet if all the high priority candidates fail to do so. Priority is given according to both the progress of each node to the surface of the sea, and the probability of packet delivery from the source to each node. Sinks deployed at the surface are responsible for receiving packets. The communication void region problem occurs when a node lacks a neighbor closer to the surface. In this case, the void node uses controlled flooding to search for a node at a depth lower than its own, and explicitly maintains a path to that node to route the data packets along the void region.

Noh et al. [94] proposed the Void-Aware Pressure Routing (VAPR) protocol. In VAPR, a data packet is routed along a directional path to a surface sonobuoy. This directional path is determined from beacon messages disseminated from the sonobuoys. When a node receives a beacon message, it updates its forwarding direction (upward or downward) according to the depth location of the sender (shallow or deep). Thus, each node becomes aware of whether it is in a communication void region. Void nodes route data packets bypassing the boundary of void regions by matching the neighbors' forwarding direction with their own.

Algorithm 3 Power control–based void node recovery algorithm

1: $R_c(v) \leftarrow$ next_level
2: $next\_hop_v \leftarrow$ undefined
3: $depth_{nh} \leftarrow \infty$
4: **for** $u \in N_e(v)$ **do**
5: **if** $depth(u) < depth_{nh}$ **then**
6: $next\_hop_v \leftarrow u$
7: $depth_{nh} \leftarrow depth(u)$
8: **end if**
9: **end for**
10: **if** $next\_hop_v \neq$ undefined **then**
11: $R_c(next\_hop_v) \leftarrow R_c(v)$
12: **else**
13: **Go to Line 1**
14: **end if**

6.1.2 Power control-based approaches

A simple way to cope with the communication void region problem is through the increment of the void node communication range, as depicted in Figure 6.1c. In this strategy, the void node increases its communication range by means of the power control, to find a neighbor node that can continue forwarding the packet.

Void-handling algorithms, using this strategy, are simple and scalable. However, a high energy cost is incurred as the transmission power is increased. Moreover, packet collisions and, consequently, more retransmissions will take place, since the increment of the interference zone.

Algorithm 3 shows a naive power control-based void-handling algorithm. Each node starts to find a next-hop forwarder using the lowest transmission power level (Lines 4-9). The node will increase to the subsequent transmission power level, regardless of whether it is in a communication void region (Lines 10-12). This algorithm is repeated until either the node determines its next-hop forwarder, or the maximum transmission power level is reached. Finally, the neighbor should also be instructed to adjust its communication range, in order to avoid asymmetric links.

Some routing protocols for underwater sensor networks adjust the power transmission to improve link reliability, as in CARP [106]. Herein, we are interested in those works in

which the power control is used to find a next-hop forwarder. In Focused Beam Routing (FBR) protocol [36], the forwarder node multicasts a request-to-send (RTS) message, using the lowest power level. This message contains the location of both the forwarder and the destination. Each receiver node that lies within a cone of angle $\pm\theta/2$ emanating from the transmitter towards the final destination is a candidate to forward the packet, and responds to the RTS message. If there is no node within the transmission cone that can be reached at the current power level, the forwarder node increases its transmission power to the next level and multicasts the RTS packet.

Al-Bzoor et al. [107] proposed a routing schema in which nodes are assigned to concentric layers centered on the sink. Data packets are forwarded to the nodes located in the next closest layer to the sink, until the packet reaches it. Adaptive power control is used by the nodes to increase their power level to ensure connectivity when the network is sparse, and decrease it to reduce the energy consumption when the network is dense and static.

6.1.3 Mobility assisted-based approaches

A more recent strategy proposed to deal with the communication void region problem in underwater sensor networks is through mobility assistance (depth adjustment) of the underwater sensor nodes (Figure 6.1d). Void nodes or auxiliary nodes are moved to new depth locations in order to resume the greedy upward forwarding strategy. The main disadvantage of the mobility-assisted methodology is the energy cost of moving void nodes. Algorithm 4 presents a void-handling algorithm based on our proposals [108, 109, 34] that will be discussed in details in the Chapters 7 and 8.

Taking advantage of node depth adjustment capabilities, O'Rourke et al [93] proposed a multi-modal communication. In their proposal, sensor nodes equipped with acoustic and radio modems compute the trade-off between energy cost and data latency, based on the amount of data needing to be sent and the cost of surfacing; they then decide what technology should be used for transmitting the data.

Depth-Controlled Routing (DCR) protocol [108] uses the mobility of the nodes by means of the depth adjustment to organize the network topology. The idea is to move some nodes to new depth locations in order to reduce the number of both void and disconnected nodes in scenarios of attached underwater sensor networks. Using a similar premise, in our previous work [109, 110] we proposed a centralized (CTC) and distributed (DTC) topology control algorithm to move void nodes to new depths, with the goal of

Algorithm 4 Mobility assisted–based void node recovery algorithm

▷ $\Im$ set of void nodes
▷ $\mathcal{D}$ set of depth candidates to the void node
for $u \in \Im$ **do**
  $\mathcal{D} \leftarrow \emptyset$
  for $v \in \mathcal{V} \setminus \Im$ **do**
    $d \leftarrow D(u, v)$ ▷ Euclidean distance considering only X,Y coordinates
    if $d \leq R_c(u)$ **then**
      determine $Z(u)_{new}$, such that
      $(X(u) - X(v))^2 + (Y(u) - Y(v))^2 + (Z(u)_{new} - Z(v))^2 \leq R_c(u)$
      if $Z(v) < Z(u)_{new}$ **then**
        $\mathcal{D} \leftarrow \mathcal{D} \cup \{Z(u)_{new}\}$
      end if
    end if
  end for
  if $|\mathcal{D}| > 0$ **then**
    $Z(u) \leftarrow Z' \in \mathcal{D} : \forall Z \in \mathcal{D}, |Z(u) - Z'| < |Z(u) - Z|$
    $\Im \leftarrow \Im \setminus \{u\}$
  end if
end for

resuming the greedy forwarding routing in long-term monitoring of underwater sensor networks. GEDAR [34, 111] routing protocol uses the depth adjustment capability of the nodes to move void nodes to new depth locations, in order to resume greedy forwarding in the scenario of short-term underwater mobile sensor networks.

6.2 Preliminaries

6.2.1 Network model

We concentrate on static underwater sensor network scenarios where self-buoyant sensor nodes are deployed with moorings. In this scenario, underwater sensor nodes such as AquaNode [93] or Telesonar SM-75 SMART modems from Teledyne Benthos [112] are deployed at specific locations, and remain static for long-term monitoring applications such as water quality [90] and hydroelectric reservoir [113] monitoring. Accordingly, we

have a set of $\mathcal{N}$ sensor nodes $N_1, \ldots, N_{|\mathcal{N}|}$ and $\mathcal{S}$ sonobuoys $S_1, \ldots, S_{|\mathcal{S}|}$ are deployed in a 3 D geographic underwater area.

Sensor nodes are randomly deployed with moorings at the bottom of the sea. They can adjust their depth by means of inflatable buoys or winch-based apparatus by adjusting the tether (e.g., AquaNode [93]), incurring in an energy cost of E_m joules/meter. We consider that each sensor node generates data packets of L_d bytes according to a Poisson process with the same parameter of λ pkts/min. Acknowledgment packets of size L_a bytes are used to confirm the successful reception of the data packet in each hop.

Sonobuoys (or sinks) can be deployed at the surface of the sea in a planned manner. They are responsible for delivering the data packets collected from the sensor network to the monitoring center. Sonobuoys are equipped with both acoustic and radio transceivers; they use acoustic links to send commands and receive data from sensor nodes, and the radio links forward the data packets to the monitoring center. As in [35, 94], we assume that a packet is correctly received and can be delivered to the monitoring center if it arrives at a sonobuoy, since the sound propagates (speed of 1.5×10^3 m/s in water) five orders of magnitudes slower than radio (with a propagation speed of 3×10^8 m/s in air).

The network topology is modeled by a graph $\mathcal{G} = (\mathcal{V}, \mathcal{E})$, where $\mathcal{V} = \{\mathcal{N} \cup \mathcal{S}\}$ is the set of nodes, and $\mathcal{E}$ is the finite set of links between them. Each node v has a communication range $R_c(v)$ and a carrier-sensing range $R_h(v)$, $R_h(v) \geq R_c(v)$. The carrier-sensing range is the area, in addition to the communication range area, in which a transmission is heard, but the signal is so weak it may not be decoded correctly. Each node v can adjust its transmission power to the corresponding communication range values of the finite set $\Gamma = \{R_{c1}, R_{c2}, \ldots, R_{cn}\}$, when using the power control-based void-handling strategy. We define $N_e(v)$ as the neighborhood set of v formed by the nodes with a distance less than or equal to $R_c(v)$, and the $N_h(v)$ formed by nodes in the region $R_c(v) - R_h(v)$.

When a node v transmits a packet, all nodes inside the sphere with the radius $R_h(v)$, $N_e(v) \cup N_h(v)$, can hear the transmission. However, only the nodes with a distance less than or equal to $R_c(v)$, $N_e(v)$, will receive the signal with sufficient power strength to be correctly decoded with high probability. Thus, all nodes inside the carrier-sensing range of v will interpret the channel as busy, and will not be capable of accessing the medium during the v's transmission [114]. Note that considering the node $u \in N_e(v)$ as the next-hop of v, the set of nodes $H(v) = N_e(v) \setminus \{u\} \cup N_h(v)$ will consume energy for the reception of the unintended v's packets, even discarding them.

In geographic routing protocols using the greedy upward forwarding strategy, the neighbor node closer to the surface is selected as the next-hop forwarder. Let $p(v, s)$ be

the routing path from the node v to a surface sonobuoy s determined from the greedy upward forwarding strategy. We define the set $P = \{p(v, s) : \forall v \in \mathcal{N}\}$ composed by the routing paths of all sensor nodes.

6.2.2 Packet collision probability

We consider that all nodes use slotted-ALOHA as the MAC layer protocol. The choice of this MAC protocol was made in light of its superior performance to random access and schedule-based MAC protocols in heavier traffic load scenarios [115, 55]. In slotted-ALOHA, the time is divided into slots of fixed duration, T_{slot}, equal to the transmission time of the maximum frame plus the guard time. Thus, each node with a packet to send starts its transmission at the beginning of the slot it has selected. If a conflict occurs, the transmission is rescheduled to a random slot in the future. The MAC layer of each node can be modeled as a M/G/1 queue with an arrival rate of λ, as the packet generation rate in each node follows a Poisson process with the same parameter λ, and service rate of $1/T_{slot}$. For a more complete description see [116]. The probability that the node's queue is not empty is:

$$P_{ne} = \min\{\rho, 1\}, \tag{6.1}$$

where $\rho = \lambda T_{slot}$, is the system utilization factor. From the n nodes affecting one another, a successful transmission occurs when only one node has a packet to transmit for a given slot; that is, the queue of the other nodes is empty. This probability is given according to:

$$P_s = \binom{n}{1} P_{ne}(1 - P_{ne})^{n-1}. \tag{6.2}$$

From Eq. 6.1 and Eq. 6.2, the collision probability P_c is [116]:

$$P_c = 1 - P_s - (1 - P_{ne})^n. \tag{6.3}$$

We use the concept of *coverage of an edge* [117] to determine the number of concurrent nodes n during a transmission from the node u to v. Let $D(u, r)$ denote the sphere centered at u with radius r, the coverage of the edge $e = (u, v)$ is defined to be the cardinality of the set of nodes covered by the sphere, induced by u and v as:

$$n = |\{w \in \mathcal{N} \mid w \text{ is covered by } D(u, R_c(u))\} \cup \{w \in \mathcal{N} \mid w \text{ is covered by } D(v, R_c(v))\}|. \tag{6.4}$$

6.3 The Proposed Analytical Framework

In the following we devise two important metrics to study the trade-offs of each methodology: *sensing coverage rate* and *energy consumption*.

6.3.1 Sensing coverage rate

The sensing coverage rate of a sensor network is defined as the portion of the monitored area from the total area of interest. A point of the area of interest is said to be covered when its Euclidean distance to a sensor node is less than or equal to the sensing coverage radius [118]. Let n_u be an underwater sensor node with a sphere sensing coverage of radius R_s, centered at ξ_u $(x_{n_u}, y_{n_u}, z_{n_u})$. The sensing coverage area of n_u is defined by the set of points:

$$\mathcal{C}_o^{n_u}(R_s) = \{\xi \in \mathfrak{R}^3 :\parallel \xi_u - \xi \parallel \leq R_s\}, \tag{6.5}$$

where $\parallel \xi_u - \xi \parallel$ is the Euclidean distance between the locations ξ_u and ξ.

In order to determine the set of covered points according to Eq. 6.5, the area of interest D is divided into $(L_x \times L_y \times L_z)/l^3$ cubes of side l. We define an indicator function $f(\xi_i, u)$ to determine whether a cube whose center point is $\xi_i(x_i, y_i, z_i)$ is covered by the sensor $n_u \in \mathcal{N}_n$, as:

$$f(\xi_i, n_u) = \begin{cases} 1, & \xi_i \in \mathcal{C}_o^{n_u}(R_s) \\ 0, & \text{otherwise.} \end{cases} \tag{6.6}$$

The points of the area monitored by a sensor node are considered to be covered only if the node covering them has a routing path to a surface sonobuoy, *i.e.*, if it can deliver the generated packet to the destination. To model that, we define the indicator function to determine the reachable nodes $n_u \in \mathcal{N}_n$ by:

$$g(n_u, s) = \begin{cases} 1, & \exists s \in \mathcal{N}_s \mid n_u \rightsquigarrow s \\ 0, & \text{otherwise.} \end{cases} \tag{6.7}$$

Finally, the coverage rate defined as the fraction of the cubes covered by at least one sensor node with a path to a sonobuoy is given as follows:

$$\mathcal{C}_o = \frac{\sum_{i=0}^{(L_x.L_y.L_z)/l^3} \max_{n_u \in \mathcal{N}_n} \{f(\xi_i, n_u) \times g(n_u, s)\}}{\frac{L_x.L_y.L_z}{l^3}}. \tag{6.8}$$

6.3.2 Energy consumption model

In this section, we concern on the network energy consumption, as it is critical in UWSNs [119]. We model the most relevant sources of energy consumption in underwater sensor networks: communication and node depth adjustment.

Regarding the energy consumption of communication, we approach only the cost relative to data and acknowledge packet transmissions and receptions, although the overhead to neighborhood discovery and routing path configuration is an important aspect to be considered in the design of routing protocols. This is because we are interested in evaluating resulting routing paths after running the next-hop forwarder selection algorithms derived from the power control-, bypassing void regions- and mobility assisted-based strategies; that is, we investigate how the peculiarities in the routing paths built from each void-handling strategy affects the network performance. Moreover, independently of the void-handling algorithm, the routing protocol will perform the neighbor discovery, which will be basically the same throughout our analysis.

6.3.2.1 Expected network energy cost

Each sensor node v will route its data packets to a sonobuoy s through the path $p(v,s) = \{v, v+1, \ldots, s\}$. The nodes belonging to the path $p(v,s)$ are determined from the greedy upward forwarding (GUF) strategy or from the void-handling algorithm when the node is a void node. Let u be a sensor node belonging to the path $p(v,s)$, the node $u+1$ ($u-1$) corresponds to the next (predecessor) from the node u. Data packets will be discarded if their nodes do not have a next-hop forwarder, even after the run of the communication void recovery algorithms.

The expected network energy cost for a network operation time of T minutes is given as:

$$E_{tot} = \sum_{u \in \mathcal{N}} \Big[T\Big(E_{trans}(u) + E_{rec}(u) + E_o(u) \Big) + E_a(u) \Big], \tag{6.9}$$

where E_{trans} is the expected transmission energy cost; E_{rec} is the expected reception energy cost; E_o is the expected overhearing energy cost; and E_a is the expected depth adjustment energy cost. In the following, we derive each expected energy cost considered in Eq. 6.9.

6.3.2.2 Expected transmission energy cost

The energy spent for each node u due to data transmission is a result of both transmissions of its generated packets ($E^t_{gen}(u)$) and relaying of the neighbors' data packets ($E^t_{rel}(u)$), computed as $E_{trans}(u) = E^t_{gen}(u) + E^t_{rel}(u)$. Let u denote a source node and $u+1$ its next-hop forwarder. The u's energy consumption per minute due to transmissions is given as:

$$E^t_{gen}(u) = \lambda \times P_t \times (\bar{N}_{u,u+1} + 1) \left(\frac{L_d}{\alpha B} \right), \tag{6.10}$$

where P_t is the transmission power given by Eq. 2.7, B is the bandwidth, α is the bandwidth efficiency, and $\bar{N}_{u,u+1}$ is the number of unsuccessful attempts to deliver the packet from u to its next-hop forwarder $u+1$.

Assuming that the number of retransmissions is not limited, the expected number of transmissions (ETX) might be used to compute the number of attempts to successfully deliver the packet between the hops u and $u+1$. As an acknowledgment packet is short compared to data packets, we assume their expected number of transmissions is equal to 1. The expected number of transmissions for data packets sent from node u to its next-hop forwarder $u+1$ is given from Eq. 5.10 and Eq. 6.3, as:

$$\bar{N}_{u,u+1} = 1 - \frac{1}{p(d,m) \times (1 - P_c)}. \tag{6.11}$$

Besides its own packet transmission, the node u will also spend energy in relaying data packets from the neighbors where it is the next-hop forwarder. The relay energy cost is due to the transmission of the acknowledgment to confirm to the node $u-1$ the successful data packet reception, and to the relaying of the data packet to the next-hop forwarder $u+1$, given as:

$$E^t_{rel}(u) \;=\; \lambda \times P_t \times \sum_{\substack{p(v,s) \in P \\ v \neq u}} \left[(\bar{N}_{u,u+1} + 1) \times \left(\frac{L_d}{\alpha B} \right) + \left(\frac{L_a}{\alpha B} \right) \right] \times 1_{\Big| u \in p(v,s)}, \tag{6.12}$$

where $1_{|u \in p(v,s)}$ is the indicator function of the condition that the node u belongs to the path $p(v,s)$, and L_a is the size of the acknowledgment packet.

6.3.2.3 Expected reception energy cost

The energy consumption for data reception is a combination of the energy cost for the reception of acknowledgment packets and data packets sent by neighbors, as $E_{rec}(u) =$

$E^r_{gen}(u) + E^r_{rel}(u)$. First, the node will consume energy for the reception of the acknowledgment of its own transmitted data packets, given as:

$$E^r_{gen}(u) = \lambda \times P_r \left(\frac{L_a}{\alpha B} \right), \tag{6.13}$$

where P_r is the reception power, the value of which depends on the acoustic modem interface. Besides, for each path P where u is part and acts as a next-hop forwarder for the node $u-1$, u will spend energy to receive the data packets that should be forwarded. This cost is given as follows:

$$E^r_{rel}(u) = \sum_{\substack{p(v,s)\in P \\ v\neq u}} \left[(\bar{N}_{u-1,u} + 1) \times \left(\frac{L_d}{\alpha B} \right) + \left(\frac{L_a}{\alpha B} \right) \right] \times 1\Big|_{u\in p(v,s)}. \tag{6.14}$$

6.3.2.4 Expected overhearing energy cost

Sensor nodes spend energy when they overhear unintended data transmissions. For each node u, this cost corresponds to the u's unintended data transmissions performed by sensor nodes inside of u's carrier-sensing range. The energy consumption relative to overhearing is given as:

$$E_o(u) = \lambda \times P_r \times \sum_{p(v,s)\in P} \sum_{i=0}^{|p(v,s)|} \left[(\bar{N}_{v_i,v_{i+1}} + 1) \times \left(\frac{L_d}{\alpha B} \right) + \left(\frac{L_a}{\alpha B} \right) \right] \times 1\Big|_{u\in H(v_i)}. \tag{6.15}$$

6.3.2.5 Expected depth adjustment energy cost

Finally, sensor nodes spend energy during the depth adjustment regardless of whether they are using a mobility assisted-based void-handling algorithm. Let u be a void node initially deployed at z'_u. If it is a void node, the recovery algorithm will move it to a new depth location, for instance z''_u. From u's displacement $\delta_u = |z''_u - z'_u|$ and the energy cost in Joules per meter for the adjustment E_m, the energy consumption of the node relative to the depth adjustment is given as

$$E_{adj}(u) = \delta_u \times E_m. \tag{6.16}$$

6.4 Numerical Results

In this section, we instantiate our analytical framework and evaluate the performance of the power control-, bypassing void regions-, and mobility assisted-based void-handling

strategies by means of the representative Algorithms 1, 3, 2 and 4 described in Section 6.1. Herein, the main goal is to observe the strengths and weakness of each void-handling paradigm according to several UWSN density scenarios and configurations.

We use the R package[1] to implement to implement and solve the proposed modeling, as well as the the considered void-handling algorithms. In our numerical evaluation, we implement the Urick's model described in Section 2.4 to simulate underwater environment and physical layer acoustic communication. As an important input of our model, we generate several network topologies for each considered density. Thus, the obtained results for each configuration correspond to an average value of 50 runs of our model, with a confidence interval of 95%.

6.4.1 Model setup

It is important to mention that in the current testbeds a few units of underwater sensor nodes are utilized and carefully deployed at specific locations [89, 120]. This is due to the high cost of these devices. However, in our study, we have explored the scenarios and system configurations that were extensively considered in the literature when simulating well-known geographic routing protocol proposed for underwater sensor networks [121, 13, 94, 93, 108, 109, 116]. The reason to consider random deployments of moderate to high density is to investigate the void-handling methodologies in future deployments of low cost underwater sensor nodes [90], as well as to be consistent with related work. Accordingly, the default simulation parameters are presented in Table 6.2. The parameter values were obtained from the Telesonar SM-75 SMART modems from Teledyne Benthos [112], as well as from related work.

We randomly deploy varying numbers of underwater sensor nodes with moorings, ranging from 80 to 400 in a 3 D region measuring 2500 m×2500 m×3500 m. It is worth noting that some nodes can work in deeper waters, such as Telesonar SM-75 SMART modems from Teledyne Benthos [112], which can be deployed to a depth of 6700 m. Surface sonobuoys are deployed in a predetermined manner. We divide the surface area into a 9-square grid with sides equal to 500 m, where $\mathcal{S} = \{3, 5, 7\}$ sonobuoys are randomly deployed on each square. We vary the number of sonobuoys to assess the upward greedily forwarding strategy that is proposed in the majority of geographic-based routing protocol designed for UWSNs [35, 13, 94].

In our numeric analysis, each node v has a communication range $R_c(v) = 250$ m.

[1] https://www.r-project.org/

Table 6.2: Model configuration

Parameter	**Value**	**Parameter**	**Value**
Sensing radius (R_s)	250 m	Bandwidth (B)	2000 Hz
Carrier sensing thres.	20 dB	Power reception (P_r)	0.62 W
Node battery	4040000 J	Bandwidth efficiency (α)	1 bps/Hz
Packet gen. rate (λ)	[0.06, 0.1]pkts/min	Energy to move nodes (E_d)	15 J/m
Mac layer protocol	slotted-ALOHA	SNR_{th}	30 dB
Frequency (f)	24 kHz	Network operation time (T)	30 day
Packet payload size	50 bytes		

For the power control-based strategy, each node can set its transmission power to the equivalent communication range of $\Gamma = \{250, 350, 450\}$ m. The carrier sensing range $R_h(v)$ is determined from the transmission power and the carrier sensing threshold.

In the plots, GUF designates Algorithm 1, a greedy upward forwarding routing protocol without a recovery mode; GUF+PA designates Algorithm 3, a greedy forwarding routing protocol with power control-based void-handling algorithm; GUF+VA designates Algorithm 2, a routing protocol with the bypassing void region-based void-handling algorithm; and GUF+DA designates Algorithm 4, a routing protocol with the mobility assisted-based void-handling algorithm.

6.4.2 Greedy forwarding analysis

In this section, we evaluate the performance of the void-handling methodologies. The main goal is to observe how the void-handling algorithms can outperform the traditional geographic-based routing without any recovery procedure.

Figure 6.2 depicts the fraction of nodes located into communication void regions. Interestingly, the use of mobility assisted (GUF+DA) and power control (GUF+PA) outperformed the widely used approach of circumventing void regions (GUF+VA). For instance, GUF+DA and GUF+PA reduced in 40% and 20%, respectively, the fraction of void nodes when as compared with GUF+VA and single GUF in the scenario of moderate density and 27 surface sonobuoy. The reason for all these trends is the same: only bypassing void region-based void handling algorithm can determine an alternative path, if one exists, from the node to a sonobuoy on the network graph model, while power control- and mobility assisted-based void handling strategies can create additional paths to the previously disconnected nodes, as both strategies change the network topology.

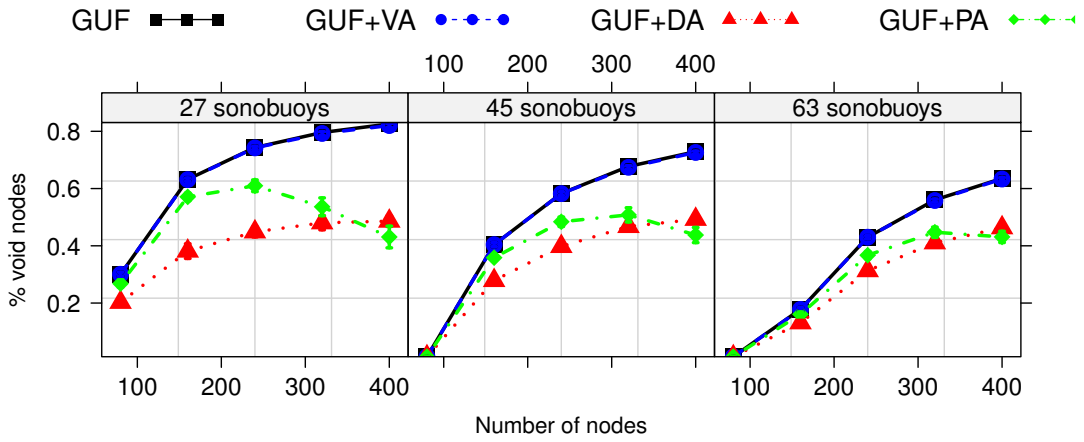

Figure 6.2: Percentage of void nodes

The aforementioned conclusion provides an useful insight. For future design of geographic-based routing protocol in low to moderate UWSN density, topology control-based methodologies are more suitable to be used as void-handling procedures. This is because they can organize the network topology in a such way that new routing paths will be created. Bypassing void region is suitable for scenarios of high density with few void nodes. In this case, it is highly probable that a void node will have a neighbor that can continue forwarding the packet through a path circumventing the void region.

6.4.3 Covered area of interest

In this section, we evaluate how the use of void-handling approaches can improve the fraction of covered area. It is important to remember that in our analytical framework, a point of the area is covered if it is inside of the sensing range of at least one node that can deliver collected data to surface sonobuoys, as modeled in Section 6.3.1.

Figure 6.3 shows the fraction of the area of interest that is covered by at least one sensor node. As expected and confirmed in the plot, the fraction of covered points increases in accordance with network density. When the number of surface sonobuoys increases, the fraction of covered area increases. This is because more nodes become connected with a routing path to a sonobuoy. Moreover and more importantly, it is possible to observe that the topology control-based void-handling algorithms (GUF+DA and GUF+PA) perform better that GUF+VA, increasing the covered area in 71% and 72% for the scenario of 27 sonobuoys, respectively. This is because these approaches

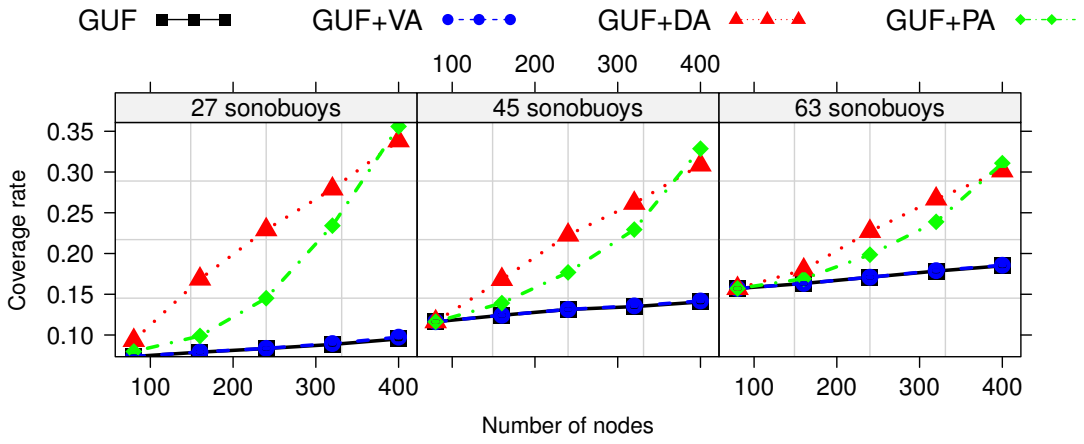

Figure 6.3: Percentage of the covered area of interest

increased the fraction of nodes that have a path to a given destination, as corroborated by Figure 6.2. Thus, more nodes are apt to deliver the collected data.

To summarize the aforementioned result, the investigated topology control-based void-handling strategies for underwater sensor networks proved efficient in coping with the void node problem, from the perspective of improving path determinations to the destinations. As an immediate consequence of this result, the sensing coverage can be improved as more nodes can deliver the gathered data packets. However, the widely used bypassing void-handling approach will not perform well especially in scenarios of low density.

6.4.4 Energy consumption analysis

In this section, we evaluate how the void-handling approaches will impact on the network lifetime. Here, we compute the network lifetime as the time until the battery depletion of the first sensor node. In order to perform a better comparative analysis, this metric is given as a ratio between each void-handling strategy by the greedy upward forwarding strategy, with no void node recovery algorithm (GUF).

Figure 6.4 depicts the normalized network lifetime for the scenario of 63 surface sonobuoys. As shown in the plot, GUF+VA has performance similar to the GUF approach. This is due its poor performance in reducing the percentage of nodes in void areas, as showed in Figure 6.2. GUF+DA outperforms GUF+PA mainly in medium- to high-density network scenarios. For the high density scenario, the network lifetime is

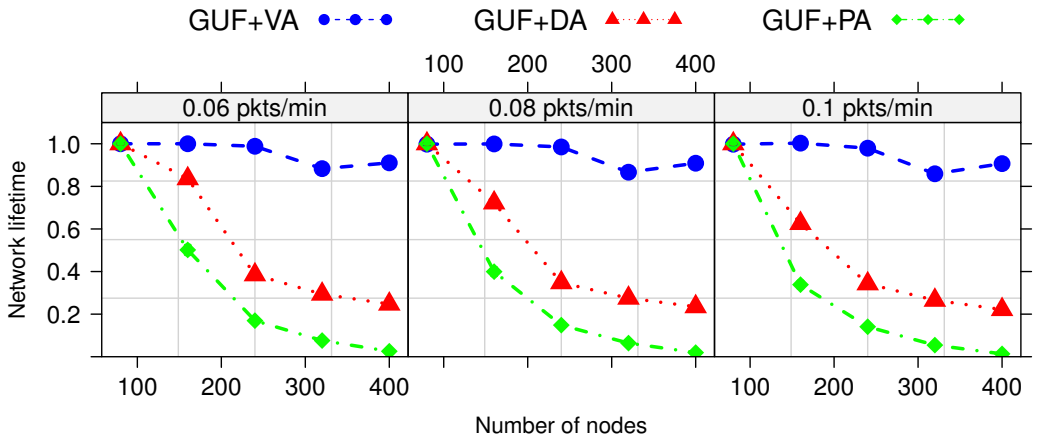

Figure 6.4: Normalized network lifetime for 63 sonobuoys

66% higher when GUF+DA is used instead of GUF+PA. This is due to the high transmission power needed to transmit data packet along long distances. The reason for this is that in high density scenarios, void nodes are moved to among short distances [110], whereas GUF+PA still result in a significant number of of nodes using more transmission power value, as shown in Figure 6.5. Moreover, the use of high communication range in the GUF+PA approach, more collisions and retransmissions will take place because of the longer carrier sensing range, and an increasing number of nodes will be within the interference zone of the transmitters, increasing the energy consumption relative to the overhearing packets operation.

To summarize the aforementioned results, GUF+VA is suitable for scenarios of low network density. This is because the three approaches have similar results in terms of reducing void nodes, but GUF+VA spends less energy than GUF+DA and GUF+PA in those scenarios. However, GUF+PA and GUF+DA are suitable for scenarios of medium to high density, in which the fraction of void nodes ranges from moderate to low. In these scenarios, GUF+PA is adequate for very low traffic loads, whereas GUF+DA suits moderate to high loads, as the energy cost to move the nodes is diluted over time.

6.4.5 Network topology analysis

In this section, we analyze various peculiarities related to the resulting network topology after each void-handling strategy, which impact on the network performance and energy consumption.

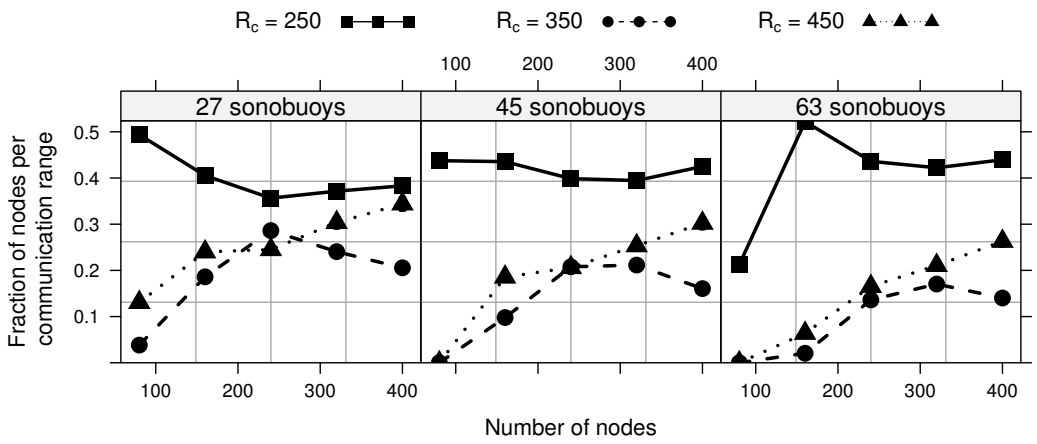

Figure 6.5: Fraction of nodes per communication range value

Figure 6.5 shows the fraction of nodes by each transmission power level on the power control-based void handling strategy. This plot shows that when the network density increases in term of number of surface sonobuoys, the fraction of nodes using 350 m or 450 m as their communication range decreases. This occurs because isolated nodes that select a large communication range in low-density scenarios to have a path to a sonobuoy will decrease with the increment of the number of sensor nodes, as confirmed by the results of GUF performance in Figure 6.2.

Figure 6.6 shows the percentage of nodes that were moved to new depths when the mobility assisted-based void-handling algorithm was used. As expected and confirmed in the plot, the increment of the surface sonobuoys decreases the percentage of moved nodes. In the hard scenario of low-density, moved nodes were reduced by approximately 95% when surface sonobuoys varied from 27 to 63. When the number of sensor nodes increases, the fraction of moved nodes increases until moderate density is reached. The reason for this is that some isolated nodes in low density scenarios cannot be moved, as they cannot communicate with sonobuoys, regardless of proximity to the surface of the sea. From moderate to high densities, the moved nodes are reduced, given that fewer nodes are in void regions. This is corroborated by the analysis of GUF performance in Figure 6.2.

Figure 6.7 shows the complementary cumulative distribution function (CCDF) of the number of hops for a different number of sensor nodes and surface sonobuoys. As a general trend, the plots show the presence of some long paths when using GUF+VA. For instance, Figure 6.7b shows that more than 20% of the paths have 10 or more hops,

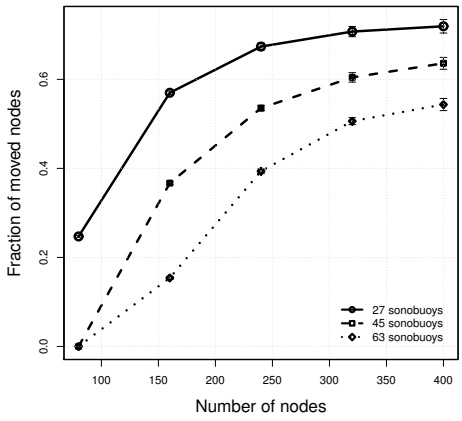

Figure 6.6: Fraction of nodes moved to new depths

whereas this value is less than 5% for GUF, GUF+DA and GUF+PA. This behavior is already expected to bypass void handling-based approaches that try to deliver the packet by routing it along an alternative path circumventing the void region.

6.5 Concluding Remarks

In this Chapter, we proposed an analytic framework to evaluate the performance of the void handling algorithms in underwater sensor networks. The proposed model considered the unique characteristics of the underwater acoustic communication and the peculiarities of power control-, bypassing void region-, and mobility assisted-based void node recovery strategies. Numeric results showed that the widely employed bypassing void region methodology is not the better strategy to cope with void nodes in low density UWSN scenarios. However, topology control-based methodologies are preferable since they change the topology creating new communication links.

More specifically, the proposed mathematical framework provided useful insights for the future design of void-handling procedures. For instance, power control-based strategy proved to be impractical for low-density scenarios, given the energy cost for data communication along long-range links. The bypassing void region-based strategy showed to be an attractive solution for low-density scenarios, as a high energy cost is incurred to use power control and mobility assisted-based strategies due to the transmission between far nodes and the cost to move void nodes in the depth adjustment strategy. The mobility assisted-based strategy with the depth adjustment of some nodes was determined as a

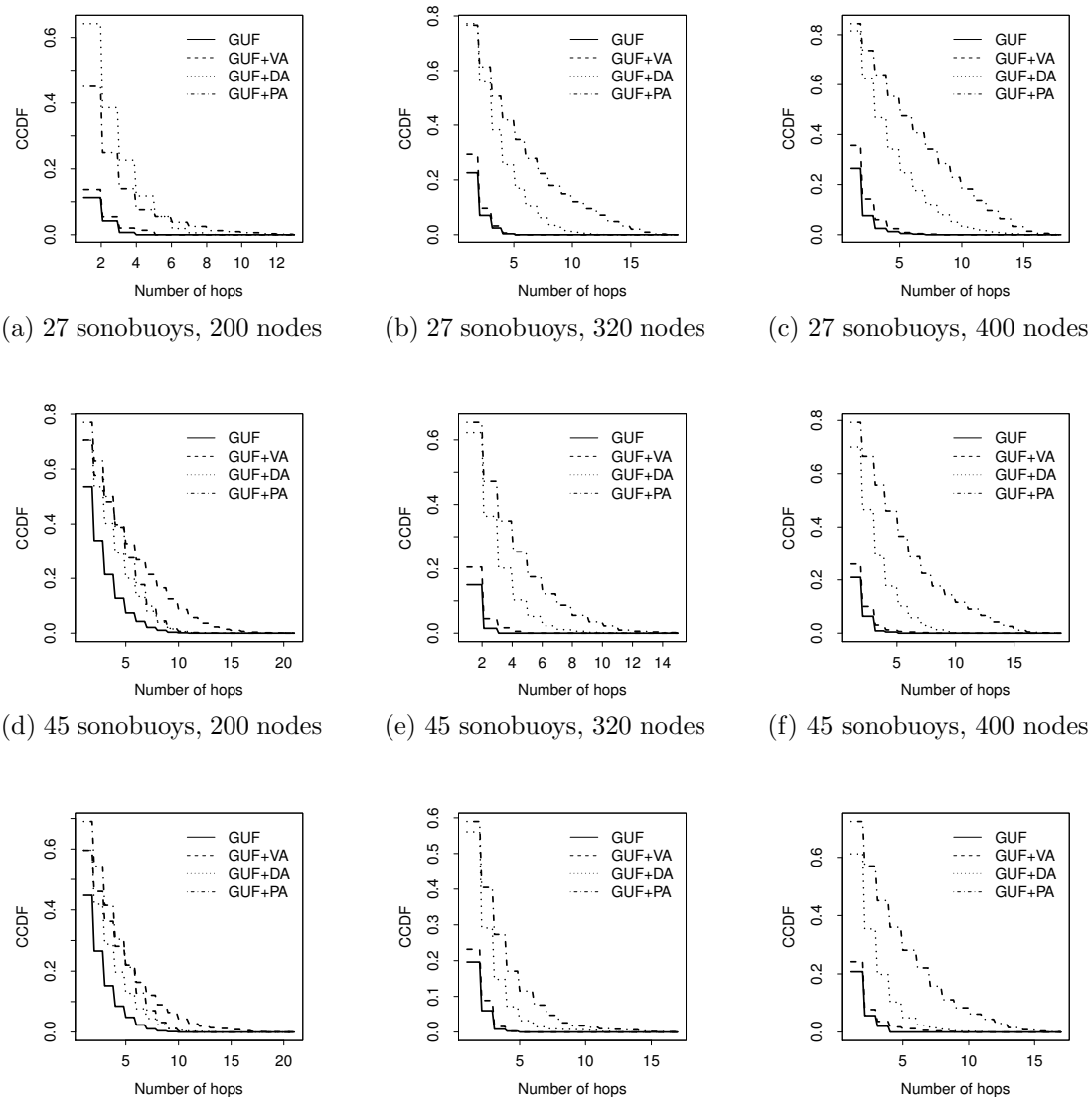

(a) 27 sonobuoys, 200 nodes (b) 27 sonobuoys, 320 nodes (c) 27 sonobuoys, 400 nodes

(d) 45 sonobuoys, 200 nodes (e) 45 sonobuoys, 320 nodes (f) 45 sonobuoys, 400 nodes

(g) 63 sonobuoys, 200 nodes (h) 63 sonobuoys, 320 nodes (i) 63 sonobuoys, 400 nodes

Figure 6.7: CCDF of the # of hops for different network densities

viable solution for moderate- to high-density and traffic load scenarios. In these scenarios, nodes will node among short distances, and the energy cost to do this is amortized as long as more data packets are transmitted.

Chapter 7

The CTC and DTC Topology Control Algorithms

In this Chapter, we propose two topology control algorithms based on the depth adjustment of some nodes: Centralized Topology Control (CTC) and Distributed Topology Control (DTC) algorithms. The goal of the proposed algorithms is to organize the network topology for the better use of the greedy packet forwarding strategy, reducing the impact of the local maximum node problem in the non-mobile underwater network performance. Our solutions consider the anycast nature of the underwater sensor network architecture, during the data packet forwarding process. Yet, they use the distance from the nodes to their closest sonobuoy to forward data packets using a greedy strategy.

This Chapter is organized as follows. Section 7.1 presents the centralized topology control (CTC) algorithm. Section 7.2 presents the distributed topology control (DTC) algorithm. Section 7.3 proposes an energy consumption model used to evaluate the CTC and DTC algorithms. Simulation results are showed in Section 7.4. Section 7.5 presents the chapter remarks.

7.1 The CTC Topology Control Algorithm

In this section, we present the proposed centralized depth adjustment-based topology control algorithm (CTC) that determines and adjusts the depth of isolated and void nodes using the location information about all nodes $\mathcal{N}$.

Algorithm 5 shows the main steps of CTC. From the network graph $\mathcal{G}$, CTC performs the depth first search (DFS) algorithm for each node $s_i \in \mathcal{N}_s$ as the root and obtains the

number of hops $d[n_i, s_i]$ n_i needs to reach the sonobuoy s_i (Lines 4-6). If $d[n_i, s_i]$ is equal to zero, node n_i does not have a path to the sonobuoy s_i. The set Φ of isolated nodes (Lines 7-11) is determined as:

$$\Phi = \{n_i \in \mathcal{N}_n : \sum_{s_i \in \mathcal{N}_s} d_{n_i}(s_i) = 0\}. \tag{7.1}$$

Afterward, CTC determines the new depth of those nodes such that they have a path to a sonobuoy. Let $\Upsilon = \overline{\Phi}$ be the set of nodes that have a path to a sonobuoy. For each node $n_i \in \Phi$, we determine the set $\mathcal{C}_{n_i}$ of candidate neighbor nodes in Υ such that n_i can reach all nodes in $\mathcal{C}_{n_i}$ and, thus, reaches a sonobuoy (Lines 19-23). Intuitively, the set of candidate neighbors for an isolated node is formed by nodes that have a path to a sonobuoy and the Euclidean distance between themselves and the isolated node, considering only the (x, y)-axes, is less than or equal to the communication radius. Thus, we determine in what depth $z_{n_i}^{n_j}$ (referred just as z_i^j for clarity purpose) the isolated node n_i must be so it can communicate with each candidate neighbor n_j in $\mathcal{C}_{n_i}$ by solving the quadratic equation:

$$(x_{n_i} - x_{n_j})^2 + (y_{n_i} - y_{n_j})^2 + (z_i^j - z_{n_j})^2 = r_c^2. \tag{7.2}$$

Finally, n_i will be moved to the new depth that will lead to the smallest displacement, *i.e.*, $z_i^* = \text{argmin}_{\forall z_i^j}\{|z_{n_i} - z_i^j|\}$, and the set Φ is updated, $\Phi = \Phi \cup \{n_i\}$. Along this adjustment, it is possible that a node, even at the surface level, *i.e.*, $z = 0$, cannot have a path to any sonobuoy. For those cases, the node is left isolated.

CTC copes with the local maximum node problem after the previous phase is finished. It determines which nodes are in the communication void region examining the neighborhood of each node and then, calculates what must be the depth such that the node can participate effectively in the routing data process using an anycast greedy geographic routing strategy. We have the set $\Gamma = \{n_i \in \mathcal{N}_n : D(n_i, s_{n_i}^*) \leq D(n_j, s_{n_j}^*), \forall n_j \in N(n_i)\}$ of nodes in the communication void region. As in the previous phase, we determine the set of candidate neighbors $\mathcal{C}_{n_k}, \forall n_k \in \overline{\Gamma}$, and the new depths z_i^k that the void node n_i must be so it can communicate with each $n_k \in \Gamma$. However, the depth z_i^k is only satisfactory if $D(n_k, s_{n_k}^*) < D(n_i, s_{n_i}^*)$ is held. As above, the void node will be moved to the new depth that will lead to the smallest displacement.

Localization and time synchronization are challenging problems even in terrestrial wireless sensor networks [122, 123, 124]. In order to obtain the position information about nodes, we use the localization system proposed by [86] to get the nodes' location. In this

Algorithm 5 CTC algorithm

procedure determine_isolated_nodes()
{d[n,s] ▷ number of hops from node n reaches the sonobuoy s}
{Φ ▷ set of isolated nodes}
for all $s \in \mathcal{N}_s$ **do**
  $d[, s] \leftarrow DFS(\mathcal{G}, s)$
end for
for all $n_i \in \mathcal{N}_n$ **do**
  if $\sum_{s_i \in \mathcal{N}_s} d[n_i, s_i] = 0$ **then**
    $\Phi \leftarrow \Phi \cup \{n_i\}$
  end if
end for
return Φ
end procedure

procedure determines_new_depth(Φ)
{$\Upsilon = \overline{\Phi}$ ▷ set of nodes that has a path to a sonobuoy}
{C_{n_i} ▷ set of neighbors candidate}
for all $n_i \in \Phi$ **do**
  for all $n_j \in \Upsilon$ **do**
    if $\sqrt{(x_{n_i} - x_{n_j})^2 + (y_{n_i} - y_{n_j})^2} \leq r_c$ **then**
      $C_{n_i} \leftarrow C_{n_i} \cup \{n_j\}$
    end if
  end for
  determine the depth z_i^j $\forall n_j \in C_{n_i}$ such that Equation 7.2 holds
  $z_i^* \leftarrow \text{argmin}_{\forall z_i^j}\{|z_{n_i} - z_i^j|\}$
  $\Phi \leftarrow \Phi \cup \{n_i\}$
end for
end procedure

localization system, an underwater autonomous vehicle (UAV) dives to a fixed depth following a predefined trajectory and then broadcasts a wake-up beacon to declare its presence. The sensor, upon receiving the beacon, starts a range measurement by sending a location request packet. When the UAV receives a location request message, it replies with a response packet the includes its coordinates. Thus, the estimated coordinates of the sensor nodes are obtained by the range measurements and the received UAV coordinates.

The abovementioned localization system does not require a priori infrastructure or synchronization between sensor nodes. At the end of the UAV-aided localization operation, the monitoring center has the position information about all sensor nodes. For this, UAVs can disseminate the nodes' location to sonobuoys along their trajectory or send directly to a monitoring center.

After CTC finishes, UAVs inform isolated and void nodes the new depth they must go. Furthermore, UAVs broadcast a beacon informing a delay that all nodes should wait before starting the data collection and reports. This delay corresponds to the time required to the UAVs to disseminate the information and the isolated and void nodes to reach their new depths.

7.2 The DTC Topology Control Algorithm

In this section, we propose the distributed topology control (DTC) algorithm where each node locally determines if it is in a communication void region and then starts the depth adjustment process, if necessary. To better understand the proposed protocol, we define the following concepts used throughout this section:

- **Waiting time for depth adjusting decision.** The decision of the depth adjustment occurs in a prioritized manner so that the shorter the distance of the node to its closest sonobuoy, the shorter the waiting time to decide if it must move or not to a new depth. Thus, when a void node starts the depth adjustment, all nodes with smaller distance to their closest sonobuoy is already done their depth adjustment and they can act as a next-hop using the greedy forwarding strategy, if it was able to find a geographic greedy path to some sonobuoy. The waiting time for the node n_i is $t_i^w = D(n_i, s_{n_i}^*)/v$, where v is the velocity of nodes' vertical movement.

- **Status of a node:** During the topology control phase, a node n_i can have different status: *waiting* (waiting for the time t_i to expire), *adjusting* (moving to a new

depth) or *done* (finalized the topology control algorithm).

- **adjusting_information_message.** Message periodically disseminated by void nodes during the depth adjustment. This message contains the *id* of the void node and *its updated distance* to its closest sonobuoy.

- **replay_message:** Replay of the adjusting_information_message, which is sent by a node with status *done* to inform the void node that it can stop its adjustment given that it must use the node id contained in the message as the next-hop. Furthermore, the replay_message contains the distance of the sender to its closest sonobuoy.

Algorithm 6 describes the DTC procedure. First of all, the sensors determine the time they must wait before starting the depth adjustment (Lines 1-5). After that, the nodes verify if they must move to a new depth or not (Lines 7-21). A node does not need to adjust its depth if *(i) it has a direct connectivity with any sonobuoy; or (ii) it has a neighbor that can act as a next-hop using the greedy geographic forward strategy.* In the first case (Lines 8-11), if the node has direct communication with its closest sonobuoy, it updates its status to *done* and broadcasts a beacon with its *id* and *distance* to its closest sonobuoy, to inform its neighbors about its status. In the second case (Lines 12-15), the node examines its neighbor table and does not adjust its depth if it has a neighbor that can be used as a next-hop.

When a node is in a communication void region and can move to a new depth (Lines 16-20), it starts the vertical movement in direction to the new depth and, periodically (with interval T), runs the procedure *depth_update()* (Lines 23-32). In this procedure, the node gets the current depth information, and if it reaches the new specified depth, it stops the depth adjustment and broadcasts a beacon. Otherwise, the node sends a adjusting_information_message and reschedules a new execution for this procedure. When a node receives an adjusting_information_message and its status is *done*, it responds to this message by saying whether it can act as a next-hop for the void node. Nodes with status equal to *waiting*, updates its neighbor table whenever it receives a beacon.

An important aspect of the DTC is that it does not perform a periodic beacon dissemination. The neighbor table is updated based on beacons sent by nodes that have either direct communication with any sonobuoy (a neighbor with status *done* that can act as a next-hop) or nodes that finished their depth adjustment and now are located in a new depth that allows to send data using the greedy geographic routing protocol. As each node independently starts the procedure to decides if it should or not to move to a new

Algorithm 6 DTC algorithm

1: **procedure** start_topology_control()
2: $t_i^w \leftarrow D(n_i, s_{n_i}^*)/v$
3: status $\leftarrow$ *waiting*
4: Schedule depth_adjustment_decision(t_i)
5: **end procedure**
6:
7: **procedure** depth_adjustment_decision(time)
8: **if** $D(n_i, s_{n_i}^*) \leq r_c$ **then**
9: status $\leftarrow$ *done*
10: next_hop $\leftarrow s_{n_i}^*$
11: Broadcast beacon
12: **else if** $\exists n_j \in N(n_i) \mid ADV(n_j) > 0$ **then**
13: status $\leftarrow$ *done*
14: next_hop $\leftarrow n_j$
15: Broadcast beacon
16: **else if** $(x_{n_i} - x_{s_{n_i}^*})^2 + (y_{n_i} - y_{s_{n_i}^*})^2 \leq r_c^2$ **then**
17: status $\leftarrow$ *adjusting*
18: $z_{n_i}^* \leftarrow \sqrt{r_c^2 - [(x_{n_i} - x_{s_{n_i}^*})^2 + (y_{n_i} - y_{s_{n_i}^*})^2]}$
19: depth_update()
20: **end if**
21: **end procedure**
22:
23: **procedure** depth_update()
24: $z_{n_i} \leftarrow \pi(n_i)$
25: **if** $z_{n_i} = z_{n_i}^*$ **then**
26: status $\leftarrow$ *done*
27: Broadcast beacon
28: **else**
29: Broadcast adjusting_information_message
30: Schedule depth_adjustment(T)
31: **end if**
32: **end procedure**

depth location, the convergence time of DTC will be given according with the distance of the nodes to their closest sonobuoys, the depth of the monitored environment and nodes' vertical movement velocity v. Let $d = \max_{\forall n_i \in \mathcal{N}_n}\{D(n_i, s^*_{n_i})\}$ and the correspondent node n. The convergence time of DTC, in that deployment, will be $\frac{d+D}{v}$, where D is the depth of the n.

7.3 CTC and DTC Energy Consumption Model

In this section we evaluate the energy consumption of the CTC and DTC topology control algorithms and the data communication.

Let $\mathcal{N}_d$ be the set of nodes that moved to a new depth and $\delta_{n_i} = |z_{n_k} - z^*_{n_k}|$ the displacement of each node $n_i \in \mathcal{N}_d$, initially located in the depth z_{n_i}, that was moved to a new depth $z^*_{n_i}$. The total displacement in the network is given by:

$$\Delta^n = \sum_{n_i \in \mathcal{N}_d} \delta_{n_i}. \tag{7.3}$$

From Eq. 7.3, the total energy consumption for the depth adjustment of nodes is:

$$E_{tc} = \Delta^n \cdot E_d. \tag{7.4}$$

In DTC, besides the cost of depth adjustment of the nodes, we have the energy spent by control messages. Let E_o be the energy consumption in DTC due to the overhead. Thus, the total energy consumption for the topology control in DTC is:

$$E_{tc} = \Delta^n \cdot E_d + E_o. \tag{7.5}$$

We derive E_o using an approach similar to the one described in [95]. An *adjusting* node updates the information about its current depth and sends an adjusting_information_message periodically within the interval T. According to Eq. 7.3, the total number of these messages disseminated in the network is $n = \Delta^n / vT$. Let L_m be the size of an adjusting_information_message and P_t the electrical transmission power of the sensor nodes. The lower bound of the energy consumption required to send n of these messages, through a channel with bandwidth equals to B kbps can be given as:

$$E^s_{MIA} = n \cdot \left(P_t \cdot \frac{L_m}{B}\right). \tag{7.6}$$

Let $\mathcal{N}_r(i)$ be the set of nodes that received the ith adjusting_information_ message and $\mathcal{N}_p(i) \subseteq \mathcal{N}_r(i)$ the set of nodes that might act as next-hop and then responded

to this message with a replay_message that has size equals L_r, and posteriorly with a beacon of size L_b. The lower bound of the energy consumption for the reception of adjusting_information_messages, when P_r is used as the energy needed by the transceiver circuit to receive one bit, and to send a replay_message is given by Eqs. 7.7 and 7.8, respectively.

$$E^r_{MIA} = P_r \cdot \sum_{i=1}^{n} \frac{|\mathcal{N}_r(i)|L_m}{B}. \tag{7.7}$$

$$E^s_{MR} = P_t \cdot \left\lceil \frac{\Big(L_r + L_b\Big) \sum_{i=1}^{n} |\mathcal{N}_p(i)|}{B} \right\rceil. \tag{7.8}$$

The energy consumption for the reception of both the replay_message and beacons can be approximated as

$$E^r_{MR} = P_r \cdot \left\lceil \frac{\Big(L_r + L_b\Big) \sum_{i=1}^{n} |\mathcal{N}_p(i)|}{B} \right\rceil. \tag{7.9}$$

Finally, the energy consumption of the send and reception operations of a control message is

$$E_o = E^s_{MIA} + E^r_{MIA} + E^s_{MR} + E^r_{MR}. \tag{7.10}$$

7.4 Performance Evaluation

We evaluate the performance of our proposed geographic routing protocol with the centralized depth adjustment-based topology control and with the distributed depth adjustment-based topology control (referred as GR + CTC and GR + DTC, respectively) against two other proposed routing protocols for UWSNs: DBR (Depth-Based Routing) [35] and VAPR (Void-Aware Pressure Routing) [94].

We implemented the routing protocols using the tool Aqua-Sim [125] v.1.0[1], which is a high fidelity and flexible packet level underwater sensor network simulator based on NS-2. Aqua-Sim effectively simulates the impairment of underwater acoustic channel such as acoustic signal attenuation and packet collisions, and the three-dimensional space

[1]http://obinet.engr.uconn.edu/wiki/index.php/Aqua-Sim

deployment. It implements the Urick's underwater acoustic physical layer model [28], described in Section 2.4.

The metrics we concentrate on during simulations are the *packet delivery ratio*, *i.e.*, the fraction of the packets that were received by the sonobuoys, the *delay*, *i.e.*, the average latency for a packet to reach any sonobuoys, the *number of redundant packets*, *i.e.*, the mean of redundant copies of data packets received by all sonobuoys, and the *energy consumption* per packet per node.

7.4.1 Simulation parameters and algorithms setup

The simulation setup was done according with the parameter values used in [35, 94]. We randomly deploy varying numbers of nodes ranging from 150 to 450 in 3D region of size 1500 m $\times$ 1500 m $\times$ 1500 m. Sensor nodes have a transmission range of $r_c = 250$ m, data rate of 50 kbps, and use the CSMA MAC protocol, as in [35, 94]. Regarding the deposition of the sonobuoys, we divide the surface area of the region of interest into $K = 9$ sub-areas with side equals to $l = 500$ m, and then we evenly deployed N_s/K sonobuoys in each sub-area to evaluate the impact of the increase in the number of surface sonobuoys in the network performance.

The size of the packet payload is 100 bytes. The values of energy consumption were $P_t = 2$ W, $P_r = 0.1$ W, $P_i = 10$ mW and $E_d = 15$ J/m [93] for the transmission, reception, idle and depth adjustment of a node, respectively. The traffic rate generated by each sensor node follows a Poisson process with the same parameter $\lambda = 0.01$ pkts/min.

In our simulation, each run lasts 24 hours. This configuration is used throughout this work if not otherwise specified. The results correspond to an average value of 50 runs with 95% confidence interval. The simulation parameters and the values used are summarized in Table 7.1.

7.4.2 Topology related results

Fig 7.1a shows the performance of the proposed topology control algorithms to the network connectivity for the scenarios with 9, 27, 45 and 63 sonobuoys. First of all, it is worth to note that more than 50% of nodes are isolated for scenarios of low network density, even when the number of surface sonobuoys increases. When the number of sensor nodes increases, the fraction of isolated nodes decreases. The result shows CTC and DTC reduce the fraction of isolated nodes for all scenarios.

Table 7.1: Simulation parameters and topology properties

Parameter	**Value**	**Parameter**	**Value**
Sub-areas (K)	9	Bandwidth (B)	50 kb/s
Sub-area size (l)	500 m×500 m	Mac layer	CSMA
Number of son. ($\mathcal{N}_s/K$)	{1,3,5,7}	Packet payload size	100 bytes
Network size	150 to 450 nodes	Power transmission (P_t)	2 W
Sensor field	$(1500\,\mathrm{m})^3$	Power reception (P_r)	0.1 W
Simulation time	1 day	Power idle (P_i)	10 mW
Packet gen. rate (λ)	0.01 pkts/min	Energy to move nodes (E_d)	15 J/m
Commun. range (r_c)	250 m		

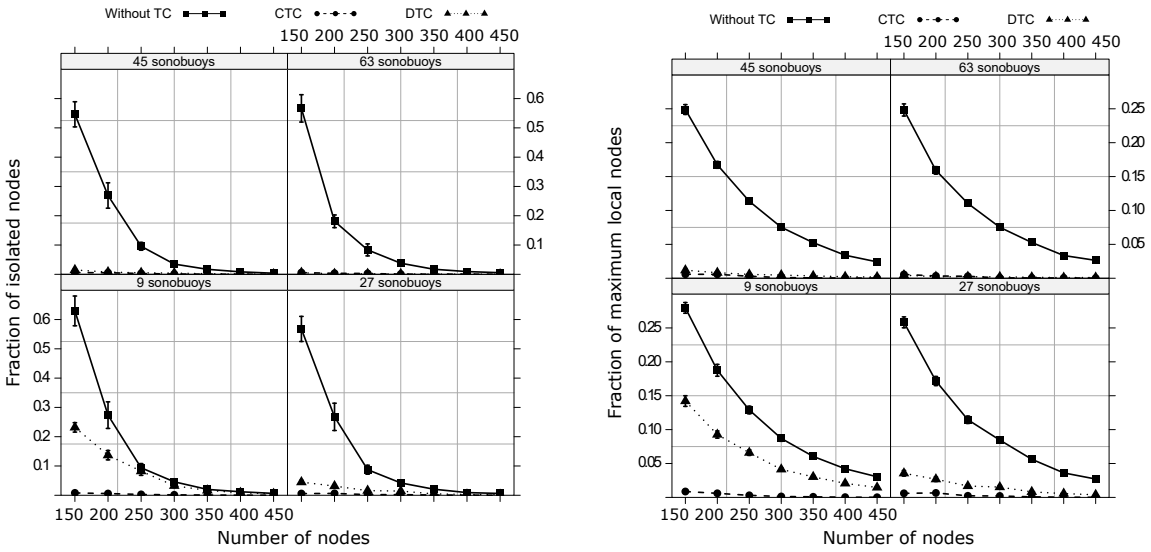

(a) Isolated nodes (b) Void nodes

Figure 7.1: Topology related results

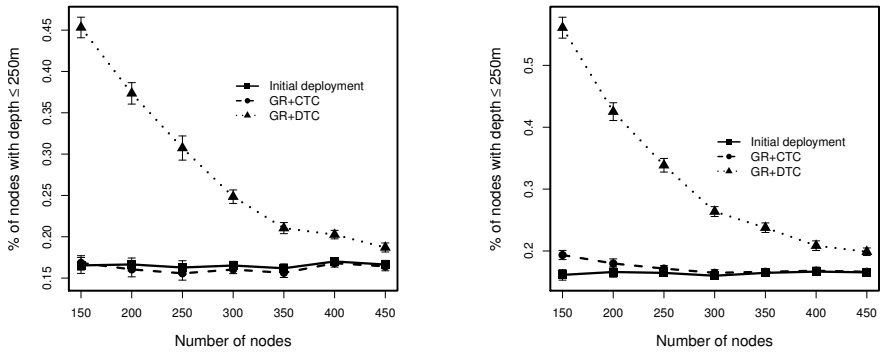

(a) 9 sonobuoys (b) 63 sonobuoys

Figure 7.2: Fraction of nodes closest to sea surface

Similar behavior happens for the fraction of void nodes as shown in Figure 7.1b. The results clearly show the efficiency of the proposed topology control algorithms to derive more adequate topologies that significantly reduce void nodes, *i.e.*, almost 25% in the network topology without the proposed topology control versus approximately 5% with topology control.

The reduction of void nodes showed in Figure 7.1b is achieved by moving some nodes to new depths. Figure 7.2 shows the fraction of nodes located closest to sea surface. As show the results, CTC efficiently moves void nodes to new depths such that the fraction of nodes closest to surface is almost the same of the initial deployment. This is because decisions are made from the whole network topology information. In DTC, as depth adjustment decisions are made locally, the nodes tend to move to depth closest to surface, in order to communicate directly with surface sonobuoys.

Figure 7.3 shows a network topology instance before and after executing the proposed topology control protocols, considering the worst-case scenario of low density. Figure 7.3a depicts the information about the depth of nodes in the initial deployment. Figure 7.3b shows that CTC effectively copes with disconnect and void regions. This is because the algorithm uses the location information of all nodes. For very low-density scenarios, DTC tends to move a significant part of the nodes closer to the surface, as depicted in Figure 7.3c. This is typically reduced once the network density increases and, thus, the number of moved nodes is reduced, as indicated in Figure 7.7a and in the resulting topology for the scenario of 200 sensor nodes showed in Figure 7.3d.

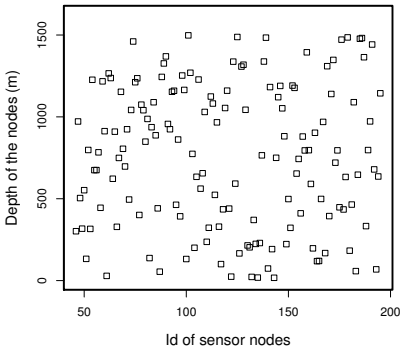

(a) Depth of the nodes in the initial deployment (150 nodes)

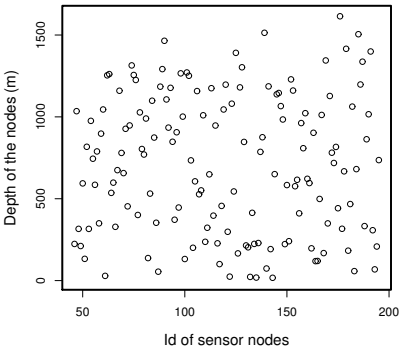

(b) Depth of the nodes after CTC (150 nodes)

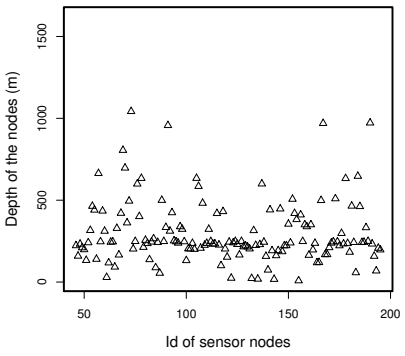

(c) Depth of the nodes after DTC (150 nodes)

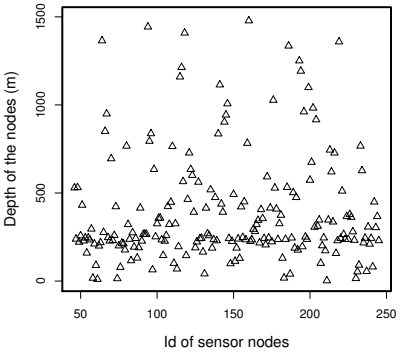

(d) Depth of the nodes after DTC (200 nodes)

Figure 7.3: Analysis of the resulting topology (45 surface sonobuoys)

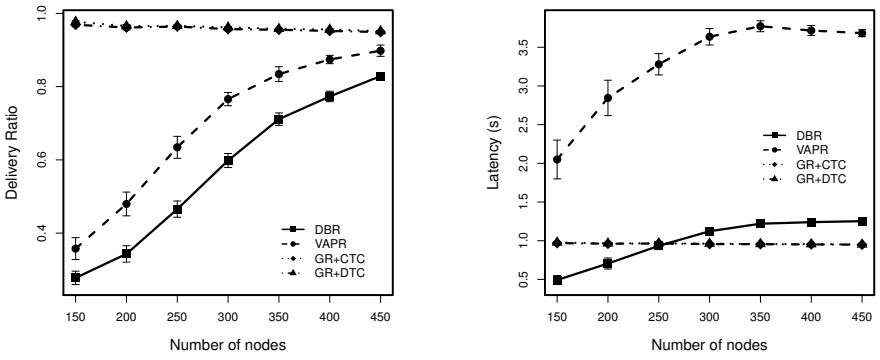

(a) Packet delivery ratio. (b) Average end-to-end delay

Figure 7.4: Simulation results (45 sonobuoys)

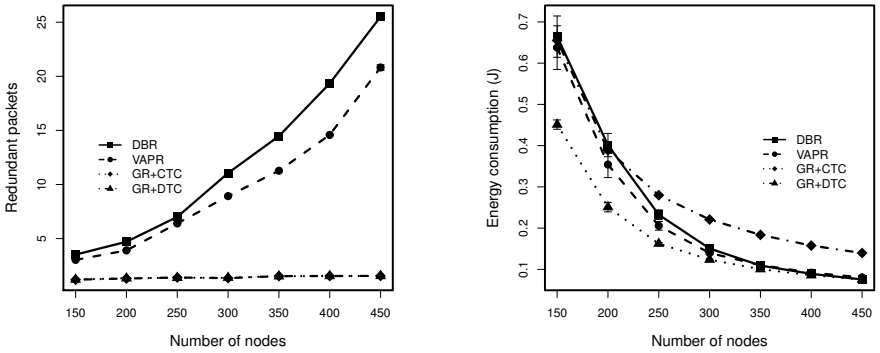

(a) Average # of redundat copies per packet (b) Energy consumption per packet per node

Figure 7.5: Simulation results (45 sonobuoys)

7.4.3 Network performance related results

Figure 7.4a shows that the overall trend of the packet delivery ratio for the protocols is quite consistent with the network topology results, shown in Figures 7.1a and 7.1b. The packet delivery ratio of GR + CTC and GR + DTC outperform those of DBR and VAPR. DBR and VAPR have similar behavior because the way of the sonobuoys are deployed at the sea surface. However, the performance of VAPR is slightly better than DBR because it is aware of void regions and routes packets through directional trails in direction to a sonobuoy.

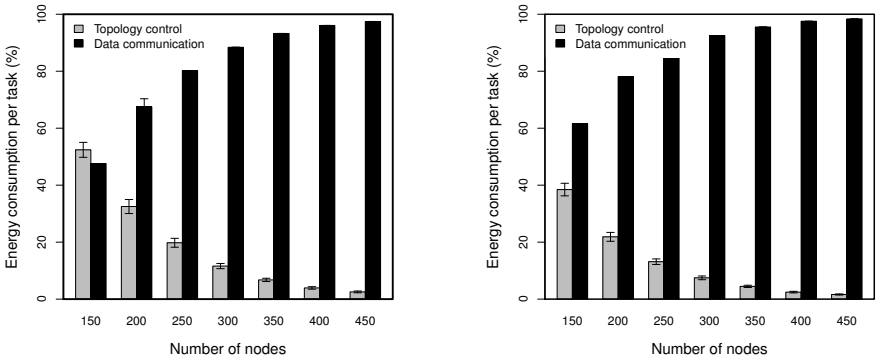

(a) GR + CTC (b) GR + DTC

Figure 7.6: Energy consumption by network operation

Figure 7.4b shows the average latency for all delivered packets. Here, VAPR shows the worst performance due to the opportunistic routing mechanism. As DBR uses a depth-based timer to schedule the forwarding transmissions, it presents a higher delay when compared with GR + CTC and GR + DTC, where data packets are immediately forwarded.

Figure 7.5a examines the average number of redundant copies of data packets received by the sonobuoys. GR + CTC and GR + DTC have similar performance. For those protocols, the redundant copy is due to the broadcast nature of the transmission. Thus, nodes next to sea surface can be located in the communication area of more than one sonobuoy, which receive the same packet. In VAPR, redundant packets are result of failures in the transmission suppression of the opportunistic routing. In DBR, the average number of redundant copies grows significantly with the increase in the number of nodes due to the failure in the suppression of the data transmission of lower priority nodes given that the heuristic to select the next-hop does not guarantee that nodes will be hearing each other.

Figure 7.5b shows the average energy consumption per packet. As a trend, this value decreases for all four protocols when the network density increases. For the case of a lower density, despite the energy consumption for the topology control in GR + CTC and GR + DTC, they have similar behavior as in DBR and VAPR because more packets are delivered.

Figure 7.6a shows the energy consumption in GR + CTC according to the data com-

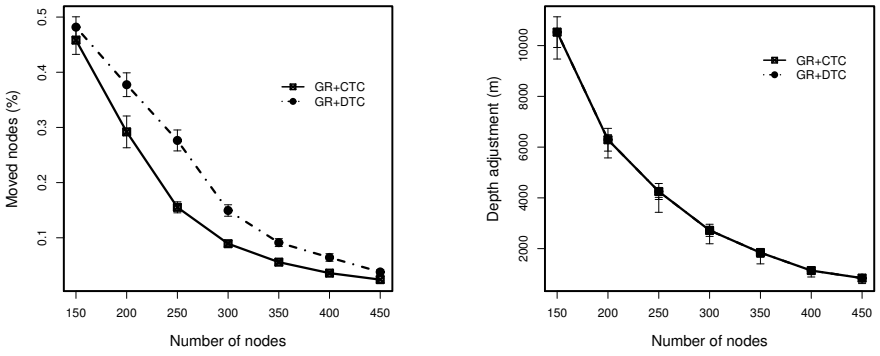

(a) Fraction of moved nodes (b) Average depth adjustment

Figure 7.7: Simulation results (45 sonobuoys)

munication and topology control operation. For lower density, the energy consumption due to the topology control corresponds to a significant part becoming higher than the data communication consumption. This is consistent with the displacement of nodes as shown in Figure 7.7b. The same trend is observed for GR + DTC in Figure 7.6b.

The energy consumption is an important metric that represents the trade-off between the cost of the topology control and the network performance. Despite the high energy consumption of topology control, it is diluted with the significant increment on the fraction of delivered packets, as shown in Figure 7.4a. Therefore, for long-term application (*e.g.*, marine life monitoring) and for applications where large amounts of data are produced in the network (*e.g.*, oil spill plumes monitoring), which need to be effectively delivered with a strong restriction in the fraction of losses that the application can support, this approach is thoroughly adequate. Besides, with mechanisms that efficiently adjust the depth of nodes with minimal energy consumption, this topology control methodology can be applied to improve the overall network performance.

7.4.4 Discussion

The topology control-based through depth adjustment of some nodes can cope with the problem of communicating in void regions and improving the overall network performance. The main weakness of this new methodology is that moving some nodes to new depths (locations) will degrade the sensing task. It is true that nodes' location changes can result in unmonitored regions that were previously covered. However, if the nodes'

deployment happens in a random way (*e.g.*, dropping sensor nodes from an airplane), all regions of the monitoring area are equally important. Otherwise, an optimal deployment, in terms of sensing and communication should take place. Of course, even in randomly deployment scenarios, we desire to have sensor nodes spread along the monitoring area leading to a high coverage.

Another motivation to move disconnected and void nodes is that if we have low or medium density deployment scenarios, where data collection cannot be performed, or due to the high percentage of disconnected nodes (nodes with no path to any sink) as was shown in Figure 7.1a, the data gathering will be done only at the end of the mission. This is what currently happens in the traditional underwater monitoring solutions without networking capabilities, such as the RAFOS floating [126]. This kind of underwater monitoring presents some disadvantages [3] such as no on-line system reconfiguration, limited storage capacity and, most critically and importantly, no failure detection. Thus, if a node fails, it will be possible to detect it only at the end of the monitoring mission, which can be after long periods (*e.g.*, months or even years).

7.5 Concluding Remarks

In this Chapter, we proposed and evaluated a geographic routing protocol and two topology control algorithms (CTC and DTC) for long-time monitoring underwater sensor networks. The topology control approach uses the movement of nodes by means of the depth adjustment, aiming to derive favorable topologies to use the anycast greedy geographic routing protocol.

Simulation results showed that when the network density is lower and consequently, the number of isolated nodes is higher, CTC and DTC effectively organize the network topology such that the fraction of delivered packet data is higher than 90% for most cases. Moreover, we investigate the impact of the depth adjustment in the network energy consumption. The results showed that the topology control through nodes movement leads to a higher energy cost, which is diluted with the increase of the fraction of delivered packets. Besides, with energy efficient depth adjustment mechanisms this methodology is very attractive to effectively use in underwater sensor networks.

Chapter 8

The GEDAR Opportunistic Routing Protocol

In this Chapter, we propose the GEDAR routing protocol. GEDAR utilizes the location information of the neighbor nodes and some known sonobuoys to select a next-hop forwarder set of neighbors to continue forwarding the packet towards the destination. To avoid unnecessary transmissions, low priority nodes suppress their transmissions whenever they detect that the same packet was sent by a high priority node. The most important aspect of the proposed GEDAR protocol is its novel void node recovery methodology. Instead of the traditional message-based void node recovery procedure, we propose a void node recovery depth adjustment based topology control algorithm. The idea is to move void nodes to new depths to resume the geographic routing whenever it is possible.

This Chapter is organized as follows. Section 8.1 presents an overview of the proposed protocol. Section 8.2 describes the opportunistic routing procedures of GEDAR to forward data packets towards the destinations. Section 8.3 describes the proposed void node recovery procedure of GEDAR. Simulation analyzes were conducted in Section 8.4 and Section 8.6 presents the final remarks.

8.1 Basic Idea of GEDAR

The proposed GEDAR routing protocol is an anycast, geographic and opportunistic routing protocol that tries to deliver a packet from a source node to some sonobuoys in mobile underwater wireless sensor network (UWSNs) scenarios. During the course, GEDAR uses the greedy forwarding strategy (please refer to Section 5.3) to advance the

packet, at each hop, towards the surface sonobuoys. A recovery mode procedure based on the depth adjustment of the void node is used to route data packet when it get stuck at a void node.

We consider that, as in [94], each sonobuoy at the sea surface is equipped with a Global Positioning System (GPS) and uses periodic beaconing to disseminate its location information to the underwater sensor nodes. We assume that each underwater sensor node knows its location. The location of the neighbors is known through periodic beaconing. Despite the exact knowledge of the node's location being a strong assumption mainly for a mobile scenario, some proposals have been devoted to solve this problem [127, 128]. Moreover, the localization problem in underwater networks continues to attract research efforts due to the importance of nodes' localization to tag the collected data, track underwater nodes and targets, and to group nodes coordinated motion.

Furthermore, GEDAR is opportunistic routing (OR) aiming to mitigate the effects of the acoustic channel. Thus, a subset of the neighbor nodes is determined to continue forwarding the packet towards some surface sonobuoy (next-hop forwarder set). The research challenge of OR next-hop forwarder set selection is how to determine a list of neighbors such that the hidden terminal problem is reduced. The next-hop forwarder set selection mechanism of GEDAR considers the position of the neighbors and known sonobuoys to select the most qualified candidate neighbors.

When a node is in a communication void region, GEDAR moves it to a new depth to find a neighboring node that can resume the greedy forwarding strategy. The motivations for the use of this new strategy are threefold. First, the node depth adjustment technology is already available, as in [85, 93, 112]. Second, the communication task in UWSNs is expensive. Third, the cost needed to move the nodes to new depths is diluted along the network operation when compared with the case where the node must route data packets along more hops.

8.2 Data Packet Forwarding of GEDAR

8.2.1 Enhanced beaconing

Periodic beaconing plays an important role in GEDAR. In highly dynamic wireless ad hoc network scenarios is desired the use of beaconless routing approaches. This is to avoid excessive overhead due to the topology changes. In aquatic environment, beaconless approach is still more demanding since the highly interference environment and energy

cost of communication. However, GEDAR needs employ a beaconing mechanism since each node must obtain the location information of its neighbors and reachable sonobuoys.

Herein, we need an efficient beaconing algorithm that keeps the size of the periodic beacon messages short as possible. For instance, if each node n_i embeds its known sonobuoy locations $|S_i|$ together with its location, the size of its beacon message in the worst case, without considering lower layer headers, is $2(m+n) \times |N_s| + 2m + 3n$ bits, where m and n are the size of the sequence number and ID fields, and each geographic coordinates, respectively. Given that the transmission of large packets in the underwater acoustic channel is impractical [129], we propose an enhanced beacon algorithm that takes this problem into consideration.

Algorithm 7 is an enhanced periodic beaconing used by GEDAR to broadcast periodic beacons and to handle received beacons. In the beacon messages, each sonobuoy embeds a *sequence number*, its *unique ID*, and its *X, Y* location. We assume that each sonobuoy at the surface is equipped with GPS and can determine its location. The sequence number of the beacon message does not need to be synchronized among all sonobuoys. It is used together with the ID to identify the most recent beacon of each sonobuoy (Line 24). The depth information of sonobuoys is omitted from the beacon message since the sonobuoys are deployed on the surface and vertical movement is negligible with respect to the horizontal movement [38].

Similarly, each sensor node embeds a *sequence number*, its unique *ID* and *X*, *Y*, and *Z* position information. Moreover, the beacon message of each sensor node is augmented with the information of its known sonobuoys from its set $S_i(t)$. Each node includes the *sequence number*, *ID*, and the *X*, *Y* location of the its known sonobuoys. The goal is for the neighboring nodes to have the location information of the all reachable sonobuoys. GPS cannot be used by underwater sensor nodes to determine their locations given that the high frequency signal is rapidly absorbed and cannot reach nodes even localized at several meters below the surface. Thus, each sensor node knows its location through localization services, such as [128]. Localization services incur additional costs in the network. However, the knowledge regarding the location of sensor nodes can eliminate the large number of broadcast or multicast queries that leads to unnecessary network flooding that reduces the network throughput [36]. In addition, the location information is required to tag the collected data, track underwater nodes and targets, and to coordinate the motion of a group of nodes.

In order to avoid long sizes of beacon messages, a sensor node includes only the position information of the sonobuoys it has not disseminated in the predecessor round

Algorithm 7 GEDAR: Periodic beaconing algorithm

```
1: procedure BroadcastPeriodicBeacon(node)
2: m: a new beacon message with the next seq_num
3: if beacon timeout expired then
4:    m.coordinate ← location(node)
5:    if node ∈ N_n then
6:       for s ∈ S_i(node) do
7:          if Λ(s) = 0 then
8:             m.addSon.(seq_num(s), ID(s), X(s), Y(s))
9:             Λ(s) ← 1
10:         end if
11:      end for
12:   end if
13:   Broadcast m
14:   Set a new timeout
15: end if
16: end procedure
17:
18: procedure ReceiveBeacon(node, m)
19: if m is from a sonobuoy then
20:   update(S_i(node), m)
21: else
22:   update_neighbor(m.seq_num, m.id, m.location)
23:   for s ∈ m do
24:      if seq_num(s, m) > seq_num(s, S_i(node)) then
25:         update(S_i(node), s)
26:      end if
27:   end for
28: end if
29: end procedure
```

(Lines 5-12). Whenever a node receives a new beacon message, if it has come from a sonobuoy, the node updates the corresponding entry in the known sonobuoy set $S_i(t)$ (Line 20). Otherwise, it updates its known sonobuoys S_i set in the corresponding entries if the information location contained in the beacon message is more recent than the location information in its set S_i. For each updated entry, the node changes the appropriate flag Λ to zero, indicating that this information was not propagated to its neighbors (Line 25). Thus, in the next beacon message, only the entries in $S_i(t)$ in which the Λ is equal to zero are embedded (Lines 7-10).

We add random jitters between 0 and 1 during the broadcast of beacon messages, to minimize the chance of both collisions and synchronization. Moreover, after a node broadcasts a beacon, it sets up a new timeout for the next beaconing.

8.2.2 Neighbors candidate set selection

Whenever a sensor node has a packet to send, it should determine which neighbors are qualified to be the next-hop forwarder. GEDAR uses the greedy forwarding strategy (Section 5.3) to determine the set of neighbors able to continue the forwarding towards respective sonobuoys. The basic idea of the greedy forwarding strategy is, in each hop, to advance the packet towards some surface sonobuoy.

The neighbor candidate set is determined as follows. Let n_i be a node that has a packet to deliver. Let $N_i(t)$ be the set of i's neighbors and $S_i(t)$ be the set of known sonobuoys at time t. We use the packet advancement (ADV) [130] metric to determine the neighbors able to forward the packet towards some destination. The packet advancement is defined as the distance between the source node S and the destination node D minus the distance between the neighbor X and D. Thus, the neighbors candidate set in GEDAR is given as:

$$\mathcal{C}_i = \{n_k \in N_i(t) : \exists s_v \in S_i(t) \mid D(n_i, s_i^*) - D(n_k, s_v) > 0\}, \tag{8.1}$$

where $D(a, b)$ is the Euclidean distance between the nodes a and b and, $s_i^* \in S_i(t)$ is closest sonobuoy of n_i as:

$$s_i^* = \underset{\forall s_j \in S_i(t)}{\operatorname{argmin}} \{D(n_i, s_j)\}. \tag{8.2}$$

8.2.3 Next-hop forwarder set selection

GEDAR uses opportunistic routing to deal with underwater acoustic channel characteristics. For each transmission, a next-hop forwarder set $\mathcal{F}$ is determined. The next-hop

forwarder set is composed of the most suitable nodes from the next-hop candidate set $\mathcal{C}_i$ so that all selected nodes must hear the transmission of each other aiming to avoid the hidden terminal problem. The problem of finding a subset of nodes, in which each one can hear the transmission of all nodes, is a variant of the maximum clique problem, that is computationally hard [13].

The next-hop forwarder set selection algorithm of GEDAR is based on the proposed in [13]. We use Normalized Advance (NADV) [131] to measure the *"goodness"* of each next-hop candidate node in $\mathcal{C}_i$. NADV corresponds the optimal trade-off between the proximity and link cost to determine the priorities of the candidate nodes. This is necessary because the greater the packet advancement is, the greater the neighbor priority becomes. However, due to the underwater channel fading, the further the distance is from the neighbor, the higher the signal attenuation becomes as well as the likelihood of packet loss. For each next-hop candidate node $n_c \in \mathcal{C}_i$, normalized packet advancement is:

$$NADV(n_c) = ADV(n_c) \times p(d_c^i, m), \tag{8.3}$$

where $ADV(n_c) = D(n_i, s_i^*) - D(n_c, s_c^*)$ is the n_c packet advancement towards its closest sonobuoy s_c^*; d_c^i is the Euclidean distance between the source node n_i and the forwarder candidate n_c and, $p(d_c^i, m)$ is the packet delivery probability of m bits over distance d_c^i given according with Eq. 5.10.

Let $\mathcal{F}_j \subseteq \mathcal{C}_i$ be a set formed by candidate forwarder nodes, ordered according to their priorities (NADV) as $n_1 > n_2 > \ldots > n_k$, that must hear each other. The Expected Packet Advancement (EPA) of the set $\mathcal{F}_j$, which is the normalized sum of advancements made by this set [132, 13], is defined by Eq. 8.4. The objective of the greedy opportunistic forwarding strategy is to determine the subset $\mathcal{F} \subseteq \mathcal{C}_i$ such that the (EPA) is maximized.

$$EPA(\mathcal{F}_j) = \sum_{l=1}^{k} NADV(n_l) \prod_{j=0}^{l-1} (1 - p(d_i^j, m)). \tag{8.4}$$

Algorithm 8 presents the next-hop forwarder set selection of GEDAR. First, Lines 2 to 4 determine the NADV of each qualified neighbor according to Eq. 8.3. Secondly, the neighbor candidate set $\mathcal{C}_i$ is ordered according to the priority of the nodes as a result of the NADV (Line 5). Thirdly, Lines 8 to 18 determine the clusters from the neighbor candidate set $\mathcal{C}_i$. Each cluster $\mathcal{F}_j$ starts with the greatest priority node from $\mathcal{C}_i$ and is expanded by including all nodes in $\mathcal{C}_i$ which have a distance less than $\frac{1}{2}r_c$. Fourthly, each cluster $\mathcal{F}_j$ is expanded to include those nodes in $\mathcal{G}_i$ (a copy from $\mathcal{C}_i$) that have a distance of less than the communication radius r_c for all nodes already in the cluster

(Lines 19-25). The idea is to expand each cluster while maintaining the restriction that each node should hear the transmissions of each other node in the cluster. Finally, the cluster $\mathcal{F}$ with the highest EPA is selected as the next-hop forwarder set.

Algorithm 8 GEDAR: Next-hop forwarder set selection algorithm

1: **procedure** GetNextHopForwarders(source node n_i)
2: **for** $n_c \in \mathcal{C}_i$ **do**
3: $NADV(n_c) \leftarrow d_c \times p(d_i^c, m)$
4: **end for**
5: Order $\mathcal{C}_i$ according with the NADV of the nodes
6: j $\leftarrow$ 1
7: $\mathcal{G}_i \leftarrow \mathcal{C}_i$ {$\mathcal{G}_i$ is a copy of $\mathcal{C}_i$}
8: **while** $\mid \mathcal{C}_i \mid > 0$ **do**
9: $\mathcal{F}_j \leftarrow \{n_1 \in \mathcal{C}_i\}$ {n_1 is the highest priority node of $\mathcal{C}_i$}
10: $\mathcal{C}_i \leftarrow \mathcal{C}_i - \{n_1\}$
11: **for** $n_u \in \mathcal{C}_i$ **do**
12: **if** $D(n_1, n_u) < \frac{1}{2} r_c$ **then**
13: $\mathcal{F}_j \leftarrow \mathcal{F}_j \cup \{n_u\}$
14: $\mathcal{C}_i \leftarrow \mathcal{C}_i - \{n_u\}$
15: **end if**
16: **end for**
17: j$\leftarrow$ j+1
18: **end while**
19: **for** $\mathcal{F}_j$ **do**
20: **for** $n_k \in \mathcal{G}_i$ **do**
21: **if** $D(n_k, n_t) < r_c \; \forall n_t \in \mathcal{F}^j$ **then**
22: $\mathcal{F}_j \leftarrow \mathcal{F}_j \cup \{n_k\}$
23: **end if**
24: **end for**
25: **end for**
26: Calculate the EPA for each cluster $\mathcal{F}_j$ according to Eq. 8.4
27: **return** the cluster $\mathcal{F}$ with the highest EPA
28: **end procedure**

8.2.4 Next-hop candidates coordination

After computing the forwarding set, the current forwarder node includes the address of the next-hop forwarder nodes in the packet and then broadcast it. Each node that has correctly received the packet, verifies if it is a next-hop forwarder and then sets the timer to broadcast it according to its priority. The greater the priority of the node is, the shorter is its waiting time. The packet will be discarded by the nodes that are not listed as the next-hop forwarder.

In opportunistic routing, the highest priority node becomes a next-hop forwarder and the rest of the lower priority nodes transmit the packet only if the highest priority node fails to do so. The lower priority nodes suppress their transmissions after listening the data packet transmission of the next-hop forwarder. In GEDAR, when the i^{th} priority node receives the packet, it will wait for the remaining time to complete propagation of the packet plus the time corresponding to the delay propagation between the 1^{th} to the 2^{th} priority nodes, the delay between the 2^{th} to the 3^{th} priority nodes, and so on until the delay between the $(i-1)^{th}$ to the i^{th} priority node. After this time, if the i^{th} node does not hear the transmission of the packet, it will broadcast it. Thus, the i^{th} waiting is:

$$T_w^i = T_p + \sum_{k=1}^{i} \frac{D(n_k, n_{k+1})}{s} + i \times T_{proc}, \tag{8.5}$$

where T_p is the remaining propagation time and T_{proc} is the packet processing time. The remaining propagation time represents the delay needed for the complete propagation of the packet broadcast by the sender node. This time is defined as

$$T_p = \frac{(r_c - D(n_a, n_b))}{s}, \tag{8.6}$$

where n_a is the receiver node, n_b is the sender node, and s is the speed of sound underwater. The second term in Eq. 8.5 corresponds to the time required for the node to hear the transmission of its predecessor priority node.

8.3 Void-Handling Procedure of GEDAR

Void node recovery procedure is used when the node fails to forward data packets using the greedy forwarding strategy. Instead of message-based void node recovery procedures, GEDAR takes advantage of the already available node depth adjustment technology to move void nodes for new depths trying to resume the greedy forwarding. We advocate

that depth adjustment-based topology control for void node recovery is more effective in terms of data delivery and energy consumption than message-based void node recovery procedures in UWSNs given the harsh environment and the expensive energy consumption of data communication.

The GEDAR depth adjustment-based topology control for a void node recovery procedure can be briefly described as follows. During the transmissions, each node locally determines if it is in a communication void region by examining its neighborhood. If the node is in a communication void region, that is, if it does not have any neighbor leading to a positive progress towards some surface sonobuoy ($\mathcal{C} = \emptyset$), it announces its condition to the neighborhood and waits the location information of two hop nodes in order to decide which new depth it should move into and the greedy forwarding strategy can then be resumed. After, the void node determines a new depth based on 2-hop connectivity such that it can resume the greedy forwarding.

Algorithm 9 is used for void node recovery. In the recovery mode procedure, the void node changes its status, stops the beaconing, sends a void node announcement message to announce its void node condition to the neighborhood, and schedules the procedure to calculate its new depth (Lines 1-7). When a neighbor node receives a void_node_announcement_message, it removes the sender from its neighbor table and, from the updated neighbor table, determines whether it is a void node or not. If the receiver node will be not a void node, it replies the received message with a void _ node _announcement _ reply message containing its location information and the location of its neighbors. Otherwise, it will start the void node recovery procedure.

The above strategy is used to avoid cascading effects during the depth adjustment of void nodes. For instance, consider the worst scenario of a "mountain-like" communication void region, as depicted in Figure 8.1. The picture shows underwater sensor nodes, such as the a, b, c, d, and e nodes, that should deliver collected data to sonobuoys at sea surface through multihop underwater acoustic communication. In this example, the node c has data packet to be sent. It discovers that it is in a communication void region and then it starts the void node recovery algorithm (Algorithm 9). At this moment, nodes b and d using node c as the next-hop forwarder. During the void node recovery, node c sends a void_node_announcement_message to its neighbor nodes (see Figure 8.1a). After receiving that control packet, nodes b and d remove c from its neighbor table and determine whether they can continue forwarding the packet, using the greedy geographic and opportunistic strategy, through other neighbor nodes. In this scenario, as they cannot, b and d start the recovery mode procedure (see Figure 8.1b). The same procedure is performed by

Algorithm 9 GEDAR: Void node recovery algorithm

procedure RecoveryMode()
is_void_node $\leftarrow$ true
Stop beaconing
$\Omega \leftarrow \emptyset$ ▷ Set of neighbors to topology control
Send void_node_announcement_message
CalculateNewDepth(t)
end procedure

{n_{vn} is the void node.}
{Ω set of neighbors to act as next-hop forwarder.}
{$\mathcal{D}$ set of depth candidates to the void node n_{vn}.}
procedure CalculateNewDepth(time)
if $\mid \Omega \mid > 0$ **then**
  for $n_u \in \Omega$ **do**
    if $D(n_{vn}, n_u) \leq r_c$ **then**
      $d_u \leftarrow D(n_u, s_u^*)$
      $(x_{vn} - x_{s_{vn}^*})^2 + (y_{vn} - y_{s_{vn}^*})^2 + (z_{vn}^* - z_{s_{vn}^*})^2 \geq d_u^2$
      $\mathcal{D} \leftarrow \mathcal{D} \cup \{z_{vn}^*\}$
    else
      $d \leftarrow \sqrt{(x_{vn} - x_u)^2 + (y_{vn} - y_u)^2}$
      if $d \leq r_c$ **then**
        $(x_{vn} - x_u)^2 + (y_{vn} - y_u)^2 + (z_{vn}^* - z_u)^2 \leq r_c^2$
        $\mathcal{D} \leftarrow \mathcal{D} \cup \{z_{vn}^*\}$
      end if
    end if
  end for
  $z = \text{argmin}_{\forall z_i \in \mathcal{D}}\{|z_{vn} - z_i|\}$
  n_{vn} moves to new depth z
  is_void_node $\leftarrow$ false
else
  RecoveryMode();
end if
end procedure

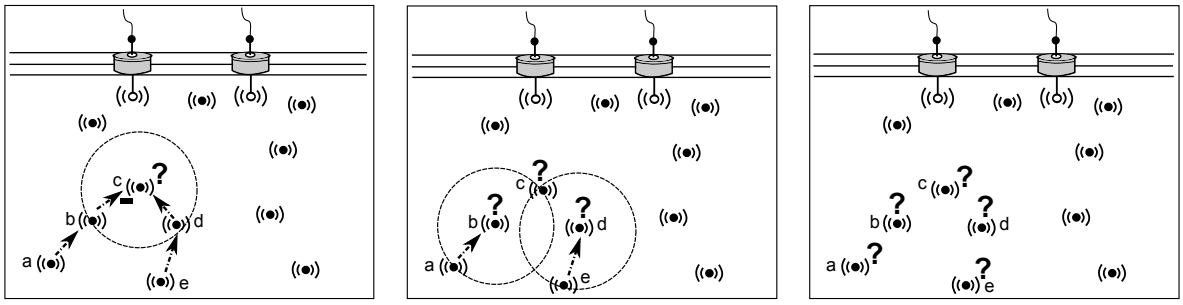

(a) Step 1 (b) Step 2 (c) Step 3

Figure 8.1: Example of a mountain-likewise shape communication void region scenario

nodes a and e. At the end, none of them can continue the recovery void node procedure as they have not received any replay of a void_node_announcement_message. Thus, all generated packets from these nodes will be discarded as they do not have a next-hop forwarder candidate, as shown Figure 8.1c.

After the waiting time t (Line 6), the void node runs the procedure *Calculate-NewDepth* (Lines 12-33). The set Ω contains the location information of the 2-hop connectivity obtained from the void_node_announcement_replay message received from the non-void node neighbors. The new depth of the void node is calculated from 2-hop connectivity neighbor set Ω. Let vn be the void node and $u \in \Omega$ a possible next-hop forwarder node. If node u is a 1-hop neighbor, the void node vn must determine a new depth such that its distance to the closest sonobuoy is larger than the distance from node u to its closest sonobuoy (Lines 15-18). This is done by solving the inequality in Line 17. The new possible depth z^*_{vn} is then added to the set of candidate depths $\mathcal{D}$ (Line 18). If node u is a 2-hop neighbor of nv, nv determines whether there is a new depth z^*_{vn} such that vn can communicate directly with u and can forward its packet through u using the greedy forwarding strategy (Lines 19-25). In Line 20, the void node vn determines its Euclidean distance to u considering only the X, Y coordinate location. This is because, in the worst scenario, vn will be at the same depth of u. If this distance is less than the communication range r_c, the void node vn determines a new candidate depth z^*_{vn} relative to the node u such that vn can use u as a next-hop forwarder (Lines 21-24). This new candidate depth is then added to the set $\mathcal{D}$ (Line 23). At the end, the void node vn chooses a new depth from the set $\mathcal{D}$ such that its displacement is minimum (Line 27), starts its vertical movement (Line 28) and changes its condition of void node (Line 29). If vn can not determine a new depth, it restarts the recovery mode procedure (Line 31).

8.4 Performance Evaluation

8.4.1 Simulation parameters and algorithms setup

In this section, we use computer simulations [133] to evaluate the performance of our proposed protocol against the simple geographic and opportunistic routing protocol (GOR) without recovery mode and the two other most popular previously proposed routing protocols for UWSN: DBR (Depth-Based Routing) [35] and VAPR (Void-Aware Pressure Routing) [94]. All evaluated routing protocols have been implemented using Aqua-Sim [125]. Aqua-Sim is a high fidelity and flexible packet level underwater sensor network simulator developed on NS-2 to simulate the impairment of the underwater acoustic channel.

In our simulations, the number of sensor nodes range from 150 to 450 and the number of sonobuoys is 45. They are randomly deployed in a region the size of 1,500 m $\times$ 1,500 m $\times$ 1,500 m. In each sensor, data packets are generated according to a Poisson process with the same parameter $\lambda = \{0.01, 0.05\}$ pkts/min to very low traffic load; $\lambda = \{0.1, 0.15\}$ pkts/min to low traffic load; and, $\lambda = \{0.2, 0.25\}$ pkts/min to medium traffic load. We adopt an extended 3 D version of the Meandering Current Mobility (MCM) [38], to simulate a mobile network scenario considering the effect of meandering sub-surface currents (or jet streams) and vortices. We set the main jet speed to 0.3 m/s. Due to the mobility, nodes would move beyond the deployment region.

In all experiments, the nodes have a transmission range (r_c) of 250 m and a data rate of 50 kbps. They use the CSMA protocol at the MAC layer. The size of the packet is determined by the size of the data payload and by the space required to include the information of the next-hop forwarder set. We consider that data packets have a payload of 150 bytes. As in [13] and [94], we use a Bloom filter to reduce the space required by the forwarding set in the data packet. Thus, a filter size of 19 bytes can be used to represent 15 items with a false positive rate smaller than 1 percent [13, 94]. The energy consumption at each sensor node is a combination of the communication and depth adjustment energy consumption. The values of the energy consumption were $P_t = 2$ W, $P_r = 0.1$ W, $P_i = 10$ mW and $E_m = 1500$ mJ/m for the respective sensor operations of transmission, reception, idle and depth adjustment per meter. In our simulation, each run lasted 1 hour.

The above mentioned parameters are similar to those ones explored in [35, 13, 134, 94, 93]. The results correspond with an average value of 50 runs with a 95 percent

confidence interval.

8.4.2 Topology-related results

In this section, we analyze the results relative to the network topology when the network density is varied. Our objective is to investigate how the greedy forwarding strategy behaves as the network density ranges from low to high densities. The results concern the greedy upward (GUF) strategy, greedy opportunistic (GOR) strategy, and GOR strategy with depth adjustment-based topology control (GEDAR). In the GUF strategy, used by DBR and VAPR, the neighbor closest to the surface is selected as the next-hop forwarder. In the GOR strategy, the neighbor closest to some sonobuoys in terms of the Euclidean distance is selected as the next-hop forwarder. GEDAR works as GOR but moves void nodes to new depths to resume the greedy forwarding.

Figure 8.2a shows the fraction of void nodes after 1 hour of simulation. As shown in the plot, the fraction of void nodes decreases when the network density increases for all greedy strategies. On the other hand, GEDAR and GOR achieve the best results as compared with the GUF. This happens because nodes deployed closest to the surface that are not in the communication range of any sonobuoy fail to maintain the greedy routing process when the GUF strategy is used. When GEDAR is used, the proposed depth adjustment-based topology control mechanism reduces 58% the fraction of void nodes for medium density scenarios in comparison to GUF and approximately 44% as compared to GOR.

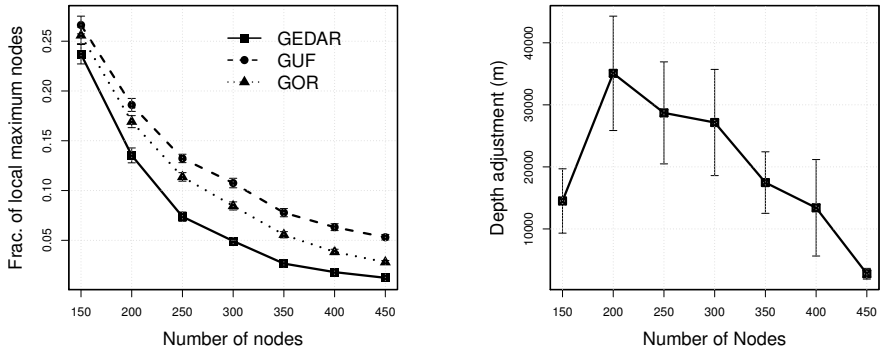

(a) Fraction of void nodes (b) Average depth adjustment

Figure 8.2: Simulation results

Figure 8.2b depicts simulation results for the average displacement of void nodes in GEDAR. When the network density is low, the displacement of void nodes is high. For instance, when the network has 200 sensor nodes where approximately 15% is in a communication void region (Figure 8.2a), each void node moves 133 meters on average. As the network density increases, the total displacement decreases. This happens because the fraction of nodes located in communication void regions decreases, as corroborated by the results of GOR in Figure 8.2a.

8.4.3 Network density-related results

In this section, we evaluate the DBR, VAPR, GOR and GEDAR for different network densities. To do this, the number of nodes was varied and the traffic load was maintained in $\lambda = 0.15$ pkts/min. We focused on the network performance mainly for the hard scenarios of low and high densities. In these scenarios, we have a high incidence of void nodes and high congestion occasioned by the concurrent transmissions of a large number of sensor nodes.

Figure 8.3a shows the results concerning the packet delivery ratio. This result is quite consistent with the topological results presented in Figure 8.2a. The overall trend is an increment in the packet delivery ratio when the network density increases. GEDAR has the best packet delivery ratio performance because of its void node recovery procedure. VAPR outperforms DBR and GOR mainly in low density scenarios. The reason is that packets generated and forwarded by void nodes are routed through directional trails to circumvent communication void regions instead of being discarded as in DBR and GOR.

Figure8.3b shows the results concerning the average number of redundant copies by received packet. As shown in Figure 8.3b, the number of redundant copies increases in DBR and VAPR when the network density increases. In DBR, this happens due to both multipath packet delivery and failures in the suppression of data transmission. For some low priority nodes, the transmission is not suppressed given that the DBR next-hop set selection heuristic does not guarantee that the selected nodes will hear the transmission of each other. The increment in redundant packets in VAPR occurs because low priority nodes cannot hear the transmission of high priority ones as we have more interferences. The redundant data packet copies in GEDAR and GOR result from the broadcast nature of the transmission of some nodes closest to the surface that are within the communication range of more than one sonobuoy.

Figure 8.4a shows the results concerning the average number of packet transmissions

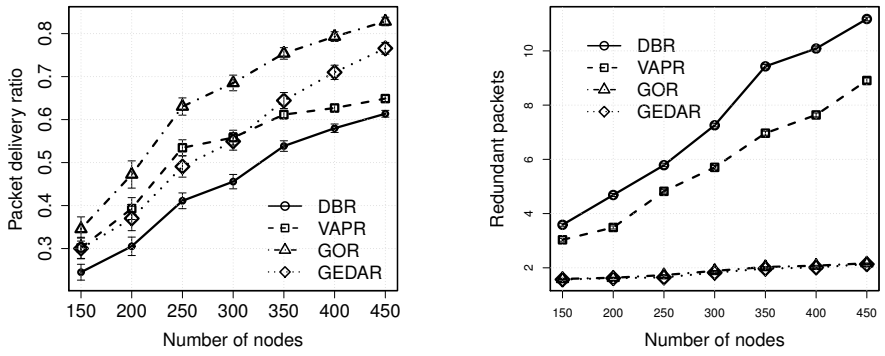

(a) Packet delivery ratio

(b) Average number of redundant packets

Figure 8.3: Simulation results

needed to deliver a data packet, including the recovery process. This plot suggests that the average number of packet transmissions needed to deliver a packet is closely related to the redundant packets shown in Figure 8.3b. As the overall trend, when the network density increases, more transmissions are necessary for delivery. This increment is significant in DBR and VAPR. In GEDAR and GOR this cost is amortized given the better performance of packet delivery ratio, as corroborated by Figure 8.3a.

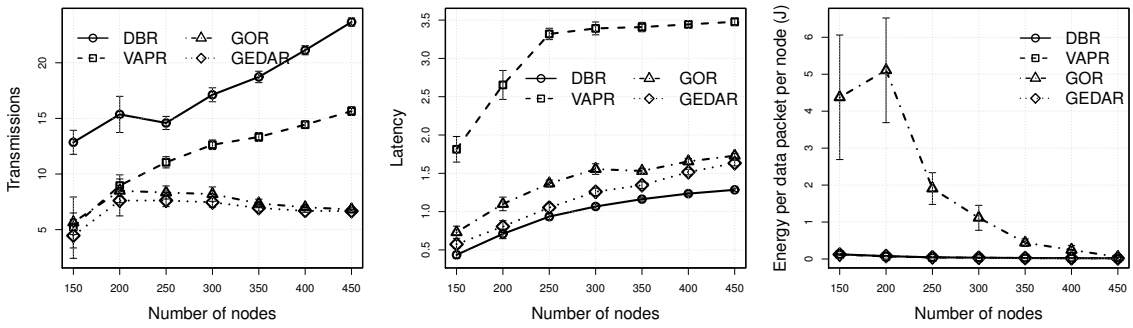

(a) Number of transmissions for delivery

(b) Average end-to-end delay

(c) Energy consumption per message per node

Figure 8.4: Simulation results

Figure 8.4b shows the results concerning the average end-to-end delay. As expected, the average delay experienced by a packet in GEDAR, VAPR and GOR is higher than

in DBR. The cause of this is that these protocols use opportunistic routing paradigm to improve the data delivery. Besides the time needed to move void nodes to new depths in GEDAR, its end-to-end delay is lower than VAPR. This is due to the fact that during the depth adjustment, the generated data packets are discarded. DBR presented the lowest delay which corresponds to the time needed to receive, process and send the data packets until they reach any sonobuoy. VAPR has the worst performance mainly due to the increment in the number of transmissions.

Figure 8.4c shows the results concerning the energy consumption per received packet per node. Notice that GEDAR has a high energy consumption for low density scenarios. This cost is relative to the depth adjustment of the void nodes. As we can see in Figure 8.2b, the average displacement per node is high in low density scenarios. However, as the network density increases, the energy consumption decreases; it becomes approximately the same as that in DBR and VAPR. This happens because the average displacement per node decreases, as shown in Figure 8.2b; and, the high packet delivery ratio (Figure 8.3a) amortizes the energy cost relative to node movement.

8.4.4 Traffic load-related results

In this section, the routing protocols are evaluated when the network traffic load is varied. The motivation for this analysis is that GOR, VAPR and GEDAR use beacon messages as an important part of the next-hop forwarding selection that can be affected by collisions when the traffic load is high. Furthermore, the multipath packet delivery of DBR can degrade the network performance when we have diverse network traffic loads.

Figure 8.5a shows the packet delivery ratio for different traffic load. As shown in the plot, the packet delivery ratio decreases when the network traffic load increases. For high traffic loads, more transmissions will compete for access to the shared acoustic medium and more transmissions will suffer from collisions, reducing the packet delivery ratio. For instance, the packet delivery ratio in DBR is reduced to 38% when we compare its performance in high density scenarios when the traffic load goes from the minimum to the maximum. The decrement of packet delivery ratio in GOR, VAPR and GEDAR is less than in DBR because they use opportunistic routing to mitigate the effects of the underwater acoustic channel more expressively experienced during high traffic load.

Figure 8.5b shows the average number of redundant copies for delivered packet. Notice that the received redundant copies in DBR decreases significantly when the traffic load increases. For the scenario of 450 nodes, this reduction is of 50% when we compare

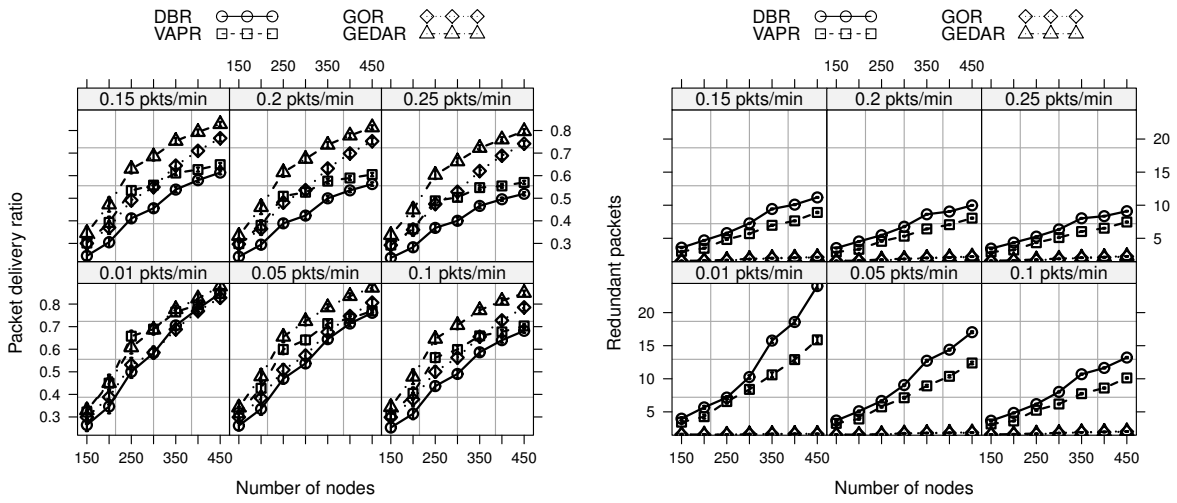

(a) Packet delivery ratio

(b) Average number of redundant packet

Figure 8.5: Simulation results

its performance with the traffic load of 0.01 and 0.25 pkts/min. The reason for this behavior is that with the network traffic load increment, more packets are lost along the routing path and less redundant copies are then generated (please refer to Figure 8.5a). Quite a trend can be observed for VAPR. Figure 8.5b shows that the redundant copies of delivered packets are low for GOR and GEDAR. This happens thanks to the proposed low priority node transmission suppression algorithm.

Figure 8.6a shows the average end-to-end latency. As a general trend, the latency increases when the network traffic load increases. This is expected given that the increment in the traffic load results in more transmissions competing to access the shared medium. This leads to nodes staying in the back-off collision avoidance mechanism of the CSMA protocol before attempting to sense the carrier again. VAPR, GOR and GEDAR have high delay when compared to DBR mainly in high traffic scenarios because of the opportunistic forwarding.

Figure 8.6b shows the average energy consumption per received packet per node. For low density and traffic load, GEDAR has a high energy cost incurred by received packets per node. However, when the traffic load increases, the energy cost per packet significantly decreases. This is because the initial energy consumption needed to move void nodes is diluted along the network lifetime. The energy cost per received packet per node for DBR, GOR and VAPR is almost constant.

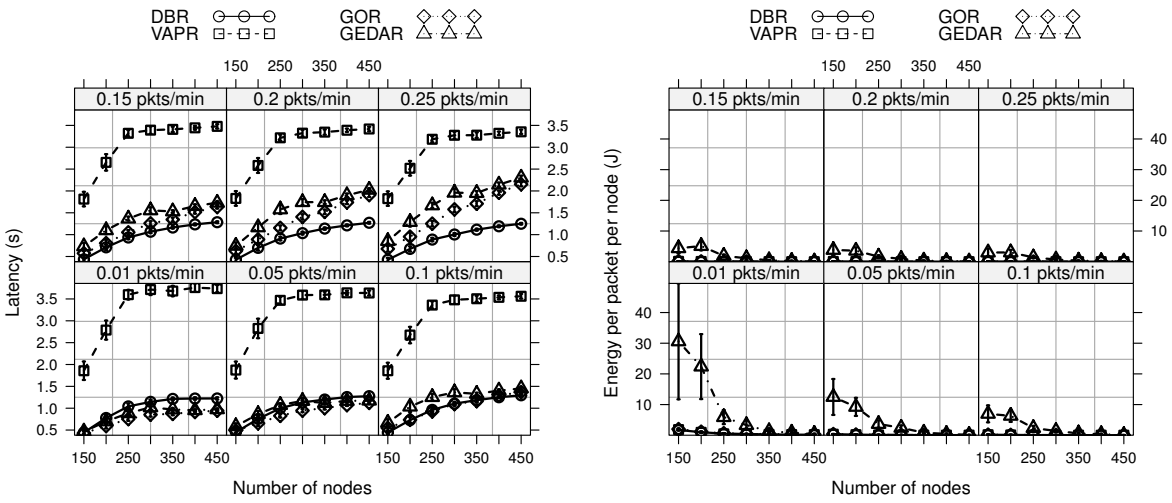

(a) Average end-to-end delay

(b) Energy consumption per message per node

Figure 8.6: Simulation results

Figure 8.7a and 8.7b show the show the percentage of the network energy consumption relative to the acoustic communication and physical actuation (nodes' depth adjustment), for a low and medium network traffic load, respectively. As depicted in the plot, the nodes' depth adjustment is responsible for most of the energy expenditure of the network. For low density network scenario, the depth adjustment task is responsible by more than 80% of the network energy consumption. This is because the high energy cost required by the depth adjustment technology to vertically move the node, as the designed in [93]. Moreover, the impact of the nodes' movement operation on the network energy consumption is high on scenarios of high traffic load (please refer to Figure 8.7b). The increment of the network traffic load increases the energy consumption's percentage of the node movement task because the highly dynamic network topology and the reactive nature of the communication void region recovery algorithm proposed in this Chapter. Thus, as more nodes have packet to be sent, more decisions of depth adjustment will take place.

8.5 Discussion

From the simulation results, the proposed GEDAR routing protocol with the depth adjustment based communication void region recovery procedure showed great potential to

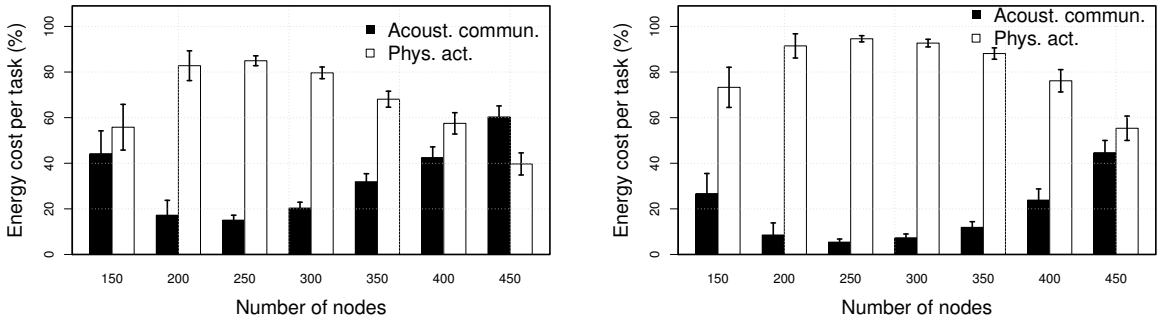

(a) Packet generation rate of 0.01 pkts/min

(b) Packet generation rate of 0.15 pkts/min

Figure 8.7: Energy consumption per task

improve the routing task in the harsh underwater acoustic communication environment. This strategy appears more useful, in terms of the energy consumption, on moderate to high network density scenarios, despite this approach improves the network performance even in harsh low density scenarios when compared against existing related solutions. This is because the energy cost to vertically move the nodes on the current technology that was considered in this work. However, as the buoyancy based nodes depth adjustment technology advances in reducing the energy cost to vertically move the nodes, the main drawback of our proposed methodology which is the energy cost of nodes movement, will be overcome.

8.6 Concluding Remarks

In this Chapter, we proposed and evaluated the GEDAR routing protocol to improve the data routing in UWSNs. GEDAR is a geographic and opportunistic routing protocol with a novel depth adjustment-based topology control mechanism used to move void nodes to new depths to overcome the communication void regions. Our simulation results showed that geographic routing protocols based on the position location of the nodes are more efficient than pressure routing protocols. Moreover, opportunistic routing proved crucial for the performance of the network besides the number of transmissions required to deliver the packet.

The use of node depth adjustment to cope with communication void regions improved significantly the network performance. GEDAR efficiently reduces the percentage

of nodes in communication void regions to 58% for medium density scenarios as compared with GUF and reduces these nodes to approximately 44% as compared with GOR. Consequently, GEDAR improves the network performance when compared with existing underwater routing protocols for different scenarios of network density and traffic load.

From the simulation results, the proposed GEDAR routing protocol with the depth adjustment-based communication void region recovery procedure showed great potential to improve the routing task in the harsh underwater acoustic communication environment. This strategy appears more useful, in terms of the energy consumption, on moderate to high network density scenarios, despite this approach improves the network performance even in harsh low density scenarios when compared against existing related solutions. This is because the energy cost to vertically move the nodes on the current technology that was considered in this work. However, as the buoyancy based nodes' depth adjustment technology advances in reducing the energy cost to vertically move the nodes, the main drawback of our proposed methodology which is the energy cost of nodes' movement, will be overcome.

Chapter 9

An Analytical Framework of Joint Duty-Cycling and Opportunistic Routing

In this Chapter, we propose a joint design of opportunistic routing (OR) and duty-cycle, towards reliable and energy-efficient mobile underwater sensor networks (UWSNs). We propose an analytical model to study the joint design OR and duty cycle protocols for UWSNs. Our goal is to shed light on the potentials and challenges of this novel designing approach in mobile UWSNs, which aims to achieve reliable and energy-efficient data collection in mobile UWSNs.

This Chapter is organized as follows. Section 9.1 discusses the motivation for the study of opportunistic routing in duty-cycled UWSNs. Section 9.2 presents a thorough discussion of opportunistic routing and duty-cycling works in the context of UWSNs. Section 9.3 describes the three approaches to the design of duty-cycling protocols. Section 9.4 thoroughly review and presents preliminary concepts for the proposal of the analytical framework. Section 9.5 proposes a refined analytical framework of opportunistic routing "meeting" duty cycle. Section 9.6 provides extensive experiments considering suitable underwater mobility model, different network densities, and several configurations of duty cycle and opportunistic routing. Section 9.7 presents a thorough discussion about the obtained insights that can be used for the design of opportunistic routing and duty cycle protocols, which consider the requirements of the mobile UWSN applications. Section 9.8 presents the final remarks.

9.1 Introduction and Motivation

In mobile UWSNs, the design of energy-efficient and reliable data collection networking protocols is challenging, due to the characteristics of the underwater acoustic communication channel. The underwater acoustic channel suffers from limited bandwidth due to the use of low frequencies, temporary losses of connectivity due to shadow zones, high bit error rate, multipath propagation, and Doppler effects [5]. Consequently, an underwater acoustic link between neighbors can perform poorly or even be temporarily down, which increases packet error rate, packet collisions and retransmissions, delay, and the already high energy consumption.

In these networks, reliable data delivery and energy conservation usually are addressed individually. On one hand, opportunistic routing (OR) can be considered for tackling the problem of low reliability in mobile UWSNs [135]. OR leverages the broadcast nature of wireless links and selects a set of next-hop forwarding candidates, instead of only a unique next-hop node, as is done in traditional multi-hop routing [136]. The selected candidates will coordinately forward the data packet towards the destination, such that a candidate forwards the packet only if all the high priority level candidates failed to do so. Therefore, a data packet is lost and needs to be retransmitted only if none of the candidates received it, which helps to reduce the energy consumption and packet collisions.

On the other hand, duty-cycling can be considered for conserving energy in mobile UWSNs. In this approach, each node periodically alternates the state of its radio between active and sleep modes. Thus, during sleep intervals, part of the radio circuitry of the node is shut down, which conserves the energy of idle listening. The schedule for the duty cycle at each node can be determined through negotiations between neighbors (synchronous protocols), or be completely independent and decoupled (asynchronous protocols).

In our understanding, mobile underwater sensor networks can benefit from the joint design of opportunistic routing and duty cycle protocols to achieve energy-efficient and reliable data collection. In fact, this combination already has been proved to improve the network performance of the counterpart terrestrial wireless sensor networks (*e.g.*, [137, 138]). However, the joint design of OR and duty cycle protocols for UWSNs can bring additional challenges, such as how to guarantee a suitable number of awake candidate forwarding nodes guaranteeing the link reliability. In this direction, there is a lack of work investigating and proposing the joint design of opportunistic routing and duty cycle

protocols for mobile UWSNs.

9.2 Background

In this section, we examine opportunistic routing and the main methodologies for the design of asynchronous duty cycling protocols protocols in UWSNs.

9.2.1 Opportunistic routing

Opportunistic routing (OR) protocol works as follows. Each sender node selects a subset of its neighboring nodes, known as the next-hop forwarding candidate set, to continue forwarding the data packet towards the destination. A candidate node that has successfully received the packet will forward it in a prioritized way (*i.e.*, it forwards the received data packet if none of the high priority candidate nodes have forwarded it). OR increases throughput by exploiting the broadcast nature and spatial diversity of the wireless medium [136]. As multiple candidates are able to continue forwarding the packet, the probability that at least one of them will receive the packet increases, compared to the traditional single next-hop routing; this improves the bandwidth utilization, reduces overhead and collisions and saves energy.

9.2.2 Duty-cycling approach

In general, duty cycle protocols has been categorized into *synchronous* and *asynchronous* approaches [73, 139, 74]. In synchronous duty-cycling, nodes negotiate a duty-cycling schedule to align their active or sleep periods. Thus, the sender node knows, a priori, when its neighbors are awake and able to receive data packets. The synchronized approach is unfeasible in UWSNs, because of the overhead for clock synchronization and schedule exchanging. In asynchronous duty-cycling, the nodes' duty cycle schedules are decoupled. At any arbitrary moment in time, only a subset of the nodes are in active mode. This approach is suitable for UWSNs, as it is simple and does not require periodic overhead. However, it can incur high delays, as the sender should wait until the next-hop node is active.

9.2.3 Opportunistic routing meeting duty cycle

It is necessary to investigate the advantages and disadvantages of cross-layer duty-cycling and opportunistic routing in mobile UWSNs. For instance, in duty-cycled terrestrial wireless sensor networks, opportunistic routing has been employed for reducing the expected delay for data packet delivery [140, 137, 141, 138]. In the single multihop routing scenario, a sender node should wait until the next-hop node is awake to transmit the data packet. By using opportunistic routing, several neighboring nodes are selected as next-hop forwarding candidates. Thus, a sender node only needs to wait until one of the candidates wakes up.

In mobile UWSNs, however, there is a lack of work investigating the benefits and drawbacks of opportunistic routing in duty-cycled scenarios. This Chapter sheds light on the aspects of cross-layer duty-cycling and opportunistic routing in underwater sensor networks. By the proposed analytical framework, we can investigate and provide useful insights for the design of opportunistic routing "meeting" duty cycle, in several configurations of network densities, sample frequency of monitoring applications, underwater mobility, and duty cycle settings.

9.3 Opportunistic Routing in Duty-Cycled Underwater Sensor Networks

Using underwater acoustic communication technology, link between neighbors can perform poorly or even be down temporarily, which increases packet error rate, packet collisions and retransmissions, delay, and energy consumption. Hence, the geographic and opportunistic routing (OR) paradigm has been adopted in designing routing protocols for UWSNs [18, 35, 13, 34]. OR protocols leverage the broadcast nature of wireless links and select a set of next-hop forwarding candidates, instead of only a unique next-hop node, as in the traditional multihop routing. The selected candidates will forward the data packet towards to the destination in a prioritized way, such that a node transmits the packet only if all the high priority candidates failed in do so. Thus, a packet should be retransmitted only if none of the candidates receive it, which helps to reduce energy consumption and packet collisions.

On the other hand, energy efficiency is a well-known challenging problem when designing wireless ad hoc & sensor networks. In those networks, each sensor node has a finite power source supplied by batteries with a limited energy budget. Commonly,

battery replacement is impossible since nodes are deployed in harsh and inhospitable environments. Thus, each sensor node should perform the designated tasks using efficiently its energy supply, aiming to extend the network lifetime as much as possible to fulfill the application requirements. Several methodologies have been studied to design energy-efficient network topologies and networking protocols. One prominent methodology is duty cycling, where the nodes periodically alternate their communication radio between active and sleep modes. The motivation to put the nodes at sleep mode come from the fact that wireless sensor networks usually have very infrequent transmissions. For instance, in underwater sensor networks, it can be once per week or less [65]. This behavior leads nodes to remain idle listening during most part of the time, wasting energy. By putting the node to sleep, part of the radio circuitry is shut down, mitigating the energy consumption of idle listening.

Duty cycle protocols can be categorized into *synchronized* and *asynchronous* approaches [73, 139, 74]. In synchronized approaches nodes negotiate a schedule in order to align their active or sleep periods. Thus, the sender node knows when its neighbors are awake and able to receive data packets. Synchronized approach is unfeasible in UWSNs since the overhead for clock synchronization and schedule exchanging. In asynchronous approaches, the nodes' duty cycle schedules are decoupled. Thus, at an arbitrary time instant, only a subset of the nodes are in active mode, providing network services. This approach is suitable for UWSNs as it is simple and does not require periodic overhead. However, it can incur in high delays as the sender should wait until the next-hop node be active. Roughly, there are three principle design guiding the proposals of asynchronous duty cycle protocols:

- **Simple asynchronous:** Node changes between active and sleep time periodically. When it has data packet to send, it simply transmits the packet addressing to the next-hop node.

- **Low power listening (LPL):** When node has data packet to send, it starts sending a preamble as long as the sleep time of the intended next-hop neighbor node. The next-hop node when wake-up and detect the preamble transmission, stay awake to receive the data packet that will be sent after the preamble transmission. A variant approach is named of *strobed preamble*, where short preambles are transmitted followed by silence time, in order to avoid energy expenditures by sending long preambles.

- **Low power probing (LPP) or receiver initiated:** Each node transmits a short

beacon when wake-up, to inform the neighborhood about its active status, and stay awake for a short interval enough to receive data packets. When a node has data packet to send, it remains awake waiting the beacon of the intended next-hop node. After receiving the beacon, the sender node transmits the data packet.

Each asynchronous duty cycle principle design has advantages and disadvantages that are more impactful in UWSNs. For instance, simple asynchronous approach does not employ any overhead. However, there is no guarantee that the next-hop is awake to receive the packet. Low power listening can discharge sender nodes quickly as they must transmit preambles before data packets. Moreover, depending on the length of the preamble, it is more efficient to have the radio always on since the transmission cost is dominating in underwater acoustic communication. Receiver initiated approach may result in unnecessary energy expenditure mainly for very low traffic generation rate since awaking nodes must send a beacon, even when there is no traffic load.

9.4 Preliminaries

In this section, we present the necessary background used to devise the proposed analytical framework described in the next section.

9.4.1 Network architecture and mobility model

We consider a swarm mobile underwater wireless sensor network architecture for 4 D (time and space) monitoring [35, 13, 94, 106, 142]. In this architecture, several sensor nodes are deployed underwater and scattered by one or multiple sonobuoys (sinks) deployed at the oceans' surface. Each sensor node monitors its surrounding variables and periodically reports the collected data to a sonobuoy through multi-hop acoustic communication. Each sonobuoy has both a radio frequency-based and an acoustic transceiver that allow it to collect data from underwater sensor nodes through underwater acoustic communication, and send the collected data to a monitoring center through radio frequency links.

Moreover, we consider scenarios of mobile underwater sensor networks where sensor nodes move freely, following the ocean's current. This particular mobility pattern is modeled by the meandering current mobility (MCM) model proposed by Caruso et al. in [38]. The MCM model considers the effects of meandering sub-surface currents (or jet streams) and vortices to determine the location of nodes over time. The mobility

Table 9.1: Examples of ocean monitoring programs in Canada

Monitoring program	**Applications (in summary)**
Atlantic Ocean Monitoring[1]	Monitoring of temperature, salinity, dissolved oxygen, fluorescence, chlorophyll a, and nutrients.
Arctic Ocean Monitoring[2]	Climate studies and monitoring of tides, currents, and water levels.
Pacific Ocean Monitoring[3]	Sea surface temperature and coastal waters monitoring; observation of marine ecosystems.

[1] http://www.dfo-mpo.gc.ca/science/oceanography-oceanographie/observations/atlantic-atlantique-eng.html

[2] http://www.dfo-mpo.gc.ca/science/oceanography-oceanographie/observations/arctic-artique-eng.html

[3] http://www.dfo-mpo.gc.ca/science/oceanography-oceanographie/observations/pacific-pacifique-eng.html

has the undesired effect of network partitions due to disruption of the network topology. However, drift nodes are desired for short-term monitoring applications, such as oil spill monitoring [143].

Accordingly, we represent the network topology as a temporal graph $G(t) = (V, E(t))$, where $V = \{V_n \cup V_s\}$ is the set of underwater sensor nodes (V_n) and sonobuoys (V_s); and $E(t)$ is the finite set of links between them, at time t. We assume that nodes have a nominal communication range of R_c meters. Thus, two nodes n_i and $n_j \in V$ are neighbors at time t, *i.e.*, $e_{i,j} \in E(t)$, if the distance between than is less than or equals to R_c.

However, due to channel fading, there is a packet delivery probability (cf. Eq. 5.10) associated with each link $e_{i,j}(t) \in E(t)$ as a function of the distance $d_{i,j}$ between nodes n_i and n_j at time t, and the size of the data packet (m bits) to be transmitted through the acoustic link. We define $N_i(t)$ as the set of n_i's neighbors with $i \notin N_i(t)$ at time instant t. Each node can know its neighborhood over time through periodic beacons dissemination.

9.4.2 Traffic model

In sensor networks, data traffic generation rates and transmission patterns are strictly dependent on the application. In general, applications relay on event-driven or periodic data collection, which results in very infrequent transmissions. However, a novel trend is the use of single sensor networks to detect composite events.

Composite events are observed through a combination of several different reading of properties (multi-modal data) that jointly determine the occurrence of the event, such as fire detection which may involve light intensity, temperature, acoustic and smoke

density sensors [144]. Therefore, traffic modeling must consider the aggregated data from multiple readings.

A mobile UWSN, more specifically, can be seen as an infrastructure for data collection in an ocean monitoring program, as shown in Table 9.1. Underwater nodes and their deployment are expensive. Thus, it would be interesting to have the network performing several monitoring tasks simultaneously, for different applications. The sampling frequency is determined by the application.

In this Chapter, we assume that each node $i \in \mathcal{V}_n$ has a constant data packet generation rate of λ_i per epoch T. In the analytical framework described in Section 9.5, the lifetime and performance measurements of the network are divided into many epochs of fixed length of T units of time. Thus, when an event-driven application is considered, λ_i would refer to an average value of nodes' n_i data generation rate given by a probabilistic distribution function (*e.g.*, Poisson) modeling the number of packets generated during a epoch. When a periodic measurement application is considered, λ_i refers to the constant number of data packets generated by the epoch.

9.4.3 Opportunistic routing modeling

Opportunistic routing (OR) protocols consist of two main procedures: the candidate set selection and candidate transmission coordination procedures. In the following, we describe these procedures and thereafter, we model important characteristics of opportunistic routing.

The candidate set selection procedure is responsible for choosing a set of next-hop forwarder nodes from the neighboring nodes. Usually, this procedure entails two basic steps. When a node has a data packet to transmit, the first step of the candidate set selection procedure is to verify which neighboring nodes are capable to continue forwarding the packet towards the destination. This is determined by considering an eligibility function, such as pressure level [35], packet advancement towards the destination [34], forwarding direction [94], delay [145], or residual energy [146]. In the next step of the candidate set selection procedure, a subset F of the apt nodes is selected as the next-hop forwarder candidate set. In the next-hop forwarder candidate set F, candidates are ordered according to the assigned transmission's priorities as $n_1 > n_2 > \ldots > n_{|F|}$, meaning that the candidate node n_2 only forwards the data packet if it does not hear the same transmission from the candidate node n_1, and so on.

The candidate transmission coordination procedure is responsible for coordinating the

transmission of the candidates according to their priority levels. In timer-based transmission coordination [135], whenever a candidate node receives a data packet, it holds the packet for a time before forwarding it. This holding time is determined according to the candidate priority level; a higher priority candidate will have lower packet holding time. Moreover, there is a redundant data packet transmission avoidance mechanism, where candidate nodes suppress their transmission as soon they detect that a high priority level candidate transmitted the same packet. Ideally, only one transmission must be performed by a candidate set to avoid redundant packets and unnecessary waste of resources. However, duplicated data transmissions may occur due to the hidden terminal problem.

9.4.3.1 Perfect transmission coordination

As in [147] and [148], we assume perfect coordination between the transmissions of the forwarding candidates. This assumption is necessary to keep the model simple and tractable.

Let us define n_i the current forwarder node and $F_i(t)$ its next-hop forwarder candidates set at time t. As previously discussed, the n_i's next-hop candidates in $F_i(t)$ are ordered according to their forwarding priorities as $n_1 > n_2 > \ldots > n_j > \ldots n_k$. Thus, from the perfect transmission coordination assumption, a node n_j forwards data packets from the node n_i the two below events hold:

1. node n_j correctly receives the data packet transmitted by node n_i;
2. the nodes $n_1, n_2, \ldots, n_{j-1}$ having higher priority level than n_j do not successfully receive the data packet transmitted by node n_i.

The candidate node n_j then forwards the data packet after the holding time. This happens with probability given as:

$$P_{f_{ij}} = p_{ij} \prod_{k=1}^{j-1} (1 - p_{ik}), \tag{9.1}$$

where p_{ij} refers to the packet delivery probability of the links between nodes n_i and n_j given by Eq. 5.10, and $\prod_{k=1}^{j-1}(1 - p_{ik})$ calculates the probability that candidate nodes $n_1, \ldots, n_{j-1}$, having higher priority than n_j, fail to receive the packet.

9.4.3.2 End-to-end probabilistic multipath

One of the main characteristics of OR is the any-path nature of data delivery (*i.e.*, multiple possible routing paths from the sender to the destination determined from the combination of candidate nodes at each hop). In traditional routing, there is a well-established deterministic path $i \rightsquigarrow s$ from the source node n_i to destination s. In opportunistic routing, however, since there is a set of candidate nodes capable to forward data packets at each hop, several routing paths are possible; these are determined from the combination of the candidate nodes at each hop, from node n_i to destination s. For instance, let us consider the network topology shown in Figure 9.1. Data packets transmitted from n_i will reach destination s through one of the three possible paths: $h_1 = \{n_i, n_j, n_s\}$, $h_2 = \{n_i, n_k, n_s\}$ or $h_3 = \{n_i, n_l, n_s\}$. We define $\mathcal{P}_i$ as the set of all possible routing paths from node n_i to each destination s (sonobuoys). In the example of Figure 9.1, this set is composed by the paths h_1, h_2, and h_3 ($\mathcal{P}_i(t) = \{h_1, h_2, h_3\}$).

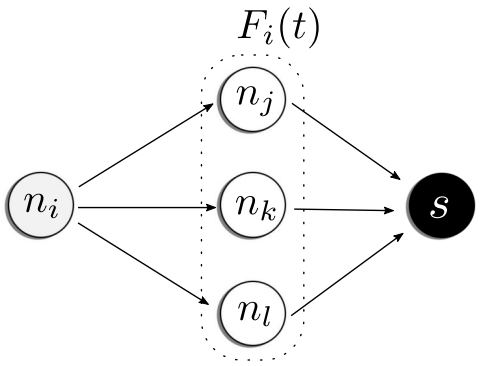

Figure 9.1: Example of opportunistic routing

We propose Algorithm 10 to obtain the set of possible routing paths from each source node $n_i \in V_n$ to all sonobuoys $s \in V_s$. The algorithm works as follows. The loop of Lines 4-15 build a directed graph where the set of vertices V_i is composed of the source node n_i and all nodes that might forward its data packets. More specifically, Line 7 selects the candidate set of the considered node n_v. This selection is given by the candidate set selection procedure of the considered opportunistic routing protocol. Lines 8-14 add the candidates and edges between the node n_v and its candidates in the graph G_i. If node n_u is not a sonobuoy (destination), it is included in the stack to have its candidates computed (Lines 11-13). The unique paths are obtained from the procedure of Lines 17-23. The paths are obtained from the shortest path search from the source node to each sonobuoy. Each found path is removed from the graph G_i and the procedure is

Algorithm 10 OR path determination

$\mathcal{P}_i = \emptyset$, $V_i = \emptyset$, $E_i = \emptyset$, $G_i = (V_i, E_i)$
S: a stack data structure
S.push(n_i)
while S is not empty **do**
  $n_v \leftarrow$ S.pop()
  $V_i \leftarrow V_i \cup \{n_v\}$
  $F_i(t) \leftarrow$ candidate_set_selection (n_v)
  for all $n_u \in F_i(t)$ **do**
    $V_i \leftarrow V_i \cup \{n_u\}$
    $E_i \leftarrow E_i \cup \{e_{n_v,n_u}\}$
    if $n_u \notin V_s$ **then**
      S.push(n_u)
    end if
  end for
end while

for all $s \in V_s$ **do**
  repeat
    $p \leftarrow$ shortest_path(G_i, n_i, s)
    $\mathcal{P}_i \leftarrow \mathcal{P}_i \cup p$
    remove(G_i, p)
  until is_not_empty(p)
end for

repeated until all the paths to the considered sonobuoy s is already in $\mathcal{P}_i$.

Each path $h_l \in \mathcal{P}_i$ has an associated probability Φ_l, which is the probability that a data packet to take it. This probability is computed as:

$$\Phi_l = \left(\prod_{m=1}^{|h_l|-2} P_{f_{v_m v_{m+1}}} \right) \times p_{v_{m-1} v_m}, \tag{9.2}$$

where $P_{f_{v_m v_{m+1}}}$, given by Eq. 9.1, is the probability of the candidate node v_{m+1} to forward the v_m's data packets and $p_{v_{m-1} v_m}$, given by Eq. 5.10, is the packet delivery probability of the last hop of h_l. Figure 9.2 shows an example of how to compute the probability of each path. Considering the path $h_1 = \{v_i, v_j, v_m, v_s\}$, its associated probability is

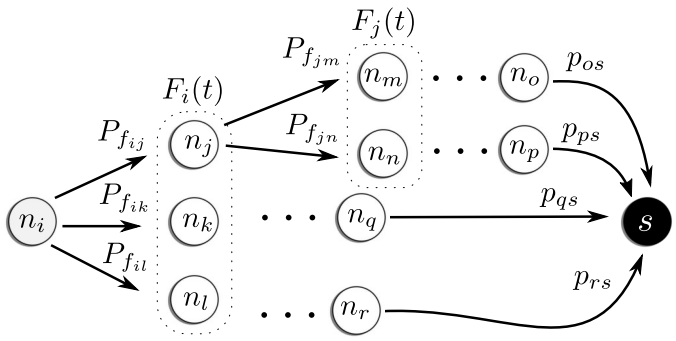

Figure 9.2: Example of calculation of the probability associated to each path of OR protocol

calculated as $\Phi_1 = f_{v_i v_j} \times f_{v_j v_m} \times p_{v_m v_s}$.

9.4.3.3 Probability of path until forwarder node k

In the previous section, we devised the probability of each one the probable multi-paths, determined from the OR protocol, from a sender node n_i to a sonobuoy s. However, one may also be interested to know the probability that a candidate node n_k, present in several paths from n_i to s, will forward the data packet.

Let us define the set $\mathcal{P}_{i,k} \subseteq \mathcal{P}_i$ composed of the unique prefix (until node n_k) of the multiple paths, determined by the OR protocol and obtained by Algorithm 10, and using node k as a vertex. The probability of each path (unique prefix) $h_l^k \in \mathcal{P}_{i,k}$ of size $\mid h_l^k \mid$ can be calculated as:

$$\Phi_l^k = \prod_{p=1}^{|h_l^k|-1} P_{f_{v_p, v_{p+1}}}. \tag{9.3}$$

9.5 The Proposed Analytical Framework

In this section, we propose an analytical framework for modeling opportunistic routing above duty cycle in mobile underwater sensor networks. In the proposed modeling, we address the following metrics for performance evaluation:

- **Packet delivery ratio:** The percentage of the generated data packets that are received by at least one sonobuoy. In the proposed modeling, this metric will be useful for understanding the impact of duty cycle in the link reliability, *i.e.*, how duty cycle affects the performance of OR protocols;

- **Energy consumption:** The average amount of energy consumed by the all underwater sensor nodes during the monitoring mission. In the proposed modeling, this metric will be useful for quantifying the benefits of the use of duty cycle;
- **Delay:** The end-to-end delay of the delivered data packets. In the proposed model, this metric will allow us to measure how duty cycle can either act to reduce and increase delay, based on the considered methodology.

When devising the aforementioned metrics, we estimate their value within an epoch. This is because these metrics relay on information regarding the network topology, which will constantly change over time due to the mobility of the nodes. At the end, we will consider the average of the packet delivery ratio and delay of each node. In regards to the energy consumption, however, the results portrays the summation of the individual costs of each epoch.

9.5.1 Always-on communication radio

We consider the always-on scenario as our baseline for the purpose of performance comparison. In this setting, underwater sensor nodes remain with their communication radio always turned on, *i.e.*, duty cycle equals 100 %. Thus, we can comparatively measure the benefits and drawbacks of duty-cycling beneath opportunistic routing. Moreover, the equations devised herein are the basis for the modeling of the duty cycle methodologies.

9.5.1.1 Packet delivery ratio estimation

A data packet transmitted from node n_i is correctly delivered if it is successfully received by any candidate node at each hop, until it reaches the destination. Therefore, we can recursively estimate the packet delivery ratio from the probability that each candidate node will receive and forward the data packet, and the packet delivery ratio from each candidate node. This can be estimated as:

$$PDR_i^{on}(t) = \sum_{\forall j \in F_i(t)} P_{f_{ij}} \times PDR_j^{on}(t), \tag{9.4}$$

where $P_{f_{ij}}$, cf. Eq. 9.1, is the probability of candidate node n_j successfully receives the data packet from n_i and forwards it. In Eq. 9.4, $PDR_j^{on}(t)$ is equal to 1 if j is a sonobuoy.

9.5.1.2 Energy consumption estimation

Herein, we estimate the energy consumption of a sensor node n_i in a given observed epoch t. To do so, it is necessary to estimate the amount of traffic that a node n_i forwards at the epoch t.

The forwarded traffic (or outgoing traffic rate) of n_i in an epoch is given by its generated data packet that n_i forwards, and the relayed traffic that comes from multiple OR paths where n_i is part (forwarder node). Therefore, we can recursively estimate this rate as:

$$\Theta_i^{on}(t) = \lambda_i + \sum_{\forall j \neq i \in V_n} \sum_{h_l^i \in \mathcal{P}_{j,i}} \Theta_j^{on}(t) \times \Phi_l^i, \tag{9.5}$$

where λ_i is the packet generation rate per epoch of node n_i (please refer to Section 9.4.2) and $\Theta_j^{on}(t)$ is the forwarded (or outgoing) traffic rate of node n_j. The outgoing traffic rate of sonobuoys are set as 0 (*i.e.*, $\forall j \in V_s, \Theta_j^{on}(t) = 0$).

From the forwarded traffic rate, we can estimate the amount of time per epoch that n_i spends transmitting and receiving data packets. The amount of time at epoch t that n_i spends transmitting data packets is:

$$T_i^{x,on}(t) = \Theta_i^{on}(t) \times \left(\frac{L_d}{\alpha B}\right). \tag{9.6}$$

The amount of time at epoch t that n_i spends receiving data packets is:

$$T_i^{r,on}(t) = \sum_{\forall j \in N_i(t)} \Theta_j^{on}(t) \times \left(\frac{L_d}{\alpha B}\right). \tag{9.7}$$

In Eq. 9.6 and Eq. 9.7, L_d is the size of a data packet, α is the channel efficiency and B is the data bit rate.

Finally, the energy consumed of node n_i at epoch t is:

$$E_i^{on}(t) = T_i^{x,on}(t) \times e_T + T_i^{r,on}(t) \times e_R + [T - T_i^{x,on}(t) - T_i^{r,on}(t)] \times e_I, \tag{9.8}$$

where T seconds is the duration of an observed epoch, and e_T, e_R and e_I refers to the electric power in transmission, reception and idle radio states, respectively.

9.5.1.3 End-to-end delay estimation

Hereafter, we estimate the end-to-end delay of data packets forwarded from a node n_i at a epoch t.

In OR protocols, the one-hop delay depends not only on the delay for packet transmission and propagation, but also on the amount of time that a forwarder holds the packet before transmitting it. The amount of this packet holding time varies at each forwarder node. In fact, it depends on the packet holding time equation of the OR protocol and the priority level of the forwarder node.

We can estimate the expected holding time of data packets forwarded from a node n_i at an epoch t as:

$$\Delta_i^{on}(t) = \sum_{\forall k \in N_i(t) \ | \ i \in F_k(t)} \delta_{ik} \times P_{f_{ki}}, \tag{9.9}$$

where δ_{ik} is the holding time of the data packet received by node n_i from a neighboring node n_k and $P_{f_{ki}}$ is the probability that n_i will forward the data packet from n_k, given by Eq. 9.1.

In order to calculate the propagation time of a data packet transmission, we approximate the speed of the sound underwater as $v = 1.5 \times 10^3$ m/s. In fact, the speed of the sound underwater is not constant and depends on the temperature of the water, salinity and pressure, which varies with depth and location [149, 39, 5]. However, this approximation is helpful for simplifying the model. Thus, the delay due to the propagation time is $H = R_c/v$, where R_c is the communication range.

Finally, we can recursively estimate the expected end-to-end delay at a epoch t of node n_i as:

$$D_i^{on}(t) = \Big(\Delta_i^{on}(t) + H\Big) + \sum_{j=1}^{|F_i(t)|} p_{ij} \prod_{k=1}^{j-1} (1 - p_{ij}) \times D_j^{on}(t), \tag{9.10}$$

where $\forall s \in V_s, D_s^{on}(t) = 0$.

9.5.2 Naive asynchronous-based duty cycle

Herein, we named naive duty-cycling the simplest duty cycle methodology, where nodes asynchronously follow their duty cycle schedule. In doing so, whenever a node has a data packet, it transmits in the hope that some of its next-hop forwarder candidate nodes are awake to receive it.

More specifically, in the naive asynchronous duty-cycling, each sensor node will independently and periodically alternate its communication radio between active and sleep states. The transition between these two modes will be purely stochastic. The amount of time in each state can be modeled according to an exponential distributed random

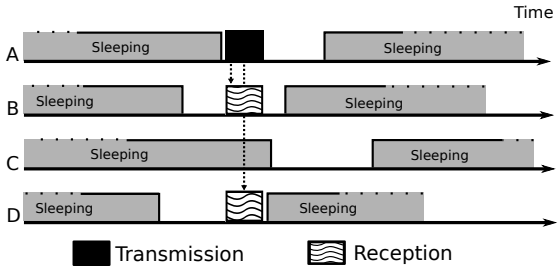

(a) **Simple asynchronous:** The transmitter sends a data packet and the next-hop candidates that are awake will receive and continue forwarding it

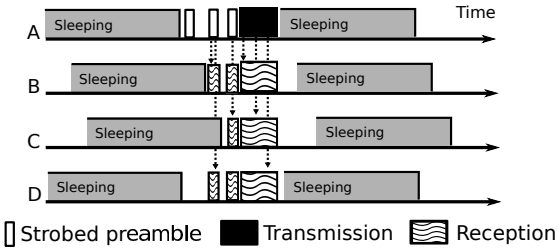

(b) **Strobed low power listening:** The transmitter sends strobed preambles before the data packet. The next-hop candidate nodes remain awake when they receive a strobed preamble, in order to further receive the data packet

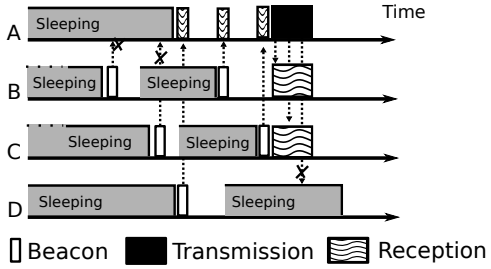

(c) **Strobed low power probing:** Each node sends a beacon whenever it wakes-up. The transmitter sends the data packet after it receives a few number of beacons

Figure 9.3: Three duty-cycling design principles

variable, with mean value of μ_a and μ_s to the active and sleep states, respectively. Therefore, the probability of having a node n_i in active mode, therefore, is $p_a = \mu_a/(\mu_a + \mu_s)$ and in sleep mode is $p_s = \mu_s/(\mu_a + \mu_s)$.

Figure 9.3a depicts an example of opportunistic routing and naive duty cycle underneath. In the depicted example, node A is the sender and $F_A(t) = \{B, C, D\}$ is its forwarder candidate set. Hereafter, when node A has a data packet to send, it broadcasts the packet in its next awake period. When node A transmits, the awake candidate nodes B and B may successfully receive the data packet. Based on the forwarding candidates' priority, each candidate that received the data packet schedules it for further transmission. This schedule is canceled if the candidate node receives the same packet from a high priority candidate.

9.5.2.1 Packet delivery ratio estimation

Herein, the same reasoning of Section 9.5.1.1 is used to calculate the packet delivery ratio of the nodes. However, active and sleep modes must be considered in this estimation. Therefore, node n_j will forward a data packet from node n_i, with probability given as:

$$P_{f_{ij}}^{nv} = p_a \times p_{ij} \prod_{k=1}^{j-1} \Big[p_s + p_a(1 - p_{ik}) \Big], \tag{9.11}$$

where p_s and p_a are the probability that the node is sleeping and in the active states, respectively. The terms p_{ij} and p_{ik} are the packet delivery probability of the link between nodes n_i and n_j and the link of nodes n_i and n_k, respectively. These probabilities are determined by Eq. 5.10.

From Eq. 9.11, the packet delivery ratio can then be estimated as:

$$PDR_i^{nv}(t) = \sum_{\forall j \in F_i(t)} P_{f_{ij}}^{nv} \times PDR_j^{nv}(t), \tag{9.12}$$

where the packet delivery ratio value of the sonobuoys is equal to 1 (*i.e.*, $\forall j \in V_s, PDR_i^{nv}(t) = 1$).

9.5.2.2 Energy consumption estimation

We must consider the effects of the sleep interval to calculate the energy consumption in the naive duty-cycling setting. The first impact of the sleep mode is in the carried traffic rate of the nodes. Since neighboring nodes can be sleeping during a transmission, some of the transmitted packets will not be received. Therefore, given $P_{f_{ij}}^{nv}$ the probability of next-hop forwarding candidate node n_j forwards a data packet from node n_i (cf. Eq. 9.11), the probability of each path $h_l^k \in \mathcal{P}_{i,k}$ in the naive duty-cycling scenario is computed as:

$$\Phi_l^{k,nv} = \prod_{m=1}^{|h_l^k|-1} f_{v_m v_{m+1}}^{nv}, \tag{9.13}$$

Similarly to the always-on settings, the outgoing traffic rate of each node i is estimated as:

$$\Theta_i^{nv}(t) = \lambda_i + \sum_{\forall j \neq i \in V_n} \sum_{h_l^i \in \mathcal{P}_j, i} \Theta_j^{nv}(t) \times \Phi_l^{i,nv}. \tag{9.14}$$

However, differently from Eq. 9.5, the Eq. 9.14 uses the probability of each path considering duty cycle (cf. Eq. 9.13).

In the naive asynchronous duty-cycling setting, the variable $\Theta_i^{nv}(t)$ is used to determine the amount of time that a node n_i spent transmitting and receiving data packets in each epoch. These values are given as $T_i^{x,nv}(t) = \Theta_i^{nv}(t) \times (L_d/\alpha B)$ and $T_i^{r,nv}(t) = \sum_{\forall j \in N_i(t)} \Theta_j^{nv} \times (L_d/\alpha B)$, respectively.

Finally, we can estimate the energy consumption rate of nodes using naive asynchronous duty-cycling as:

$$E_i^{nv}(t) \;=\; T_i^{x,nv} \times e_T + T_i^{r,nv} \times e_R + \underbrace{\left[\left(\frac{1}{T\mu_s} \times \mu_a\right) - T_i^{x,nv} - T_i^{r,nv}\right]}_{\text{Term 3}} \times e_I\,. \quad (9.15)$$

In Eq. 9.15, the third term estimates the amount of energy consumed when the node's radio is on. We determine the average number of awake intervals during an epoch length T, from the relationship between exponential and Poisson distributions. Accordingly, we can view exponential random variables with mean value $1/\lambda$ as waiting times between events modeled as Poisson process with mean value λ. Let the time between awake states be exponentially distributed with mean value μ_s. Thus, the number of active states can be modeled as a Poisson process with mean $1/T\mu_s$.

9.5.2.3 End-to-end delay estimation

The end-to-end delay of opportunistic routing and naive duty-cycling beneath can be derived in a straightforward manner, as in Section 9.5.1.3. The expected data packet holding time of a node n_i is $\Delta_i^{nv}(t) = \sum_{\forall k \in N_i(t) \;|\; i \in F_k(t)} \delta_{ik} \times P_{f_{ki}^{nv}}$, where δ_{ik} is the holding time of data packet received from node n_k and $P_{f_{ki}^{nv}}$ is the probability that the node n_i will forward the data packet received from node n_k, given by Eq. 9.11. We estimate the expected lower bound end-to-end data packet delay, at an epoch t, of a node n_i as:

$$D_i^{nv}(t) \;=\; \Big(\Delta_i^{nv}(t) \;+\; H\Big) \;+\; \sum_{j=1}^{|F_i(t)|} p_a p_{ij} \;\times\; \prod_{k=1}^{j-1} \Big[p_s \;+\; p_a(1 \;-\; p_{ij})\Big] D_j^{nv}(t), \quad (9.16)$$

where $H = R_c/v$ is the packet propagation time and $\forall s \in V_s, D_s^{nv}(t) = 0$.

9.5.3 Strobed preamble LPL-based duty cycle

Low-power listening (LPL) duty-cycling has been proposed in wireless sensor networks [74, 150]. In this duty-cycling approach, each node asynchronously remains active for the period of t_a, after which is goes to sleep for the period of t_s. Thus, an observed node is active and sleeping with probability $p_a = t_a/(t_a + t_s)$ and $p_s = t_s/(t_a + t_s)$, respectively.

In this approach, whenever a sender node has a data packet to send, it transmits a preamble before its data packet transmission. The transmission of the preamble lasts for a slightly longer duration than the intended neighbor nodes' sleep interval. It is to ensure that the intended receiver will be awake when the data packet is transmitted. When the receiver wakes up, it detects the preamble transmission and remains awake to receive the data packet.

The abovementioned traditional LPL duty-cycling approach is not feasible for UWSNs. This is due to the high energy cost of the preamble transmissions. In order to overcome this drawback, strobed preamble version of LPL duty-cycling has been investigated. Figure 9.3b depicts an example of our proposed strobed preamble LPL and opportunistic routing scenario. Short preambles are transmitted by the sender node A, followed by pause periods. The number of strobed preambles is determined by the maximum sleep interval of the next-hop forwarder candidate nodes, B, C and D. Whenever a forwarding candidate node receives a strobed preamble, it remains awake, waiting for further data packet transmissions. This approach ensures that all candidates are awake prior to data packet transmission.

9.5.3.1 Packet delivery ratio estimation

In this approach, once all next-hop forwarder candidate nodes are awake when a sender transmits, the packet delivery ratio of strobed preamble LPL duty-cycling is the same of the always-on configuration of the radio, given by Eq. 9.4.

9.5.3.2 Energy consumption estimation

In strobed LPL duty-cycling setting, it is necessary to know the average amount of time spent transmitting strobed preambles ($T_{i,X}^{pre}$) before data packet transmission when estimating the energy consumption rate of each node i. Moreover, it is necessary to know the average amount of time that a node i spends receiving strobed preambles ($T_{i,R}^{pre}$) from neighboring nodes. We derive these averages in the following.

Let $t_{preamble}$ and t_{pause} be the duration time of a strobed preamble transmission and silence interval, between strobed preamble transmissions, respectively. The amount of time that a node spent during a cycle transmitting strobed preambles and receiving them from neighboring nodes is given by Eq. 9.17 and Eq. 9.18, respectively.

$$T_{i,X}^{pre} = \frac{t_s}{t_{preamble} + t_{pause}} \times t_{preamble}. \tag{9.17}$$

$$T_{i,R}^{pre} = \frac{t_s/2}{t_{preamble} + T_{pause}} \times t_{preamble}. \tag{9.18}$$

The overall amount of time that a node i will spend transmitting in an epoch will be $T_i^{x,sp} = \Theta_i^{on}(t)(L_d/\alpha B + T_{i,X}^{pre})$ and receiving will be $T_i^{r,sp} = \sum_{\forall k \in N_i(t) \mid i \in F_k(t)} \Theta_j^{on}(t)(L_d/\alpha B + T_{i,R}^{pre})$. Finally, the energy consumption rate a node i can therefore be calculated as:

$$E_i^{sp}(t) = T_i^{x,sp} \times e_T + T_i^{r,sp} \times e_R + \Big(C \times t_a - T_i^{x,sp} - T_i^{r,sp}\Big)e_I, \tag{9.19}$$

where $C = (t_a + t_s)/T$ is the number of cycles during an epoch and the expression $C \times t_a$ computes the amount of time that a node remains active during an epoch. In the third term of Eq. 9.19, $T_i^{x,sp}$ and $T_i^{r,sp}$ are used to reduce the amount of time that the node is awake but not in an idle state; that is, it is transmitting or receiving data packets. It should be mentioned that, in this last expression, only data packets transmitted by neighboring nodes in which i is a next-hop forwarding candidate are considered for the calculation of the reception energy consumption. This is because a node will not receive unintended data packets, despite the broadcast nature of the wireless medium, since it could infer the designated forwarders from strobed preambles. It can verifies whether it is one of them. If it is not a designated forwarder, the node can proceed with the sleep operation and avoid receiving the further transmitted data packet.

9.5.3.3 End-to-end delay estimation

Finally, the end-to-end data packet delay from node i can be estimated recursively by:

$$D_i^{sp}(t) = \frac{t_s}{2} + H + \Delta_i^{on}(t) + \sum_{j=1}^{m} p_{ij} \prod_{k=1}^{j-1}(1 - p_{ij}) \times D_j^{sp}(t). \tag{9.20}$$

where $H = R_c/v$ is the packet propagation time, $\Delta_i^{on}(t)$ is the average packet holding time at node i, given by Eq. 9.9, and $\forall s \in V_s, D_s^{sp}(t) = 0$.

9.5.4 Low-power probing (LPP)-based duty cycle

In the previously described duty-cycling strategy, sender nodes will be in higher demand and will incur higher energy costs due to strobed preamble transmissions. This behavior can lead to network partitions, particularly in applications with high traffic generation rates.

In order to overcome this aspect, Sun et al. [139] proposed a different strategy of receiver-initiated (low-power probing) data transmission. In this approach, the sender node remains active and silently waits for an indication that the intended receiver has woken up. Whenever a node wakes up, it transmits a short packet to inform all sender nodes. The receiver initiated-based or low-power probing duty-cycled MAC protocols aim to reduce the energy consumption of the long preamble transmissions of low-power listening-based MAC protocols. Moreover, this technique reduces the end-to-end delay, as there is no need for preamble transmissions.

Herein, we propose a low-power probing duty-cycling and opportunistic routing strategy. Figure 9.3c depicts an example of our LPP duty-cycling and opportunistic routing scenario. Accordingly, whenever a node wakes up, it sends out a beacon of t_b duration to notify its neighboring nodes that it is awake. During an amount of time of t_r, an awaking node checks the channel activity for incoming data packets. If a data packet is received during this time and the node is a next-hop forwarding candidate for the sender, it schedules the packet to be forwarded according to its priority level. Otherwise, it goes back to sleep for the t_s time. At the sender side, when a data packet is ready to be transmitted, it remains awake, waiting for the beacon packets from its neighbor.

9.5.4.1 Packet delivery ratio estimation

Packet delivery ratio of low power probing duty-cycling and OR protocols is calculated similarly to the naive duty-cycling approach presented in Section 9.5.2. However, herein, the periods of time a node is asleep or active during a cycle, t_s and t_a, are deterministic instead of stochastic. Therefore, in calculating the packet delivery ratio, we use $p_a = t_a/(t_s + t_a)$ and $p_s = t_s/(t_s + t_a)$ as the probabilities of a node being active and sleeping, respectively.

9.5.4.2 Energy consumption estimation

In calculating energy consumption, we use Eq. 9.14 to estimate the carried traffic rate per epoch of each sensor node. For the purpose of clarity, hereafter, we gave the carried traffic rate of Eq. 9.14 the notation $\Theta_i^{lpp}(t)$, computed using $p_a = t_a/(t_s+t_a)$ and $p_s = t_s/(t_s+t_a)$. At each epoch, a node i will spent $T_i^{x,lpp} = \Theta_i^{lpp}(t)\frac{L_d}{\alpha B} + C \times t_b$ amount of time transmitting packets and $T_i^{r,lpp} = \mid N_i(t) \mid p_a t_b C + p_a \frac{L_d}{\alpha B} \sum_{j \in N_i(t)} \Theta_j^{lpp}(t)$ amount of time receiving

packets. We can compute the energy consumption rate of a node i per epoch as:

$$E_i^{lpp}(t) \;=\; T_i^{x,lpp} \times e_T + T_i^{r,lpp} \times e_R + \Big(C \times t_a - T_i^{x,lpp} - T_i^{r,lpp}\Big) e_I. \quad (9.21)$$

In the above equation, it is worth mentioning that, due to the receiver-initiated mechanism, a receiver node cannot know in advance whether or not the data packet to be transmitted is intended to reach it. Therefore, due to the broadcast nature of wireless communication, a node will hear the data packet transmission of all of its neighbors. In the low-power probing duty-cycling strategy, it does not happen because a node can know if it is a next-hop forwarding candidate node from strobed preambles. Thus, it can go sleep if it is not in the forwarding candidate set. The third term of Eq. 9.21 calculates the energy consumption cause by the idle period. This amount of time corresponds to the awake time, in which node i was not transmitting or receiving packets.

9.5.4.3 End-to-end delay estimation

The end-to-end delay for each node in the LPL duty-cycling scenario can be estimated following the same reasoning of the abovementioned duty-cycling strategies. Accordingly, it is given as:

$$D_i^{lpp}(t) \;=\; \left\{ \Delta_i^{lpp}(t) + H + \frac{t_s}{2} + \sum_{j=1}^{|F_i(t)|} p_a p_{ij} \prod_{k=1}^{j-1} \Big[p_s + p_a \Big(1 - p_{ij}\Big) \Big] D_j^{lpp}(t) \right\}, \quad (9.22)$$

where $\Delta_i^{lpp}(t) = \sum_{\forall k \in N_i(t) \;|\; i \in F_k(t)} \delta_{i,k} \times f_{ki}^{nv}$; $\delta_{i,k}$ is the holding time of data packet received from node k; $f_{ki}^{n}v$ is the probability of the node i forwards the data packet received from node k, given by Eq. 9.11; $H = R/v$ is the packet propagation delay; and $\forall s \in V_s, D_s^{lpp}(t) = 0$.

9.6 Performance Evaluation

In this section, we instantiate the proposed analytical framework to evaluate the performance of joint opportunistic routing and duty-cycling in underwater sensor networks.

We use MATLAB to implement the proposed model and generate several network topologies. Moreover, we implement the Urick's underwater acoustic channel model [28] and the noise sources revised in Section 5.5, to simulate the dynamics of underwater acoustic communication.

In our study, we consider a mobile underwater sensor network in which underwater nodes move according to the dynamics of the ocean's movements. It is worth mentioning that ocean mobility has a high impact on the connectivity of the underwater sensor network [134]. The mobility of underwater nodes highly influences UWSN topology, changing the average degree of the nodes and network connectivity over time [151]. This factor will diminish the performance of UWSNs' applications. In order to make our analysis more realistic, we used the extended 3 D version of the meandering current mobility to simulate that movement. The mobility model considers the effects of meandering sub-surface currents (or jet streams) and vortices. The value parameters of the MCM model are the same as in [38].

9.6.1 Model setup

We simulate the underwater sensor network deployment as follows. We consider a region of size 10 km×10 km×10 km. It is important to mention that the average ocean depth is 2.3 miles (≈ 3.7 km). The vertical 10 km is about the depth of the deepest known point in the oceans (Mariana Trench).

We divide the surface area into a grid, with 25 squares with sides equal to 2000 m. Regarding the deployment of sonobuoys at the sea surface, we simulate the continuously random deployment of one sonobuoy at each cell of the grid, until all 64 sonobuoys are completely deployed. Underwater sensor nodes are evenly deployed in the considered area of interest. We simulate the deployments of 35 and 75 underwater sensor network scenarios, corresponding to network densities of average degrees of 5 and 12.

Regarding the duty-cycling settings in our modeling, we consider that each epoch lasts for 1 min. We have varied duty cycle in the following values of 5 %, 10 %, 15 %, 20 % and 25 %. We have set the duration of a cycle as 20 seconds. Remaining that for each considered length of cycle t_c and a duty cycle of σ, the active and sleep intervals are calculated as $t_a = \sigma \times t_c$ and $t_c = (1 - \sigma) \times t_c$, respectively. Thus, with these settings, active and sleep interval values are $t_a = \{1, 2, 3, 4, 5\}$ seconds and $t_s = \{19, 18, 17, 16, 15\}$ seconds, respectively.

We use the nodes' configuration according to the specifications of the Telesonar SM-75 SMART modem by Teledyne Benthos [112]. The transmission power of the nodes is set to 190 dB μ re Pa. The transmission frequency, bit rate and channel efficiency are $f = 14$ kHz, $B = 18700$ bps and $\alpha = 1$, respectively. The unitary transmission, reception and idle energy costs are $e_T = 18$ W, $e_R = 0.8$ W and $e_I = 0.08$ W, respectively.

Finally, we consider that each sensor node generates one packet size of $L_d = 250$ bytes per epoch. Strobed preamble and beacon packets used by low-power listening and low-power probing duty-cycling approaches are 4 bytes in size. In our experiments, we use DBR and Hydrocast opportunistic routing protocols. These are two pressure-based routing protocols designed for underwater sensor networks. In our simulations, each run lasts 1 h. The results correspond to an average value or the empirical cumulative density function of 30 runs, with a 95 % confidence interval.

9.6.2 Numerical results

Figure 9.4 shows the complementary empirical cumulative density function (CCDF) of the packet forwarding probability of candidate nodes having high (level 1) and low (level 5) priorities. We plot the results of DBR and Hydrocast routing protocols for several configurations of duty cycle, and low and high network densities of 35 and 125 nodes. In the plots, the curves portray the results regarding naive and low-power probing (LPP) duty cycling approaches, where there is no mechanism for awaking all candidate nodes during a transmission of the sender node.

The first trend that can be observed in Figure 9.4 is that duty cycle impacts the probability that a candidate node will forward data packets. For instance, as shown in Figure 9.4a, approximately 18 % of the high level priority candidates has 20 % probability of forwarding received data packet when duty cycle is 100 %. Conversely, as duty cycle decreases, the probability that a high priority candidate will forward data packets drastically decreases. In fact, for a duty cycle of 5 %, there is no candidate that has a probability higher than 10 % of forwarding the packet.

When we compare the results of low duty cycle, independently of the considered routing protocols and network density, the packet forwarding probabilities are similar. This is because in this setting, it is very unlikely to find a neighboring node awake during a packet transmission. Therefore, opportunistic routing protocols in this duty-cycling setting should be more concerned with increasing candidate set density than in best priority level assignment between candidates. Moreover, transmission coordination through different packet holding times is unnecessary and should even be avoided. Since the probability of finding a node awake will be the dominant factor in the packet forwarding, the use of timer-based transmission coordination will only increase the end-to-end delay.

Another trend that can be observed in Figure 9.4 is the low packet forwarding probability for high priority nodes, particularly in low duty cycle. For instance, Figures 9.4a,

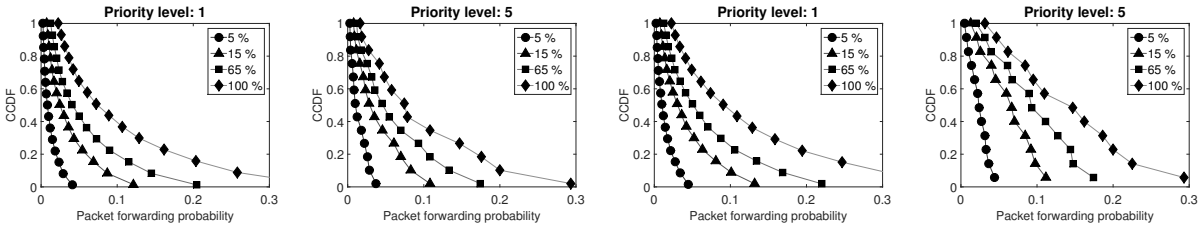

(a) DBR routing protocol, 35 nodes (b) DBR routing protocol, 35 nodes (c) Hydrocast routing protocol, 35 nodes (d) Hydrocast routing protocol, 35 nodes

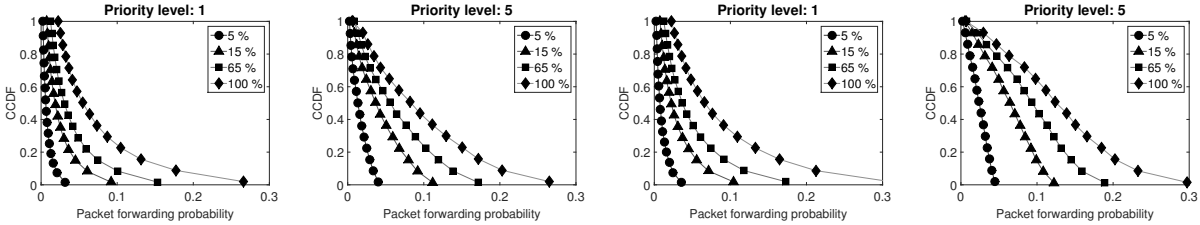

(e) DBR routing protocol, 125 nodes (f) DBR routing protocol, 125 nodes (g) Hydrocast routing protocol, 125 nodes (h) Hydrocast routing protocol, 125 nodes

Figure 9.4: Packet forwarding probability according to the priority level

9.4c, 9.4e and 9.4g show that, for a duty cycle of 25 %, the packet forwarding probability of the highest priority node is less than 25 %. This means that the greatest fraction of data packets is forwarded by low level priority nodes. This is an important insight for designing candidate set selection procedures of opportunistic routing protocols in duty cycled networks. In this case, these high priority nodes should be removed from the candidate set, since they will only have the undesired effect of increasing end-to-end delay, as low priority level nodes should wait to see if a high priority node will continue forwarding the packet.

Figure 9.5 depict the average packet delivery ratio of naive/low-power probing duty-cycling, as network operation time elapses. We consider a scenario of low (5%) and moderate (20%) duty cycle. As expected, packet delivery ratio decreases as the network operation time increases. This is due to the underwater nodes' displacement occasioned by ocean currents, which leads to disconnections in the network topology.

Figure 9.6 portrays the results of packet delivery ratio when duty cycle varies. We remember that the packet delivery ratios for always-on and LPL settings are the same, as well as those for naive and LPP, as discussed in Section 9.5. As shown in Figure 9.6a, the use of naive and LPP duty-cycling settings decreased the PDR by approximately 85 % and 65 % for the worst-case scenario of duty cycle of 5 %, with a network density of

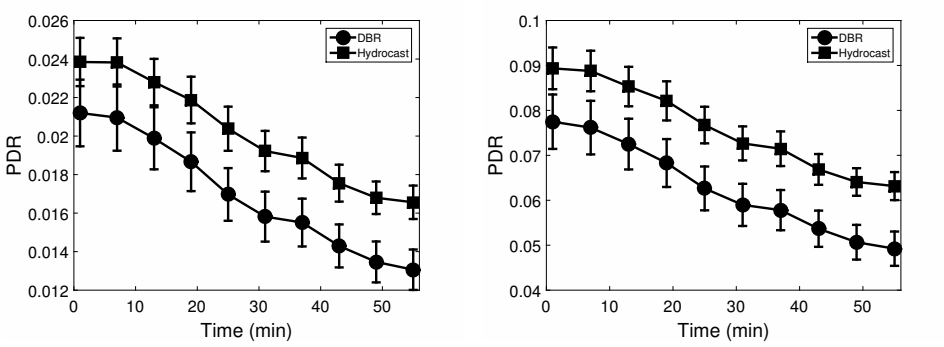

(a) 75 nodes, duty cycle of 5% (b) 75 nodes, duty cycle of 20%

Figure 9.5: Packet delivery ratio

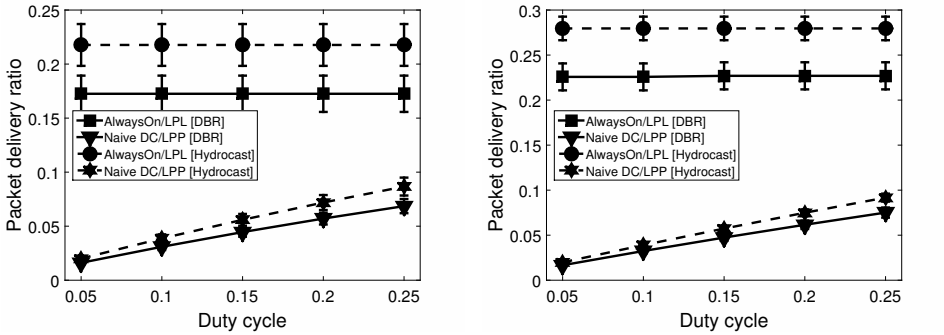

(a) 35 nodes (b) 75 nodes

Figure 9.6: Packet delivery ratio

35 nodes, for DBR and Hydrocast, respectively. Even increasing the average node degree (from 5 to 7), Figure 9.6 shows that PDR is still lower when using duty-cycling. As the duty cycle increases, the PDR increases. This expected behavior occurs because these duty-cycling settings do not guarantee that all candidates will be awake during a packet transmission. With the increment of the duty cycle, the probability that a sender node will find awake candidate nodes also increases, as corroborated in the following analysis.

Figure 9.7 shows the average energy consumption. In the plots, this metric is normalized by the energy consumption of the network when duty-cycling is not employed. In all of the considered scenarios, low power probing (LPP) duty-cycling had lower energy consumption. This is due to the fact that a sender node only transmits when it knows that at least one forwarding candidate node is awake, in contrast to the naive approach. Interestingly, when network density is high, naive asynchronous duty-cycling incurred higher energy consumption (please refer to Figures 9.7b and 9.7d). This is because an

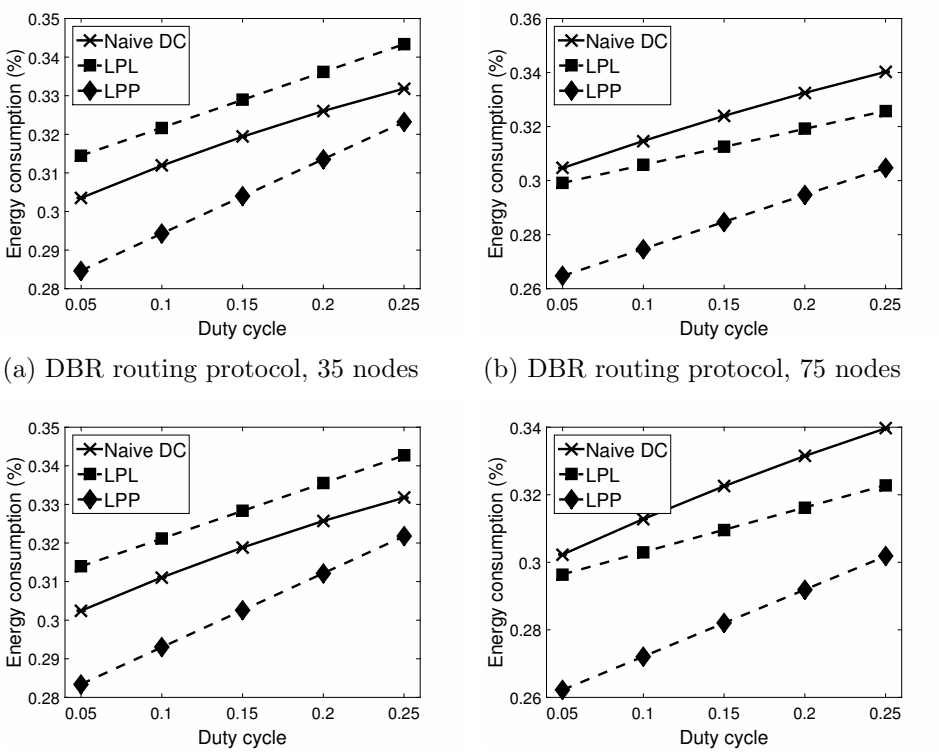

(a) DBR routing protocol, 35 nodes

(b) DBR routing protocol, 75 nodes

(c) Hydrocast routing protocol, 35 nodes

(d) Hydrocast routing protocol 75 nodes

Figure 9.7: Avgerage energy consumption

increase in network density also increases the traffic load head by a node. In the LPL approach, a sensor node goes to sleep when it hears a strobed preamble of an unintended data packet, thus avoiding spending energy listening for data packets that are not addressed to it. Conversely, in the naive duty-cycling approach, an awake node will receive all the transmitted data packets within its communication range.

Figure 9.8 depicts the results of the average end-to-end delay. As already expected, for both routing protocols duty cycle affects delay on LPL approach. In this duty-cycling approach, lower duty cycle results in higher delay. This is due to the strobed preambling period before a data packet transmission. Moreover, for both protocols, when network density increases, the average end-to-end delay increases. This is due to the delivery of data packets from distant nodes, to high density scenarios that could be not delivered to low density scenarios, as corroborated by an increase in the packet delivery ratio shown in Figure 9.6b.

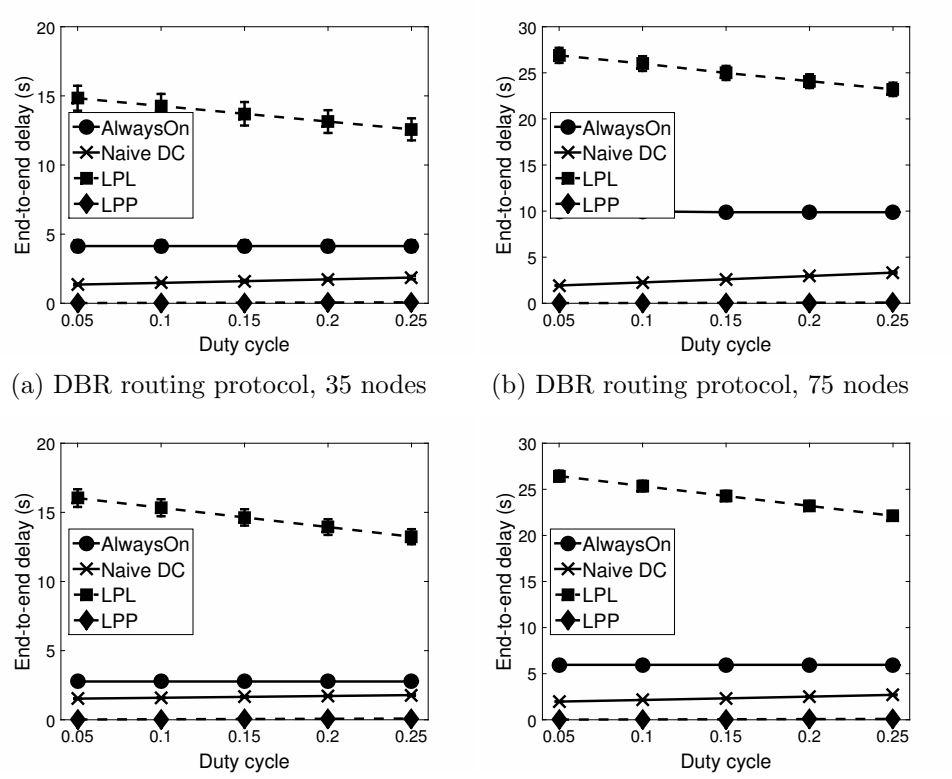

(a) DBR routing protocol, 35 nodes

(b) DBR routing protocol, 75 nodes

(c) Hydrocast routing protocol, 35 nodes

(d) Hydrocast routing protocol 75 nodes

Figure 9.8: Avgerage end-to-end delay

9.7 Discussion

Nowadays, opportunistic routing has been extensively proposed for efficient data collection in mobile underwater sensor networks. However, there is a lack of works investigating this routing paradigm under duty cycle settings, to achieve energy efficiency. In this sense, the proposed analytical framework is helpful for obtaining insights in this direction. In the evaluated scenarios, it was possible to observe that packet delivery ratio, energy consumption and delay of opportunistic routing protocols were impacted by the use of duty-cycling.

Overall, duty-cycling might reduce the benefits of the traditional opportunistic routing proposals. In fact, when there is no guarantee that all forwarding candidates will be awake during a packet transmission, the packet delivery ratio is drastically reduced. However, the use of duty cycle showed enormous benefits in conserving energy in mobile underwater sensor networks. This is an achievement that must be explored. Thus, novel

cross-layer design of opportunistic routing and duty cycle protocols for mobile underwater sensor networks must be investigated.

The abovementioned characteristics obtained from the proposed model are insightful. Depending on the requirements of the application, we might select a better approach for designing cross-layer duty-cycling and opportunistic routing protocols. For instance, for short-term applications requiring high fidelity for data collection (*e.g.*, oil spill monitoring or underwater surveillance), the strobed preambling low-power listening duty-cycling approach is suitable, since it reduces energy consumption and keeps packet delivery ratio as in the always-on scenarios. However, if the application can tolerate a certain degree of packet loss, low-power probing or even naive asynchronous duty-cycling could be considered. This is the case for applications requiring periodic measurement of underwater variables. Accordingly, a few obtained measurements could be used to predict overall trends on the monitored variables.

9.8 Concluding Remarks

In this Chapter, we propose an analytical model for evaluating joint designs of duty-cycling and opportunistic routing protocols in mobile underwater sensor networks. We proposed a desired collision of duty-cycling and opportunistic routing to conserve energy and prolong the network lifetime of mobile UWSNs, whilst maintaining data delivery reliability. Our proposed model considered the characteristics of the most common approaches for designing duty-cycling protocols: naive asynchronous, low-power listening and low-power probing approaches. Moreover, it considered the unique characteristics of underwater environment, underwater acoustic communication, underwater sensor mobility, and opportunistic routing.

Numerical results showed the benefits and drawbacks of the combination of duty-cycling and opportunistic routing in mobile UWSNs. The use of duty-cycling leads to energy conservation in the network. However, for some duty-cycling approaches, the data delivery ratio is decreased. In this context, the proposed model proves useful for obtaining insights for duty-cycling and opportunistic routing protocol designs and scenario configurations to achieve a desired performance, according to the requirements of the applications.

Chapter 10

An Optimization Model of the Sleep Interval Adjustment Problem in Duty-Cycled UWSNs

In this Chapter, we propose a new modeling framework to study the fixed and optimized sleep interval settings of duty-cycled UWSNs running opportunistic routing protocols. Our framework considers the underwater acoustic communication characteristics, network density and traffic load, and the peculiarities of the opportunistic routing and strobed preamble LPL duty-cycling. Moreover, we formulate the on-the-fly sleep interval control as an optimization problem, with the goal of to prolong the network lifetime. We explore several possible traffic load and duty-cycling configurations for a mobile UWSN scenario running opportunistic routing protocols.

This Chapter is organized as follows. Section 10.1 provides the motivation for the study of the sleep interval in duty-cycled UWSNs using opportunistic routing protocols. Section 10.2 provides more details about opportunistic routing and LPL duty cycle in underwater networks. Section 10.3 describes the network architecture considered in this work. Section 10.4 presents the proposed energy consumption model and the sleep interval control optimization problem. Section 10.5 shows the performance evaluation and the preliminary results achieved from the proposed model. Finally, the conclusion and future work are presented in Section 10.6.

10.1 Introduction and Motivation

Duty-cycling protocols have been proposed to save energy in underwater sensor networks [152, 153, 5, 75]. In this approach, nodes periodically alternate their communication radio between active and sleep modes. The idea is to put the nodes in the sleep mode during the most part of the time, to save the energy relative to the idle listening since underwater monitoring applications have very infrequent data sample rates, leading to sporadic transmissions (*e.g.*, once a week or less in underwater sensor networks [65]). Duty cycling protocols can be classified in synchronous and asynchronous approaches. In synchronous duty-cycling, nodes must negotiate a schedule to align their awake and sleep periods. Advantageously, the source node is aware when its next-hop node is awake and ready to receive the packet. However, a periodic overhead is incurred to synchronize the nodes' clock and duty cycle schedules. In asynchronous duty-cycling, the nodes' duty cycle schedules are decoupled. Whenever a node has a packet to transmit, it informs the next-hop node to be awake during the transmission interval. The control signaling traffic will be locally and proportional to the data traffic load between the communicating pair nodes, which makes this approach most suitable for underwater sensor network scenarios.

One strategy to align the awake time of the source and next-hop node in asynchronous duty-cycling is through signaling packet transmissions. In low power listening (LPL) technique [154], the sender is responsible for sending preambles before the data packet transmission. The preamble duration lasts for the time corresponding to the sleep interval of the next-hop node. It is important mentioning that LPL preamble transmission is prohibitive in UWSNs due to the high energy cost for transmissions. However, LPL using strobed preambles can be effective in UWSN applications. In this variant, the sender interleaves strobed preamble transmission and silent time. The next-hop node remains awake when it wakes-up and detects a strobed preamble transmission.

The combination of opportunistic routing and duty cycling is desired for underwater sensor networks. By using both techniques, the energy consumption decreases whereas the data packet delivery ratio is still maintained at high level, as we showed in the previous Chapter. However, the effects of the sleep interval and its on the fly adjustment is still an open research question in UWSNs despite some works in wireless sensor networks [155, 156, 157, 74]. Identical sleep interval among the nodes does not account for different traffic loads in the routing path, which may result in unbalanced energy consumption.

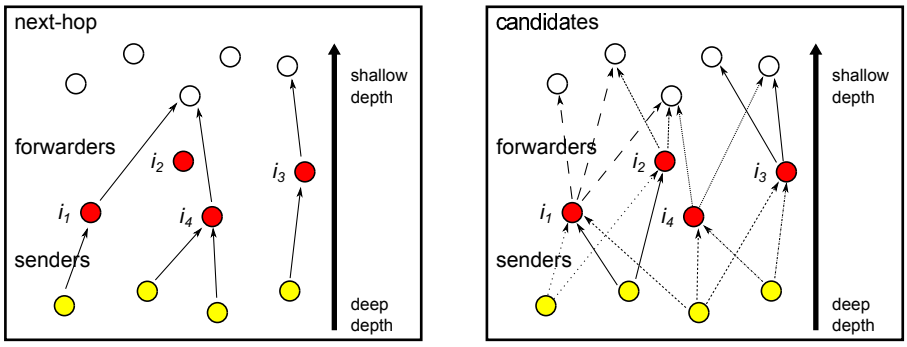

(a) Traditional multi-hop (b) Opportunistic routing

Figure 10.1: Multi-hop routing paradigms

10.2 Related Work and Problem Statement

Recently, some works have been proposed to the properly sleep interval selection and on-the-fly adjustment in the context of the multihop routing (Figure 10.1a) on terrestrial wireless ad hoc and sensor networks.

The ZeroCal protocol [155] adjusts the sleep interval of the nodes according to traffic load variations. The pTunes framework [156] adapts the duty-cycled MAC parameters based on the network lifetime, end-to-end latency and end-to-end reliability. The I^2C approach [157] adjusts the sleep interval of the nodes based on the energy consumption rate of the child nodes in the routing path. In those proposals, the parent and child node tune-up their sleep interval considering the fact that long sleep interval at a node will save its energy but it will increase the energy consumption of its children nodes, due to strobed preamble transmissions. Moreover, the sleep interval control should consider the traffic load at the nodes in order to avoid them waste energy because of unnecessary channel polling. Zhu et al. in [158] and [159] investigated the sleep scheduling for geographic routing and top-k query in duty-cycled wireless sensor networks.

In this Chapter, we consider an underwater sensor network scenario where each node, at the MAC layer, operates in duty-cycling way employing the strobed preamble variant of the low power listening (LPL) technique; and at the network layer, uses an opportunistic routing protocol. In this scenario of duty-cycle meeting opportunistic routing, the sleep interval control should consider the next-hop candidates' sleep interval information, as shown in Figure 10.1b. This is because the sleep interval of a node will affect the energy consumption of itself, its next-hop candidate nodes and all its neighbors having the node as a next-hop candidate. By choosing a short sleep interval, a node saves the

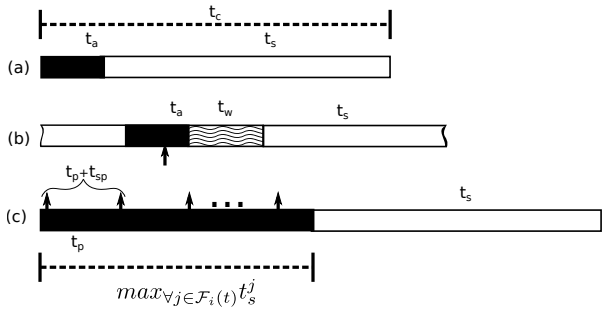

Figure 10.2: Illustration of the strobed preamble low power listening duty-cycling

energy relative strobed preamble receptions. However, the sender node using it as a candidate, will need transmit more strobed preambles. Moreover, nodes in the candidate set waking up earlier will spend energy receiving unnecessary preambles since it will last to the maximum sleep interval of the next-hop candidates. This behavior makes the sleep interval control in OR scenarios a challenging task.

Figure 10.2a shows the cycle of a node. The cycle has the duration of t_c. The interval t_a is the awake time of a node during the cycle. The interval t_s is the sleep time of a node during the cycle. If the node receives a strobed preamble during its awake time t_a, it remains awake for an additional time t_w, where it waits for the packet transmission, as showed in Figure 10.2b. Figure 10.2c shows the behavior of a source node when it has data packet to transmit. Firstly, it transmits strobed preambles of duration t_{sp} interleaved of silent intervals of duration t_p. This procedure lasts for the time corresponding to the maximum sleep interval of the next-hop candidates. It will ensure that all next-hop candidates will be awake when the data packet is transmitted. Secondly, the node broadcast the data packet after the preambling phase discussed previously.

10.3 Network Model

We consider a mobile UWSN comprising of several sensor nodes deployed underwater and sonobuoys (sinks) deployed at sea's surface. The network topology is represented by a graph $G = (V, E(t))$, where $V = \{V_n \cup V_s\}$ is the finite set of nodes (V_n) and sonobuoys (V_s), and $E(t)$ is the finite set of link between the nodes at a time t. At time t, there is an edge between the nodes i and j, *i.e.*, $e_{ij}(t) \in E(t)$, if they are neighbors and can communicate each other directly and consistently over a wireless acoustic link.

Each sensor node i monitors its surrounding variables. We model the packet gener-

ation at each sensor node i according to a Poisson process with rate λ_i, as it has been done on several works proposing and evaluating medium access control and routing analytical framework models and protocols proposed for underwater sensor networks (*e.g.*, [160, 161]). The sensor nodes report collected data to a surface sonobuoy through multihop acoustic communication. Each sonobuoy is equipped with both a radio frequency-based and an acoustic transceiver. They collect data from underwater nodes using underwater acoustic communication and send them to a monitoring center by means of radio frequency-based links.

Due to the channel fading, there is a packet delivery probability $p_{ij}(t)$ associated with each link $e_{ij}(t) \in E(t)$. This parameter is a function of distance between communicating nodes i and j, and the packet size of m bits to be transmitted between them. We define $\Omega_i(t)$ as the neighborhood set of node i ($i \notin \Omega_i(t)$). Each node can know its neighbors along the time through periodic beaconing.

Using opportunistic routing protocol, when a node i has data packet to send it should determine its next-hop candidate set. Several heuristics have been proposed to select the candidate set according to different metrics and provided information [13, 35]. OR protocol selects a subset $\mathcal{F}_i(t)$ of the neighbor set $\Omega_i(t)$ of the nodes enabled to continue forwarding the data packet towards to the destination.

10.4 The Proposed Modeling Framework

10.4.1 Energy consumption analysis

In our modeling framework, the energy consumption rate of a node i at time t is:

$$E_i(t) = E_t^i(t) + E_r^i(t), \tag{10.1}$$

where $E_t^i(t)$ and $E_r^i(t)$ are the energy consumption due to packet transmissions and receptions, respectively. Basically, these transmissions are relative to the strobed preambles and data packets. We detail each cost in the following.

10.4.1.1 Energy consumption for receiving packets

Each node spends energy when it receives data packets and strobed preambles. Due to the broadcast nature of the wireless medium, a node will hear intended and unintended transmissions when it is awake. Let $\Omega_i(t)$ be the neighborhood set of node i and $\mathcal{F}_j(t) \mid j \in$

$\Omega_i(t)$ be the candidate set of its neighbor j at time t. Due to the asynchronously duty-cycle schedule of the nodes, the node i may wake-up during at any portion of the j's strobe preamble transmissions. Therefore, on average, the node i receives $N_j^r(t)$ strobed preambles from the neighbor node j, at each data packet transmissions, given by:

$$N_j^r(t) = \frac{\max\limits_{\forall k \in \mathcal{F}_j(t)} \{t_s^k(t)\}}{2(t_{sp} + t_p)}. \tag{10.2}$$

Given $\lambda_j(t)$ the data packet generation rate at the node j, the incoming strobed preamble packets rate at node i and time t is:

$$\mathcal{I}_p^i(t) = \sum_{\forall j \in \Omega_i(t)} \lambda_j(t) N_j^r(t). \tag{10.3}$$

Hereafter, we estimate the incoming data packet rate at the node i and time t. Denote $p_{a|j}^i$ the probability of a node i is awake when its neighbor node j transmits a data packet. If i is a next-hop candidate from j, *i.e.*, $i \in \mathcal{F}_j(t)$, it will be awake when j transmits its data packet. Otherwise, i will receive the data packet only if its awake time overlaps j's data packet transmission time. Thus, i is awake when its neighbor j transmits a data packet with probability:

$$p_{a|j}^i = \begin{cases} 1 & \text{, if } i \in \mathcal{F}_j(t) \\ \frac{t_a}{t_a + t_s^i(t)} & \text{, otherwise.} \end{cases} \tag{10.4}$$

From Eq. 10.4 and the packet generation rate of the neighbor nodes, we can estimate the incoming data packet rate at node i and time t as:

$$\mathcal{I}_d^i(t) = \sum_{\forall j \in \Omega_i(t)} \lambda_j(t) p_{a|j}^i. \tag{10.5}$$

Finally, the energy consumption for packet reception is:

$$E_r^i(t) = e_R \Big[\mathcal{I}_p^i(t) t_{sp} + \mathcal{I}_d^i(t) t_d \Big], \tag{10.6}$$

where e_R is electrical power in reception radio on mode, $\mathcal{I}_p^i(t)$ and $\mathcal{I}_d^i(t)$ are the incoming strobed preamble and data packet rates given by Eqs. 10.3 and 10.5, respectively.

10.4.1.2 Energy consumption for transmitting packets

Each node spends energy to transmit and relay data packets and strobed preambles. A node i relays data packets when: i) it receives them from its neighbors, ii) it is in the candidate set and iii) the high priority level nodes failed in relay the packet.

The outgoing data transmission rate of i's generated packet is λ_i. The outgoing data rate of i's relayed packets depends of the i's priority in the candidate set of its each neighbor. Denote $p^i_{f|j}$ the probability of the node i relays the data packet received from its neighbor j. Assuming that there is a perfect transmission coordination between next-hop candidates [162, 163], the node i relays data packets coming from the neighbor j with probability:

$$p^i_{f|j} = \frac{p_{ji}(t)\prod_{k=1}^{j-1}(1-p_{jk}(t))}{1-\prod_{k=1}^{m}(1-p_{jk}(t))}, \tag{10.7}$$

where $p_{ab}(t)$ is the packet delivery probability from node a to b. Term $\prod_{k=1}^{j-1}(1-p_{jk}(t))$ calculates the probability of the high priority candidates fail in receiving, and consequently relaying, the data packet. We can estimate the overall outgoing data packets traffic rate of node i at time t as:

$$\Theta^i_d(t) = \lambda_i(t) + \sum_{\forall j \in \Omega_i(t) \wedge i \in \mathcal{F}_j(t)} \lambda_j(t) p^i_{f|j}. \tag{10.8}$$

Using the low power listening duty-cycling approach, a strobed preambling phase will behave a data packet transmission. The number of transmitted short preambles will depend of the sleep interval of the candidates. It can be estimated as:

$$N^t_i(t) = \frac{\max_{\forall k \in \mathcal{F}_i(t)}\{t^k_s(t)\}}{(t_{sp}+t_p)}. \tag{10.9}$$

From Eqs. 10.8 and 10.9, we estimate the outgoing preamble packets rate as:

$$\Theta^i_p(t) = \Theta^i_d(t) N^t_i(t). \tag{10.10}$$

Finally, we can estimate the energy consumption due to the transmissions as:

$$E^i_t(t) = e_T\Big[\Theta^i_p(t)t_{sp} + \Theta^i_d(t)t_d\Big], \tag{10.11}$$

where e_T is electrical power in transmission radio on mode and t_d is the time to transmit a data packet.

10.4.2 The formulation of the sleep interval control problem

In this section, we formulate the sleep interval control in opportunistic routing scenario as an optimization problem. Although this strategy is not suitable for mobile UWSN distributed nature, it will be helpful in providing insights for further distributed duty-cycle medium access control and routing protocol proposals.

Formally, the sleep interval control at each node with the goal of prolonging the network lifetime can be described as the optimization problem formulation showed in Figure 10.3. In this formulation, Eq. 10.12 is the objective function to be maximized. The goal is to maximize the minimum residual energy of the node i at time t, given by Eq. 10.16. The constraint 10.13 restricts the sleep interval of the nodes for a non-negative value with upper bound corresponding to the complementary value of the awake time t_a in a cycle with length of t_c. The constraint 10.14 ensures that the surface sonobuoys will not operate in duty-cycled way, *i.e.*, they will be always on. The constraint 10.15 represents flow-conservation, *i.e.*, at each node, the amount of incoming flow is equal to the amount of outgoing flow.

$$\max \min_{\forall i \in V_n} \{L_i(t)\} \tag{10.12}$$

$$s.t.$$

$$\forall i \in V_n, 0 \leq t_s^i \leq (1-\epsilon)t_c \tag{10.13}$$

$$\forall k \in V_s, t_s^k = 0 \tag{10.14}$$

$$\lambda_i(t) + \sum_{\forall j \in \Omega_i(t) \wedge i \in \mathcal{F}_j(t)} \lambda_j(t) p_{f|j}^i = \Theta_d^i(t) \tag{10.15}$$

Figure 10.3: LP formulations to optimize the nodal lifetime

$$L_i(t) = L_i(t-1) - [E_t^i(t) + E_r^i(t)]. \tag{10.16}$$

10.5 Performance Evaluation

10.5.1 Model setup

We implement our model using MATLAB and evaluate the performance of the network consisting of 100 underwater nodes and 64 sonobuoys. In our analysis, we implement the Urick's channel model [28], described in Section 2.4, to simulate the underwater acoustic communication characteristics.

In our analysis, the underwater sensor nodes are randomly distributed in a 3 D area of size 10 km × 10 km × 10 km. We deploy the surface sonobuoys in a preplanned way as follows. Firstly, the surface area is divided in a grid with 25 squares of side equals to 2000 m. Secondly, we continuously deploy randomly one sonobuoy at each cell of the grid, until all 64 sonobuoys are completely deployed. We used the extended 3 D version of the meandering current mobility (MCM) [38] to simulate the mobility of the nodes. Accordingly, they move as an effect of meandering sub-surface currents (or jet streams) and vortices. We set up the parameters of the radio of the nodes according to the values of the Telesonar SM-75 SMART modem [112]. Accordingly, the transmission power of the nodes is set to 190 dB μ re Pa, the frequency is $f = 14$ kHz and their data rate is $B = 18700$ bps.

We run experiments were the nodes use DBR [35] and Hydrocast [13] protocols. Communication void regions are not addressed and the performance of void nodes are not considered. The depth threshold of DBR is set to $\Delta_{DBR} = 500$ m. The values of energy cost are set to $e_T = 18$ W and $e_R = 0.8$ W, respectively. Strobed preamble and data packet size are set to $L_{sp} = 4$ bytes and $L_d = 250$ bytes, respectively. The silent time is $t_p = 2$ s and the length of the cycle is set to $t_c = 30$ s. We have varied the duty cycle in the interval of $\epsilon = \{0.05, 0.10, 0.15, 0.20, 0.25, 0.30, 0.35, 0.40\}$. The awake time is $t_a = \epsilon \times t_c$ and the sleep interval is $t_s = (1 - \epsilon) \times t_c$.

We plot the energy consumption results considering different traffic loads as will be presented in the next section. In the plots, the acronym FI designates the fixed sleep interval scenarios and OP to the optimized sleep interval scenarios. Due to the traffic load and grouped mobility characteristics, the sleep interval of the nodes are optimized in intervals of 10 min. The results corresponds to an average of 15 runs, with a confidence interval of 95 %. Each run last for 3 h.

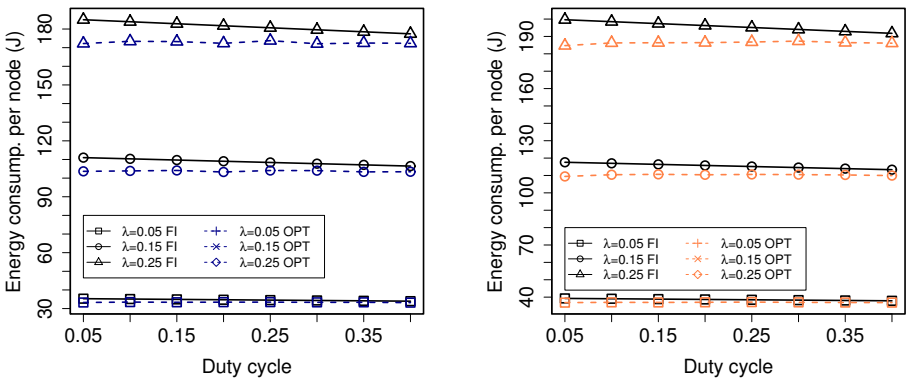

(a) DBR routing protocol (b) Hydrocast routing protocol

Figure 10.4: Avg. energy consumption over different traffic loads and duty-cycle values

10.5.2 Numerical results

Figures 10.4a and 10.4b show the results we have obtained for the average energy consumption per node, using the DBR and Hydrocast OR protocols, respectively. The plots show that, as expected, the energy consumption increases when the traffic load increases. An interesting trend that can be observed in this plot is that the energy consumption does not increased significantly when the fixed sleep interval duty-cycling increased. This is because, despite the nodes spent more energy polling the channel and receiving unintended packets, they send less strobed preambles, which save energy since the packet transmission energy cost is dominant over the packet reception one.

Figure 10.5 portrays the results we have obtained for the nodes' energy consumption when the duty cycle was varied. Figures 10.5a and 10.5b show the results for the low and high traffic load scenarios of nodes using the DBR routing protocol, respectively. The plot shows that the sleep interval control can prolong the network lifetime by reducing the high energy consumption value which happens in central nodes from the routing viewpoint. This reduction is more significant for the scenario of high traffic load (please refer to Figure 10.5b). Figures 10.5c and 10.5d show the results for nodes using the Hydrocast routing protocol. As showed in the plots, the median and high energy consumption decreases when sleep interval control is used. Interestingly, we can note that the sleep interval control was more efficient for the DBR scenario. This is because the candidate set of DBR usually have more nodes than in Hydrocast.

Figure 10.6 depicts the cumulative density function of the nodes' energy consumption for two different traffic load and duty cycle scenarios. Figures 10.6a and 10.6b depict the results for DBR routing protocol. We can see that the sleep interval control reduces the

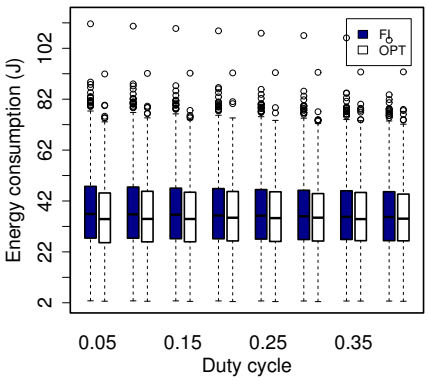

(a) DBR routing protocol, $\lambda = 0.05$

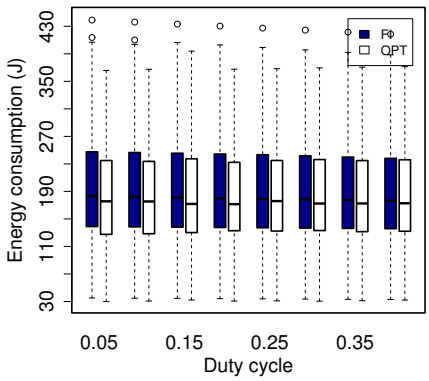

(b) DBR routing protocol, $\lambda = 0.25$

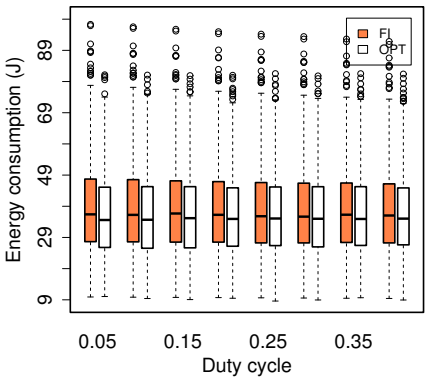

(c) Hydrocast routing protocol, $\lambda = 0.05$

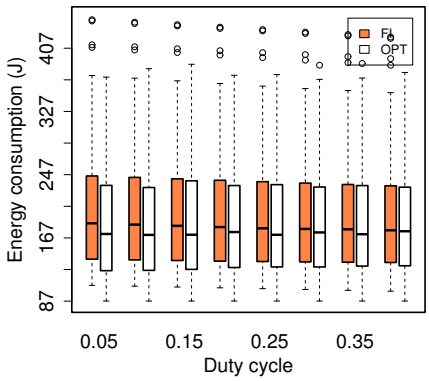

(d) Hydrocast routing protocol, $\lambda = 0.25$

Figure 10.5: Energy consumption over different traffic loads and duty-cycle values

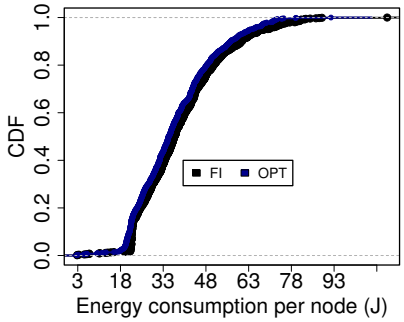

(a) DBR routing protocol, $\lambda = 0.05$, $\epsilon = 0.10$

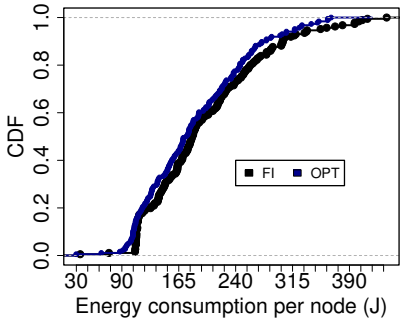

(b) DBR routing protocol, $\lambda = 0.25$, $\epsilon = 0.10$

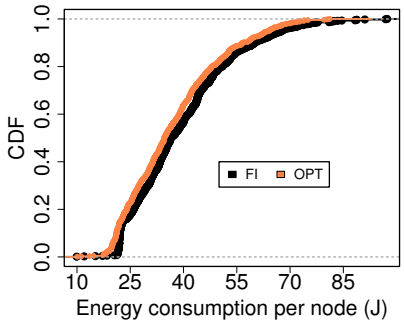

(c) Hydrocast routing protocol, $\lambda = 0.05$, $\epsilon = 0.10$

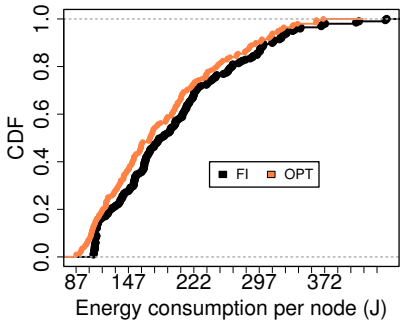

(d) Hydrocast routing protocol, $\lambda = 0.25$, $\epsilon = 0.10$

Figure 10.6: Cumulative density function (CDF) of the energy consumption

nodes' energy consumption. As already expected, this reduction is significant when the traffic load is high (Figure 10.6b). The same trend is observed when the nodes use the Hydrocast routing protocol (please refer to Figures 10.6c and 10.6d).

10.6 Concluding Remarks

In this Chapter, we proposed a modeling framework to evaluate the the sleep interval effects on the energy consumption, in duty-cycled, opportunistic routing underwater sensor networks. The proposed modeling considered the underwater acoustic communication characteristics as well as the low power listening strobed preamble duty-cycling and opportunistic routing ones.

Preliminary results showed that different fixed sleep intervals do not significantly affected the average energy consumption because of the strobed preambling mechanism. However, the results' trend showed that the sleep interval control of the nodes can prolong the network lifetime by reducing the energy consumption at central nodes from routing viewpoint.

Chapter 11

Conclusion and Future Work

This Chapter is organized as follows. Section 11.1 presents the summary of this thesis. Section 11.2 present future research directions related to this topic.

11.1 Summary of this Thesis

In this thesis, we proposed the symbiotic design of topology control and opportunistic routing in underwater sensor networks (UWSNs). Overall, the contribution of this work was the design of analytical frameworks and protocols towards efficient data collection in underwater sensor networks (UWSNs).

By doing so, we developed a novel depth adjustment-based topology control methodology to improve position-based opportunistic routing in UWSNs. We then proposed a framework modeling to evaluate the performance of our methodology in comparison to the related work: power control and bypassing void region-based. The proposed model considered the characteristics of the network architecture, underwater acoustic communication, and void node recovery strategies.

From the aforementioned methodology and observed results, we designed the CTC and DTC topology control algorithms. Both algorithms are intended to reduce disconnected and void nodes in long-term UWSN applications. CTC is a centralized topology control algorithm where a monitoring center determine which node must be moved and for which depth. To do so, the location of the nodes are known through UAV-aided underwater node localization systems. DTC, conversely, is a distributed algorithm performed prior to the network operation. Each node will solely determine whether it must adjust its depth or not. This decision is based on the one-hop neighborhood information.

In non-mobile UWSN, we designed the opportunistic routing protocol, named of GEDAR. Different from related work, GEDAR relays on the location information of the underwater nodes for data routing. Moreover, it has a depth adjustment-based procedure for the selection of new depth locations for void nodes. In terms of data delivery, GEDAR outperformed related work as fewer nodes stayed in void regions. Moreover, the improved data delivery ratio is also explained by the fact that the proposed depth adjustment on void nodes does not create long routing paths as in the related work. Thus, less transmission will take place in the network, which also reduces the chances of packet collisions.

Next, we proposed the cross-layer design of opportunistic routing in duty-cycled UWSNs. We devised a framework modeling to investigate this approach. The proposed model considered the main methodologies currently used for the design of duty-cycling protocols: naive, low power listening and low power probing. Moreover, it considered the characteristics of the underwater environment and acoustic channel, network density, and traffic load aspects. This proposed model enabled us to observe how the overhead of duty-cycling protocols diminished the performance of UWSN applications. Moreover, it allowed us to identified a set of configuration scenarios where each duty-cycle approach could be advantageous or disadvantageous for the application.

Finally, we observed that the lack of balanced energy consumption of duty-cycle leads to poor performance of UWSN applications. Hence, we proposed an analytical framework to investigate how adjustable sleep interval on the nodes can be leveraged towards balanced energy consumption. The motivation for this study came from the fact that fixed and equal sleep interval will penalize those high priority candidate nodes in our OR considered scenarios. This model proved to be useful for guiding the further design of protocols for the on-the-fly sleep interval adjustment on duty-cycled UWSNs.

11.2 Future Research Directions

The future research work consists in further investigating additional shortcomings of opportunistic routing and topology control in UWSNs. Hence, the proposal of novel mathematical models might enable the assessment of the impact of some other peculiar characteristics of topology control and opportunistic routing on the performance of UWSN applications. This investigation might enable the proposal of a novel cross-layer design of efficient topology control and opportunistic routing protocols for UWSNs. In addition, centrality metric might be proposed to measure the importance of the nodes

in these symbiotic designs. Thus, we can propose local topology control protocols with low and confined overhead. As future work, we plan to investigate the following aspects.

- Transmission power control is fundamental for UWSNs. This is because, as in the traditional WSNs, energy consumption for data transmission is high and related to the communication distance between nodes. However, in UWSN scenarios, the optimal frequency for communication is related to the distance between the nodes. Thus, we can leverage the transmission power control capabilities of the underwater acoustic modems to adjust it accordingly, to reduce the energy consumption and improve the network performance.

- Towards balanced energy consumption in UWSNs, the depth adjustment methodology can be leveraged move a node with a high centrality score, from hot-spots to locations at the edge of the network, when its battery level is below a determined threshold.

- The design of topology control-aided heterogeneous underwater sensor networks. In this approach, a few number of nodes with more capabilities (i.e., more energy budget) can be used to occupy key locations making them highly central for the routing task. Moreover, efficient deployment strategies should be investigated in order to have an adequate topology. In addition, we plan to use mobile nodes for repositioning at determined locations.

- Opportunistic routing protocol may shorten the network lifetime if no mechanism is employed for the transmission priority rotation of the candidate nodes. Candidate set selection procedures of OR could use centrality metric to rotate the priority of the nodes. Moreover, to better balance the centrality of the nodes, we plan to propose position-based upward and downward routing strategies instead of the classical pressure-based methodology. We plan to incorporate the centrality information of the nodes in scenarios of cross-layer topology control and OR designs, to decides which data flows will go in the upward/downward direction.

We are also planning further investigating OR protocols in duty-cycled UWSNs. Considering an opportunistic routing scenario of UWSNs, we proposed analytical frameworks to study the performance of the common methodologies used for the design of duty-cycle protocols. We also studied the effects of the sleep interval on the performance of duty-cycled UWSNs. The step ahead is the proposal of protocols for the reactive sleep interval adjustment of duty-cycled UWSNs.

Bibliography

[1] Woods Hole Oceanographic Institution (WHOI), "Know your ocean." `http://www.whoi.edu/know-your-ocean`, (accessed March 23, 2017).

[2] National Oceanic and Atmospheric Administration, "How much of the ocean have we explored?." `http://oceanservice.noaa.gov/facts/exploration.html`, (accessed March 23, 2017).

[3] I. F. Akyildiz, D. Pompili, and T. Melodia, "Underwater acoustic sensor networks: research challenges," *Ad Hoc Networks*, vol. 3, no. 3, pp. 257–279, 2005.

[4] J. Heidemann, M. Stojanovic, and M. Zorzi, "Underwater sensor networks: applications, advances and challenges," *Philosophical Trans. of the Royal Society of London A: Mathematical, Physical and Engineering Sciences*, vol. 370, no. 1958, pp. 158–175, 2012.

[5] M. Stojanovic and J. Preisig, "Underwater acoustic communication channels: Propagation models and statistical characterization," *IEEE Communications Magazine*, vol. 47, pp. 84–89, Jan. 2009.

[6] A. Boukerche, S. K. Das, and A. Fabbri, "Analysis of a randomized congestion control scheme with dsdv routing in ad hoc wireless networks," *Journal of Parallel and Distributed Computing*, vol. 61, no. 7, pp. 967 – 995, 2001.

[7] A. Boukerche, S. K. Das, and A. Fabbri, "Swimnet: A scalable parallel simulation testbed for wireless and mobile networks," *Wireless Networks*, vol. 7, no. 5, pp. 467–486, 2001.

[8] A. Boukerche and L. Bononi, *Simulation and Modeling of Wireless, Mobile, and AD HOC Networks*, pp. 373–409. John Wiley & Sons, Inc., 2005.

[9] A. Boukerche, R. W. N. Pazzi, and R. B. Araujo, "A fast and reliable protocol for wireless sensor networks in critical conditions monitoring applications," in *Proceedings of the 7th ACM Int'l Symposium on Modeling, Analysis & Simulation of Wireless and Mobile Systems (MSWiM)*, pp. 157–164, 2004.

[10] A. Shukla and H. Karki, "Application of robotics in offshore oil and gas industry – a review part II," *Robotics and Autonomous Systems*, 2015.

[11] Woods Hole Oceanographic Institution (WHOI), "Ocean intruments: How they work, what they do, and why they do it. rafos float." `http://www.whoi.edu/instruments/viewInstrument.do?id=1061`, (accessed Marc 23, 2017.

[12] Argo, "About argo." `http://www.argo.ucsd.edu/`, (accessed March 23, 2017).

[13] U. Lee, P. Wang, Y. Noh, L. F. M. Vieira, M. Gerla, and J.-H. Cui, "Pressure routing for underwater sensor networks," in *Proceedings of the IEEE INFOCOM*, pp. 1–9, Mar. 2010.

[14] Z. Wang and B. Wang, "A novel node sinking algorithm for 3d coverage and connectivity in underwater sensor networks," *Ad Hoc Networks*, pp. –, 2016.

[15] A. Boukerche, X. Cheng, and J. Linus, "A performance evaluation of a novel energy-aware data-centric routing algorithm in wireless sensor networks," *Wireless Networks*, vol. 11, no. 5, pp. 619–635, 2005.

[16] R. W. Pazzi and A. Boukerche, "Mobile data collector strategy for delay-sensitive applications over wireless sensor networks," *Computer Communications*, vol. 31, no. 5, pp. 1028 – 1039, 2008.

[17] F. Cunha, L. Villas, A. Boukerche, G. Maia, A. Viana, R. A. Mini, and A. A. Loureiro, "Data communication in vanets: Protocols, applications and challenges," *Ad Hoc Networks*, vol. 44, pp. 90 – 103, 2016.

[18] P. Xie, J.-H. Cui, and L. Lao, "Vbf: Vector-based forwarding protocol for underwater sensor networks," in *Proceedings of the 5th Int'l IFIP-TC6 Conf. on Networking Technologies, Services, and Protocols; Performance of Computer and Communication Networks; Mobile and Wireless Communications Systems (NETWORKING)*, pp. 1216–1221, Springer Berlin Heidelberg, 2006.

[19] Y. Noh, U. Lee, P. Wang, B. S. C. Choi, and M. Gerla, "Vapr: Void-aware pressure routing for underwater sensor networks," *IEEE Trans. on Mobile Comput.*, vol. 12, pp. 895–908, May 2013.

[20] J. M. Jornet, M. Stojanovic, and M. Zorzi, "Focused beam routing protocol for underwater acoustic networks," in *Proceedings of the 3rd ACM Int'l Workshop on Underwater Networks (WuWNeT)*, pp. 75–82, 2008.

[21] H. Yan, Z. J. Shi, and J.-H. Cui, "DBR: depth-based routing for underwater sensor networks," in *Proceedings of the 7th Int'l IFIP-TC6 NETWORKING*, pp. 72–86, 2008.

[22] R. W. L. Coutinho, L. F. M. Vieira, and A. A. F. Loureiro, "Dcr: Depth-controlled routing protocol for underwater sensor networks," in *Proceedings of the IEEE Symposium on Computers and Communications (ISCC)*, pp. 453–458, July 2013.

[23] R. W. L. Coutinho, A. Boukerche, L. F. M. Vieira, and A. A. F. Loureiro, "Design guidelines for opportunistic routing in underwater networks," *IEEE Communications Magazine*, vol. 54, pp. 40–48, Feb. 2016.

[24] R. W. L. Coutinho, A. Boukerche, L. F. M. Vieira, and A. A. F. Loureiro, "On the design of green protocols for underwater sensor networks," *IEEE Communications Magazine*, vol. 54, pp. 67–73, Oct. 2016.

[25] R. W. L. Coutinho, L. F. M. Vieira, and A. A. F. Loureiro, "Movement assisted-topology control and geographic routing protocol for underwater sensor networks," in *Proceedings of the 16th ACM Int'l Conf. on Modeling, Analysis & Simulation of Wireless and Mobile Systems (MSWiM)*, pp. 189–196, 2013.

[26] M. Jouhari, K. Ibrahimi, and M. Benattou, "Topology control through depth adjustment and transmission power control for uwsn routing protocols," in *Proceedings of the Int'l Conf. on Wireless Networks and Mobile Communications (WINCOM)*, pp. 1–5, Oct. 2015.

[27] H. Yang, B. Liu, F. Ren, H. Wen, and C. Lin, "Optimization of energy efficient transmission in underwater sensor networks," in *Proceedings of the IEEE Global Telecommunications Conference (GLOBECOM)*, pp. 1–6, Nov. 2009.

[28] R. J. Urick, *Principles of Underwater Sound*. McGraw-Hill, 1983.

[29] L. M. Brekhovskikh and Y. P. Lysanov, *Fundamentals of Ocean Acoustics*. Springer, 2003.

[30] M. Stojanovic, "On the relationship between capacity and distance in an underwater acoustic communication channel," in *Proceedings of the 1st ACM Int'l Workshop on Underwater Networks (WUWNet)*, pp. 41–47, 2006.

[31] A. Boukerche and A. Darehshoorzadeh, "Opportunistic routing in wireless networks: Models, algorithms, and classifications," *ACM Computing Surveys*, vol. 47, pp. 22:1–22:36, Nov. 2014.

[32] L. F. M. Vieira, "Performance and trade-offs of opportunistic routing in underwater networks," in *Proceedings of the IEEE Wireless Communications and Networking Conf. (WCNC)*, pp. 2911–2915, Apr. 2012.

[33] Y. Li, W. Chen, and Z.-L. Zhang, "Optimal forwarder list selection in opportunistic routing," in *Proceedings of the IEEE 6th Int'l Conf. on Mobile Adhoc and Sensor Systems (MASS)*, pp. 670–675, Oct 2009.

[34] R. W. L. Coutinho, A. Boukerche, L. F. M. Vieira, and A. A. F. Loureiro, "Gedar: Geographic and opportunistic routing protocol with depth adjustment for mobile underwater sensor networks," in *Proceedings of the IEEE Int'l Conf. on Communications (ICC)*, pp. 251–256, June 2014.

[35] H. Yan, Z. J. Shi, and J.-H. Cui, "DBR: depth-based routing for underwater sensor networks," in *Proceedings of the 7th Int'l IFIP-TC6 NETWORKING*, pp. 72–86, 2008.

[36] J. M. Jornet, M. Stojanovic, and M. Zorzi, "Focused beam routing protocol for underwater acoustic networks," in *Proceedings of the 3rd ACM Int'l Workshop on Underwater Networks (WuWNet)*, pp. 75–82, 2008.

[37] S. Basagni, C. Petrioli, R. Petroccia, and D. Spaccin, "Channel-aware routing for underwater wireless networks," in *Proc of the OCEANS - Yeosu*, pp. 1–9, May 2012.

[38] A. Caruso, F. Paparella, L. F. M. Vieira, M. Erol, and M. Gerla, "The meandering current mobility model and its impact on underwater mobile sensor networks," in *Proceedings of the IEEE INFOCOM*, 2008.

[39] F. Guerra, P. Casari, and M. Zorzi, "World ocean simulation system (woss): A simulation tool for underwater networks with realistic propagation modeling," in *Proceedings of the 4th ACM Int'l Workshop on UnderWater Networks (WUWNet)*, pp. 4:1–4:8, 2009.

[40] P. Qarabaqi and M. Stojanovic, "Adaptive power control for underwater acoustic communications," in *Proceedings of IEEE OCEANS - Spain*, pp. 1–7, June 2011.

[41] P. Santi, "Topology control in wireless ad hoc and sensor networks," *ACM Comput. Surv.*, vol. 37, pp. 164–194, June 2005.

[42] A. Porto and M. Stojanovic, "Optimizing the transmission range in an underwater acoustic network," in *Proceedings of the OCEANS*, pp. 1–5, Sept. 2007.

[43] A. F. Harris-III, M. Stojanovic, and M. Zorzi, "When underwater acoustic nodes should sleep with one eye open: Idle-time power management in underwater sensor networks," in *Proceedings of the 1st ACM Int'l Workshop on Underwater Networks (WUWNet)*, pp. 105–108, 2006.

[44] I. F. Akyildiz, D. Pompili, and T. Melodia, "Challenges for efficient communication in underwater acoustic sensor networks," *SIGBED Rev.*, vol. 1, pp. 3–8, July 2004.

[45] P. Casari and A. F. Harris, "Energy-efficient reliable broadcast in underwater acoustic networks," in *Proceedings of the 2nd Workshop on Underwater Networks (WUWNet)*, pp. 49–56, 2007.

[46] P. Casari, M. Stojanovic, and M. Zorzi, "Exploiting the bandwidth-distance relationship in underwater acoustic networks," in *Proceedings of the OCEANS*, pp. 1–6, Sept. 2007.

[47] L. M. Feeney and M. Nilsson, "Investigating the energy consumption of a wireless network interface in an ad hoc networking environment," in *Proceedings of the 20th Annual Joint Conf. of the IEEE Computer and Communications Societies (INFOCOM)*, vol. 3, pp. 1548–1557, 2001.

[48] T. Rappaport, *Wireless Communications: Principles and Practice*. Upper Saddle River, NJ, USA: Prentice Hall PTR, 2nd ed., 2001.

[49] M. Al-Bzoor, Y. Zhu, J. Liu, R. Ammar, J.-H. Cui, and S. Rajasekaran, "Adaptive power controlled routing for underwater sensor networks," in *Proceedings of the 7th*

Int'l Conf. on Wireless Algorithms, Systems, and Applications (WASA), pp. 549–560, 2012.

[50] Z. Zhou and J.-H. Cui, "Energy efficient multi-path communication for time-critical applications in underwater sensor networks," in *Proceedings of the 9th ACM Int'l Symp. on Mobile Ad Hoc Networking and Computing (MobiHoc)*, pp. 221–230, 2008.

[51] J. Xu, K. Li, G. Min, K. Lin, and W. Qu, "Energy-efficient tree-based multipath power control for underwater sensor networks," *IEEE Trans. on Parallel and Distributed Systems*, vol. 23, pp. 2107–2116, Nov. 2012.

[52] S. Kim, S. Park, and Y. Yoo, "Dynamic transmission power control based on exact sea surface movement modeling in underwater acoustic sensor networks," in *Proceedings of the IEEE 10th Int'l Conf. on Wireless and Mobile Computing, Networking and Communications (WiMob)*, pp. 666–672, Oct. 2014.

[53] S. Lmai, M. Chitre, C. Laot, and S. Houcke, "Throughput-maximizing transmission schedules for underwater acoustic multihop grid networks," *IEEE Journal of Oceanic Engineering*, vol. 40, pp. 853–863, Oct. 2015.

[54] P. Anjangi and M. Chitre, "Unslotted transmission schedules for practical underwater acoustic multihop grid networks with large propagation delays," in *Proceedings of the IEEE 3rd Underwater Communications and Networking Conference (UComms)*, pp. 1–5, Aug. 2016.

[55] Y. Su, Y. Zhu, H. Mo, J.-H. Cui, and Z. Jin, "A joint power control and rate adaptation mac protocol for underwater sensor networks," *Ad Hoc Networks*, vol. 26, pp. 36 – 49, 2015.

[56] K. Kredo-II, P. Djukic, and P. Mohapatra, "Stump: Exploiting position diversity in the staggered tdma underwater mac protocol," in *Proceedings of the IEEE INFOCOM*, pp. 2961–2965, Apr. 2009.

[57] C.-C. Hsu, K.-F. Lai, C.-F. Chou, and K. C. J. Lin, "St-mac: Spatial-temporal mac scheduling for underwater sensor networks," in *Proceedings of the IEEE INFOCOM*, pp. 1827–1835, Apr. 2009.

[58] S. C. Ergen and P. Varaiya, "Pedamacs: power efficient and delay aware medium access protocol for sensor networks," *IEEE Transactions on Mobile Computing*, vol. 5, pp. 920–930, July 2006.

[59] W. Bai, H. Wang, X. Shen, and R. Zhao, "Link scheduling method for underwater acoustic sensor networks based on correlation matrix," *IEEE Sensors Journal*, vol. 16, pp. 4015–4022, June 2016.

[60] A. Shashaj, R. Petroccia, and C. Petrioli, "Energy efficient interference-aware routing and scheduling in underwater sensor networks," in *Oceans - St. John's*, pp. 1–8, Sep 2014.

[61] P. Anjangi and M. Chitre, "Scheduling algorithm with transmission power control for random underwater acoustic networks," in *OCEANS - Genova*, pp. 1–8, May 2015.

[62] B. Peleato and M. Stojanovic, "A mac protocol for ad-hoc underwater acoustic sensor networks," in *Proceedings of the 1st ACM Int'l Workshop on Underwater Networks (WUWNet)*, pp. 113–115, 2006.

[63] J. M. Jornet and M. Stojanovic, "Distributed power control for underwater acoustic networks," in *Proceedings of the OCEANS*, pp. 1–7, Sept. 2008.

[64] E. Gallimore, J. Partan, I. Vaughn, S. Singh, J. Shusta, and L. Freitag, "The whoi micromodem-2: A scalable system for acoustic communications and networking," in *Proceedings of the MTS/IEEE OCEANS - SEATTLE*, pp. 1–7, 2010.

[65] J. Heidemann, W. Ye, J. Wills, A. Syed, and Y. Li, "Research challenges and applications for underwater sensor networking," in *Proceedings of the IEEE Wireless Communications and Networking Conf. (WCNC)*, vol. 1, pp. 228–235, Apr. 2006.

[66] A. F. Harris-III, M. Stojanovic, and M. Zorzi, "Idle-time energy savings through wake-up modes in underwater acoustic networks," *Ad Hoc Netw.*, vol. 7, pp. 770–777, June 2009.

[67] I. Tumar, A. Sehgal, and J. Schonwalder, "Power management for acoustic underwater networks," in *Proceedings of the 6th IEEE Annual Communications Society Conference on Sensor, Mesh and Ad Hoc Communications and Networks Workshops (SECON)*, pp. 1–3, June 2009.

[68] R. W. L. Coutinho, A. Boukerche, L. F. M. Vieira, and A. A. F. Loureiro, "Modeling and analysis of opportunistic routing in low duty-cycle underwater sensor networks," in *Proceedings of the 18th ACM Int'l Conf. on Modeling, Analysis and Simulation of Wireless and Mobile Systems (MSWiM)*, pp. 125–132, 2015.

[69] M. Cardei and D.-Z. Du, "Improving wireless sensor network lifetime through power aware organization," *Wirel. Netw.*, vol. 11, pp. 333–340, May 2005.

[70] J. Wills, W. Ye, and J. Heidemann, "Low-power acoustic modem for dense underwater sensor networks," in *Proceedings of the 1st ACM International Workshop on Underwater Networks (WUWNet)*, pp. 79–85, 2006.

[71] A. Sanchez, S. Blanc, P. Yuste, I. Piqueras, and J. J. Serrano, "A low-power wake-up system for underwater wireless sensor modems," in *Proceedings of the Sixth ACM International Workshop on Underwater Networks (WUWNet)*, pp. 18:1–18:2, 2011.

[72] X. Li, M. Zhu, and Y. Wu, "Low-power system design for underwater acoustic modems," in *Proceedings of the 10th International Conference on Underwater Networks & Systems (WUWNET)*, (New York, NY, USA), pp. 38:1–38:2, 2015.

[73] M. Buettner, G. V. Yee, E. Anderson, and R. Han, "X-mac: A short preamble mac protocol for duty-cycled wireless sensor networks," in *Proceedings of the 4th Int'l Conf. on Embedded Networked Sensor Systems (SenSys)*, pp. 307–320, 2006.

[74] Z. Li, M. Li, and Y. Liu, "Towards energy-fairness in asynchronous duty-cycling sensor networks," *ACM Trans. Sen. Netw.*, vol. 10, pp. 38:1–38:26, May 2014.

[75] F. Zorzi, M. Stojanovic, and M. Zorzi, "On the effects of node density and duty cycle on energy efficiency in underwater networks," in *Proceedings of the IEEE OCEANS - Sydney*, pp. 1–6, May 2010.

[76] L. Hong, F. Hong, B. Yang, and Z. Guo, "Ross: Receiver oriented sleep scheduling for underwater sensor networks," in *Proceedings of the Eighth ACM International Conference on Underwater Networks and Systems (WUWNet)*, pp. 4:1–4:8, 2013.

[77] R. W. L. Coutinho, A. Boukerche, L. F. M. Vieira, and A. A. F. Loureiro, "Modeling the sleep interval effects in duty-cycled underwater sensor networks," in *Proceedings of the IEE Int'l Conf. on Communications (ICC)*, pp. 1997–2002, May 2016.

[78] M. Younis, I. F. Senturk, K. Akkaya, S. Lee, and F. Senel, "Topology management techniques for tolerating node failures in wireless sensor networks: A survey," *Computer Networks*, vol. 58, pp. 254 – 283, 2014.

[79] S. Basagni, L. Bölöni, P. Gjanci, C. Petrioli, C. A. Phillips, and D. Turgut, "Maximizing the value of sensed information in underwater wireless sensor networks via an autonomous underwater vehicle," in *Proceedings of the IEEE INFOCOM*, pp. 988–996, Apr. 2014.

[80] P. A. Forero, S. K. Lapic, C. Wakayama, and M. Zorzi, "Rollout algorithms for data storage- and energy-aware data retrieval using autonomous underwater vehicles," in *Proceedings of the Int'l Conf. on Underwater Networks & Systems (WUWNET)*, pp. 22:1–22:8, 2014.

[81] E. Cayirci *et al.*, "Wireless sensor networks for underwater survelliance systems," *Ad Hoc Networks*, vol. 4, no. 4, pp. 431–446, 2006.

[82] M. Erol, L. F. M. Vieira, and M. Gerla, "Localization with dive'n'rise (dnr) beacons for underwater acoustic sensor networks," in *Proceedings of the 2nd Workshop on Underwater Networks (WuWNet)*, pp. 97–100, 2007.

[83] F. A. Khan, S. A. Khan, D. Turgut, and L. Bölöni, "Greedy path planning for maximizing value of information in underwater sensor networks," in *Proceedings of the 39th Annual IEEE Conf. on Local Computer Networks Workshops (LCN Workshops)*, pp. 610–615, Sept. 2014.

[84] M. O'Rourke, E. Basha, and C. Detweiler, "Multi-modal communications in underwater sensor networks using depth adjustment," in *Proceedings of the 7th ACM Int'l Conf. on Underwater Networks and Systems (WUWNET)*, pp. 31:1–31:5, 2012.

[85] J. Jaffe and C. Schurgers, "Sensor networks of freely drifting autonomous underwater explorers," in *Proceedings of the 1st ACM Int'l Workshop on Underwater Networks (WUWNet)*, pp. 93–96, 2006.

[86] M. Erol, L. F. M. Vieira, and M. Gerla, "Auv-aided localization for underwater sensor networks," in *Proceedings of the Int'l Conf. on Wireless Algorithms, Systems and Applications (WASA)*, pp. 44–54, Aug. 2007.

[87] E. Basha, N. Yuen, M. O'Rourke, and C. Detweiler, "Analysis of algorithms for multi-modal communications in underwater sensor networks," in *Proceedings of the Int'l Conf. on Underwater Networks & Systems (WUWNET)*, pp. 17:1–17:8, 2014.

[88] R. W. L. Coutinho, A. Boukerche, L. F. M. Vieira, and A. A. F. Loureiro, "Local maximum routing recovery in underwater sensor networks: Performance and trade-offs," in *Proceedings of the IEEE 22nd Int'l Symposium on Modelling, Analysis Simulation of Computer and Telecommunication Systems (MASCOTS)*, pp. 112–119, Sept. 2014.

[89] L. Pu, Y. Luo, H. Mo, S. Le, Z. Peng, J.-H. Cui, and Z. Jiang, "Comparing underwater mac protocols in real sea experiments," *Computer Communications*, vol. 56, pp. 47–59, 2015.

[90] D. Pinto, S. S. Viana, J. A. M. Nacif, L. F. M. Vieira, M. A. M. Vieira, A. B. Vieira, and A. O. Fernandes, "Hydronode: A low cost, energy efficient, multi purpose node for underwater sensor networks," in *Proceedings IEEE 37th Conf. on Local Computer Networks (LCN)*, pp. 148–151, 2012.

[91] J.-H. Cui, J. Kong, M. Gerla, and S. Zhou, "The challenges of building mobile underwater wireless networks for aquatic applications," *IEEE Network*, vol. 20, pp. 12–18, May 2006.

[92] Z. Zhou, Z. Peng, J.-H. Cui, Z. Shi, and A. Bagtzoglou, "Scalable localization with mobility prediction for underwater sensor networks," *IEEE Trans. on Mobile Comput.*, vol. 10, no. 3, pp. 335–348, 2011.

[93] M. O'Rourke, E. Basha, and C. Detweiler, "Multi-modal communications in underwater sensor networks using depth adjustment," in *Proceedings of the 7th ACM Int'l Conference on Underwater Networks and Systems (WUWNet)*, pp. 31:1–31:5, 2012.

[94] Y. Noh, U. Lee, P. Wang, B. S. C. Choi, and M. G., "VAPR: void-aware pressure routing for underwater sensor networks," *IEEE Trans. on Mobile Comput.*, vol. 12, no. 5, pp. 895–908, 2013.

[95] T. Melodia, D. Pompili, and I. F. Akyildiz, "Optimal local topology knowledge for energy efficient geographical routing in sensor networks," in *Proceedings of the IEEE INFOCOM*, vol. 3, pp. 1705–1716, 2004.

[96] A. Mostefaoui, M. Melkemi, and A. Boukerche, "Routing through holes in wireless sensor networks," in *Proceedings 15th ACM Int'l Conf. on Modeling, Analysis & Simulation of Wireless and Mobile Systems (MSWiM)*, pp. 395–402, 2012.

[97] D. Chen and P. Varshney, "A survey of void handling techniques for geographic routing in wireless networks," *IEEE Commun. Surveys and Tuts.*, pp. 50–67, 2007.

[98] S. Durocher, D. Kirkpatrick, and L. Narayanan, "On routing with guaranteed delivery in three-dimensional ad hoc wireless networks," *Wireless Networks*, vol. 16, pp. 227–235, Jan. 2010.

[99] M. Stojanovic, "Recent advances in high-speed underwater acoustic communications," *IEEE J. Oceanic Eng.*, pp. 125–136, 1996.

[100] C. Carbonelli and U. Mitra, "Cooperative multihop communication for underwater acoustic networks," in *Proceedings of the 1st ACM Int'l Workshop on Underwater Networks (WUWNet)*, pp. 97–100, 2006.

[101] L. Freitag, M. Grund, S. Singh, J. Partan, P. Koski, and K. Ball, "The WHOI micro-modem: An acoustic communcations and navigation system for multiple platforms," in *Proceedings of the MTS/IEEE Oceans*, 2005.

[102] H. Yang, B. Liu, F. Ren, H. Wen, and C. Lin, "Optimization of energy efficient transmission in underwater sensor networks," in *Proceedings of the IEEE Global Telecommun. Conf. (GLOBECOM)*, pp. 1–6, 2009.

[103] T. Rappaport, *Wireless Communications: Principles and Practice*. Upper Saddle River, NJ, USA: Prentice Hall PTR, 2nd ed., 2001.

[104] N. Nicolaou, A. SEE, P. Xie, J.-H. Cui, and D. Maggiorini, "Improving the robustness of location-based routing for underwater sensor networks," in *Proceedings MTS/IEEE OCEANS*, pp. 1–6, 2007.

[105] P. Xie, Z. Zhou, Z. Peng, J.-H. Cui, and Z. Shi, "Void avoidance in three-dimensional mobile underwater sensor networks," in *Wireless Algorithms, Systems, and Applications*, vol. 5682, pp. 305–314, Springer, 2009.

[106] S. Basagni, C. Petrioli, R. Petroccia, and D. Spaccini, "Carp: A channel-aware routing protocol for underwater acoustic wireless networks," *Ad Hoc Networks*, vol. 34, pp. 92 – 104, 2015.

[107] M. Al-Bzoor, Y. Zhu, J. Liu, A. Reda, J.-H. Cui, and S. Rajasekaran, "Adaptive power controlled routing for underwater sensor networks," in *Wireless Algorithms, Systems, and Applications*, vol. 7405 of *Lecture Notes in Computer Science*, pp. 549–560, Springer Berlin Heidelberg, 2012.

[108] R. W. L. Coutinho, L. F. M. Vieira, and A. A. F. Loureiro, "DCR: depth-controlled routing protocol for underwater sensor networks," in *Proceedings of the IEEE Symp. on Comput. and Commun. (ISCC)*, pp. 453–458, 2013.

[109] R. W. L. Coutinho, L. F. Vieira, and A. A. F. Loureiro, "Movement assisted-topology control and geographic routing protocol for underwater sensor networks," in *Proceedings of the 6th ACM Int'l Conf. on Modeling, Analysis & Simulation of Wireless and Mobile Systems (MSWiM)*, pp. 189–196, 2013.

[110] R. W. Coutinho, A. Boukerche, L. F. M. Vieira, and A. A. F. Loureiro, "A novel void node recovery paradigm for long-term underwater sensor networks," *Ad Hoc Networks*, vol. 34, pp. 144 – 156, 2015.

[111] R. W. L. Coutinho, L. F. M. Vieira, and A. A. F. Loureiro, "Geographic and opportunistic routing for underwater sensor networks," *IEEE Transactions on Computers*, vol. 65, pp. 548–561, Feb. 2016.

[112] Teledyne-Benthos, Acoustic Modems. http://www.benthos.com, 2015. [Online].

[113] L. F. M. Vieira, M. A. M. Vieira, D. Pinto, J. A. M. Nacif, S. S. Viana, and A. B. Vieira, "Hydronode: An underwater sensor node prototype for monitoring hydroelectric reservoirs," in *Proceedings 7th ACM Int'l Conference on Underwater Networks and Systems (WUWNet)*, pp. 43:1–43:2, 2012.

[114] F. Bouabdallah, N. Bouabdallah, and R. Boutaba, "On balancing energy consumption in wireless sensor networks," *IEEE Transactions on Vehicular Technology*, vol. 58, no. 6, pp. 2909–2924, 2009.

[115] P. Xie and J.-H. Cui, "Exploring random access and handshaking techniques in large-scale underwater wireless acoustic sensor networks," in *Proceedings of the OCEANS*, pp. 1–6, 2006.

[116] Y. Zhu, Z. Jiang, Z. Peng, M. Zuba, J.-H. Cui, and H. Chen, "Toward practical mac design for underwater acoustic networks," in *Proceedings of the IEEE INFOCOM*, pp. 683–691, 2013.

[117] M. Burkhart, P. von Rickenbach, R. Wattenhofer, and A. Zollinger, "Does topology control reduce interference?," in *Proceedings of the 5th ACM Int'l Symposium on Mobile Ad Hoc Networking and Computing (MobiHoc)*, pp. 9–19, 2004.

[118] B. Liu, F. Ren, C. Lin, Y. Yang, R. Zeng, and H. Wen, "The redeployment issue in underwater sensor networks," in *Proceedings IEEE Global Telecommunications Conference (GLOBECOM)*, pp. 1–6, 2008.

[119] R. W. L. Coutinho, A. Boukerche, L. F. M. Vieira, and A. A. F. Loureiro, "On the design of green protocols for underwater sensor networks," *IEEE Communications Magazine*, vol. 65, pp. 548–561, Oct. 2016.

[120] H. Zhang, S. Xiong, Z. Yue, and Z. Wang, "Sea trials of an underwater acoustic network in the east china sea 2015," in *IEEE/OES China Ocean Acoustics (COA)*, pp. 1–5, Jan 2016.

[121] L. F. M. Vieira, J. Kong, U. Lee, and M. Gerla, "Analysis of Aloha Protocols for Underwater Acoustic Sensor Networks," in *Proceedings of the ACM WUWNet*, 2006.

[122] A. Boukerche, S. Hong, and T. Jacob, "An efficient synchronization scheme of multimedia streams in wireless and mobile systems," *IEEE Transactions on Parallel and Distributed Systems*, vol. 13, pp. 911–923, Sep 2002.

[123] A. Boukerche, H. A. B. F. Oliveira, E. F. Nakamura, and A. A. F. Loureiro, "Secure localization algorithms for wireless sensor networks," *IEEE Communications Magazine*, vol. 46, pp. 96–101, April 2008.

[124] H. A. B. F. de Oliveira, A. Boukerche, E. F. Nakamura, and A. A. F. Loureiro, "An efficient directed localization recursion protocol for wireless sensor networks," *IEEE Transactions on Computers*, vol. 58, pp. 677–691, May 2009.

[125] P. Xie, Z. Zhou, Z. Peng, H. Yan, T. Hu, J.-H. Cui, Z. Shi, Y. Fei, and S. Zhou, "Aqua-sim: An ns2 based simulator for underwater sensor networks," in *Proceedings of the IEEE OCEANS*, 2009.

[126] T. Rossby, D. Dorson, and J. Fontaine, "The RAFOS system," *Journal of atmospheric and oceanic technology*, vol. 3, pp. 672–680, 1986.

[127] M. Erol, F. Vieira, and M. Gerla, "AUV-Aided localization for underwater sensor networks," in *Proceedings of the Int'l Conf. on Wireless Algorithms, Systems and Applications (WASA)*, pp. 44–54, 2007.

[128] Z. Yu, C. Xiao, and G. Zhou, "Multi-objectivization-based localization of underwater sensors using magnetometers," *IEEE Sensors J.*, vol. 14, no. 4, pp. 1099–1106, 2014.

[129] D. Pompili, T. Melodia, and I. F. Akyildiz, "Routing algorithms for delay-insensitive and delay-sensitive applications in underwater sensor networks," in *Proceedings of the 12th Annu. Int'l Conf. on Mobile Computing and Networking (MobiCom)*, pp. 298–309, 2006.

[130] T. Melodia, D. Pompili, and I. F. Akyildiz, "Optimal local topology knowledge for energy efficient geographical routing in sensor networks," in *Proceedings of the IEEE INFOCOM*, vol. 3, pp. 1705–1716, 2004.

[131] S. Lee, B. Bhattacharjee, and S. Banerjee, "Efficient geographic routing in multihop wireless networks," in *Proceedings of the 6th ACM Int'l Symp. on Mobile Ad Hoc Network. & Comput. (MobiHoc)*, pp. 230–241, 2005.

[132] K. Zeng, W. Lou, J. Yang, and D. R. Brown, "On geographic collaborative forwarding in wireless ad hoc and sensor networks," in *Proceedings of the Int'l Conf. on Wireless Algorithms, Systems and Applications (WASA)*, pp. 11–18, 2007.

[133] A. Boukerche, S. K. Das, A. Fabbri, and O. Yildiz, "Exploiting model independence for parallel pcs network simulation," in *Proceedings 13th Workshop on Parallel and Distributed Simulation (PADS)*, pp. 166–173, 1999.

[134] Y. Ren, W. K. G. Seah, and P. D. Teal, "Performance of pressure routing in drifting 3d underwater sensor networks for deep water monitoring," in *Proceedings of the 7th ACM Int'l Conf. on Underwater Networks and Systems (WUWNet)*, pp. 28:1–28:8, 2012.

[135] R. W. L. Coutinho, A. Boukerche, L. F. M. Vieira, and A. A. F. Loureiro, "Design guidelines for opportunistic routing in underwater networks," *IEEE Commun. Mag.*, vol. 54, pp. 40–48, Feb. 2016.

[136] K. Zeng, W. Lou, and H. Zhai, "On end-to-end throughput of opportunistic routing in multirate and multihop wireless networks," in *Proceedings of the IEEE INFOCOM*, pp. 1490–1498, Apr. 2008.

[137] O. Landsiedel, E. Ghadimi, S. Duquennoy, and M. Johansson, "Low power, low delay: Opportunistic routing meets duty cycling," in *Proceedings of the 11th Int'l Conf. on Information Processing in Sensor Networks (IPSN)*, pp. 185–196, 2012.

[138] M. Cattani, A. Loukas, M. Zimmerling, M. Zuniga, and K. Langendoen, "Staffetta: Smart duty-cycling for opportunistic data collection," in *Proceedings of the 14th ACM Conf. on Embedded Network Sensor Systems (SenSys)*, pp. 56–69, 2016.

[139] Y. Sun, O. Gurewitz, and D. B. Johnson, "Ri-mac: A receiver-initiated asynchronous duty cycle mac protocol for dynamic traffic loads in wireless sensor networks," in *Proceedings of the 6th ACM Int'l Conf. on Embedded Network Sensor Systems (SenSys)*, pp. 1–14, 2008.

[140] P. Spachos, P. Chatzimisios, and D. Hatzinakos, "Energy aware opportunistic routing in wireless sensor networks," in *Proceedings of the IEEE Globecom Workshops*, pp. 405–409, Dec. 2012.

[141] E. Ghadimi, O. Landsiedel, P. Soldati, S. Duquennoy, and M. Johansson, "Opportunistic routing in low duty-cycle wireless sensor networks," *ACM Trans. Sen. Netw.*, vol. 10, pp. 67:1–67:39, June 2014.

[142] V. D. Valerio, F. L. Presti, C. Petrioli, L. Picari, and D. Spaccini, "A self-adaptive protocol stack for underwater wireless sensor networks," in *Proceedings of the OCEANS - Shanghai*, pp. 1–8, Apr. 2016.

[143] F. J. L. Ribeiro, A. d. C. Pedroza, and L. H. M. K. Costa, "Underwater monitoring system for oil exploration using acoustic sensor networks," *Telecomm. Systems*, vol. 58, no. 1, pp. 91–106, 2015.

[144] J. Gao, J. Li, Z. Cai, and H. Gao, "Composite event coverage in wireless sensor networks with heterogeneous sensors," in *Proceedings of the IEEE INFOCOM*, pp. 217–225, Apr. 2015.

[145] C. C. Hsu, H. H. Liu, J. L. G. Gmez, and C. F. Chou, "Delay-sensitive opportunistic routing for underwater sensor networks," *IEEE Sensors Journal*, vol. 15, pp. 6584–6591, Nov. 2015.

[146] A. Wahid, S. Lee, H.-J. Jeong, and D. Kim, "EEDBR: Energy-Efficient Depth-Based Routing Protocol for Underwater Wireless Sensor Networks," *Advanced Computer Science and Information Technology*, vol. 195, pp. 223–234, Sept. 2011.

[147] W. Hu, J. Xie, and Z. Zhang, "Practical opportunistic routing in high-speed multi-rate wireless mesh networks," in *Proceedings of the 14th ACM Int'l Symposium on Mobile Ad Hoc Networking and Computing (MobiHoc)*, pp. 127–136, 2013.

[148] A. Darehshoorzadeh, R. E. D. Grande, and A. Boukerche, "Toward a comprehensive model for performance analysis of opportunistic routing in wireless mesh networks," *IEEE Transactions on Vehicular Technology*, vol. 65, pp. 5424–5438, July 2016.

[149] J. Preisig, "Acoustic propagation considerations for underwater acoustic communications network development," *SIGMOBILE Mob. Comput. Commun. Rev.*, vol. 11, pp. 2–10, Oct. 2007.

[150] J. Wang, Z. Cao, X. Mao, X. Y. Li, and Y. Liu, "Towards energy efficient duty-cycled networks: Analysis, implications and improvement," *IEEE Trans. on Comput.*, vol. 65, pp. 270–280, Jan. 2016.

[151] F. D. Rienzo, M. Girolami, S. Chessa, F. Paparella, and A. Caruso, "Signals from the depths: Properties of percolation strategies with the argo dataset," in *Proceedings of the IEEE Symposium on Computers and Communication (ISCC)*, pp. 372–378, June 2016.

[152] V. Rodoplu and M. K. Park, "An energy-efficient mac protocol for underwater wireless acoustic networks," in *Proceedings of the MTS/IEEE OCEANS*, pp. 1198–1203 Vol. 2, Sept. 2005.

[153] A. A. Syed, W. Ye, and J. Heidemann, "T-Lohi: a new class of mac protocols for underwater acoustic sensor networks," in *Proceedings of the IEEE INFOCOM*, pp. 789–797, Apr. 2008.

[154] J. Polastre, J. Hill, and D. Culler, "Versatile low power media access for wireless sensor networks," in *Proceedings of the 2nd ACM SenSys*, pp. 95–107, 2004.

[155] A. Meier, M. Woehrle, M. Zimmerling, and L. Thiele, "ZeroCal: automatic mac protocol calibration," in *Distributed Computing in Sensor Systems*, vol. 6131, pp. 31–44, Springer Berlin Heidelberg, 2010.

[156] M. Zimmerling, F. Ferrari, L. Mottola, T. Voigt, and L. Thiele, "ptunes: Runtime parameter adaptation for low-power mac protocols," in *Proceedings of the 11th Int'l Conf. on Information Processing in Sensor Networks (IPSN)*, pp. 173–184, 2012.

[157] Y. Peng, Z. Li, D. Qiao, and W. Zhang, "I^2C: a holistic approach to prolong the sensor network lifetime," in *Proceedings of the IEEE INFOCOM*, pp. 2670–2678, Apr. 2013.

[158] C. Zhu, L. T. Yang, L. Shu, V. C. M. Leung, J. J. P. C. Rodrigues, and L. Wang, "Sleep scheduling for geographic routing in duty-cycled mobile sensor networks," *IEEE Transactions on Industrial Electronics*, vol. 61, pp. 6346–6355, Nov. 2014.

[159] C. Zhu, L. T. Yang, L. Shu, V. C. M. Leung, T. Hara, and S. Nishio, "Insights of top- k query in duty-cycled wireless sensor networks," *IEEE Transactions on Industrial Electronics*, vol. 62, pp. 1317–1328, Feb. 2015.

[160] Y. Zhu, Z. Peng, J.-H. Cui, and H. Chen, "Toward practical mac design for underwater acoustic networks," *IEEE Transactions on Mobile Computing*, vol. 14, pp. 872–886, Apr. 2015.

[161] A. Capossele, G. D. Cicco, and C. Petrioli, "R-CARP: A reputation based channel aware routing protocol for underwater acoustic sensor networks," in *Proceedings of the ACM WUWNet*, Oct. 2015.

[162] H. Dubois-Ferrière, M. Grossglauser, and M. Vetterli, "Valuable detours: Least-cost anypath routing," *IEEE/ACM Transactions on Networking*, vol. 19, pp. 333–346, Apr. 2011.

[163] W. Hu, J. Xie, and Z. Zhang, "Practical opportunistic routing in high-speed multi-rate wireless mesh networks," in *Proceedings of the 14th ACM MobiHoc*, pp. 127–136, 2013.